STUDY OF SELECTIVE WITHDRAWAL FROM TWO LAYER FLUID

By

ANWAR HOSSAIN

A thesis submitted to the Department of Mechanical Engineering in partial fulfillment of the requirements for the degree of

Master of Science

in

Mechanical Engineering

JUNE, 1995

BANGLADESH UNIVERSITY OF ENGINEERING AND TECHNOLOGY
DHAKA, BANGLADESH.

The thesis titled " STUDY OF SELECTIVE WITHDRAWAL FROM TWO LAYER FLUID ", submitted by ANWAR HOSSAIN, Roll no. 911416P, Registration no. 85464 has been accepted as satisfactory in partial fulfillment of the degree of Master of Science in Mechanical Engineering on 25th June, 1995.

BOARD OF EXAMINERS

1. Dr. Md. Quamrul Islam — Chairman (Supervisor)
Professor
Mechanical Engineering Department
BUET, Dhaka.

2. Dr. Md. ~~Abdur~~ Razzaq Akhanda — Member (Ex-officio)
Professor & Head
Mechanical Engineering Department
BUET, Dhaka.

3. Dr. A. K. M. Sadrul Islam — Member
Professor
Mechanical Engineering Department
BUET, Dhaka.

4. Dr. Md. Refayet Ullah — Member (External)
Associate Professor
Naval Architecture and Marine Engineering Department
BUET, Dhaka.

CERTIFICATE OF RESEARCH

This is to certify that the work presented in this dissertation is outcome of the investigation carried out by the candidate under the supervision of Dr. Md. Quamrul Islam in the Mechanical Engineering Department of Bangladesh University of Engineering and Technology, Dhaka, Bangladesh.

Supervisor

Candidate

ABSTRACT

Selective withdrawal from stratified fluid system is a technique of water quality management. Stagnant water in most of the reservoirs are stably stratified throughout most or all of the year. This stratification is caused primarily by temperature variation with depth, and secondarily by a variable concentration of dissolved or suspended solid. Selective withdrawal is one, where one can select the strata of the fluid at the sink level. Here the flow in the horizontal direction is restricted and thus enables the water to be withdrawn in horizontal layers. This method of reservoir fluid quality management is becoming popular day by day. This method is used in cooling ponds, solar ponds, salt producing industry.

The flow from different layers in a stably stratified fluid system depends on many parameters. They are; nature of stratification, thickness of the interface, flow rate, shape of the sink, location of the sink, rotation etc.. The change in any of this parameter effect the drawdown significantly. By changing these variables effectively one can efficiently control fluid quality from a stably stratified fluid system.

Starting from the middle of this century, still today, numerous experimental and analytical work has been done on this topic. Location of sink effects the percentage drawdown significantly. It is found from the experiment that when the sink is elevated to a certain height Densimetric Froude number becomes the governing parameter in controlling the drawdown history of the stratified fluid system and all other parameter becomes less significant. From the experimental data a generalized equation is developed which can predict drawdown efficiently.

ACKNOWLEDGEMENTS

The author likes to express his deep gratitude to his supervisor, Dr. Md. Quamrul Islam, Professor, Mechanical Engineering Department, Bangladesh University of Engineering and Technology, Dhaka, and Dr. A. K. M. Sadrul Islam for their encouraging and valuable suggestions, superb guidance and continuous encouragement during whole period of this research.

CONTENTS

APPENDICES

LIST OF FIGURES

LIST OF TABLES

NOMENCLATURE

a	Intake diameter normalized by tank radius, d/R
a_i	Description coefficients
C_n	Speed of internal wave of mode n
b	Half thickness of the interface, mm
d	Intake hole diameter, mm
d_c	Cap diameter, mm
D	Molecular thermal diffusivity, m^2/s
EX	Extension of the intake from the ground level of the tank, mm
F	Densimetric Froude number at cross flow, $U(g'H^5)^{1/2}$
Fi	Froude number defined as $q/(2g'h^3)^{1/2}$
F_r	Densimetric Froude number for line sink, $q/(g'h^3)^{1/2}$
Fr	Densimetric Froude number for axisymmetric sinks, $Q/(g'H^5)^{1/2}$
Fr_c	Critical densimetric Froude number
F_d	Intake Froude number, $Q/(g'd^5)^{1/2}$
F_D	Intake Froude number defined as, $4Q/\pi(g'd^5)^{1/2}$
F_l	Interface Froude number, $q/(g'l^5)^{1/2}$
Fr_s	Intake Froude number based on cap height, $Q/(g'S^5)^{1/2}$
Fr_δ	Froude number based on withdrawal layer thickness, $U/N\delta$
F_R	Froude number based on tank radius, $(Q^2/g'R^5)^{1/2}$

g	Gravitational acceleration, mm/sec^2
g'	Reduced gravitational acceleration, $g\Delta\rho/\rho$, mm/sec^2
h	Difference between the elevation of the interface and intake, mm
H	Initial mean height of interface from the ground level of the tank, mm
l	Interface thickness, mm; characteristic length scale
L	Length of tank
mv	Millivolt reading
n	Mode number of internal wave
N	Buoyancy frequency, $(\gamma' g)^{1/2}$
P	Pressure, central node of a discretisation cell
Pe	Peclet number, Ul/D
q	Withdrawal rate per unit width of a line sink, m^2/sec
Q	Withdrawal rate in an axisymmetric sink, m^3/sec
r	radial axis of cylindrical coordinate system
R	Tank radius
Ra	Raleigh number, $(\nu D)^{1/2}/NH^2$
Re	Reynolds number, UH/ν
Ri	Richardsons number
S	Cap height, mm
Sc	Schimidt number, ν/D
S_t	Cap thickness, mm
t	Time, sec

Δt	Time step, sec
T	Temperature, °C
ΔT	Temperature difference, °C
u	Axial velocity in cylindrical coordinate system
U	Cross-flow velocity, m/s
x_c	Critical distance, $(2F)^{3/2}$ Ra^{-1}

Greek symbols:

β	$\Delta\rho/(\rho_1+\rho_2)$
γ	Length scale for density gradient, $-\partial\rho/\rho_o\partial y$), m^{-1}
Γ	Coefficient of diffusivity transport of φ, kg/ms
δ	Withdrawal layer thickness
θ	Normalized temperature $(T-T_2)/(T_1-T_2)$
ν	Kinematic viscosity, μ/ρ, m^2/s
ρ	Density, kg/m^3
ρ_o	Reference density, kg/m^3
$\Delta\rho$	Density difference, kg/m^3
τ	Time scale, 1/N
λ	Drawdown fraction

Λ Percentage drawdown, 100λ

φ Dependent variable for transport equation

ψ Stream function, m^2/s

∞ Infinity

$\propto$ Proportional to

Subscript:

c Critical

1 Upper layer

2 Lower layer

o Incipient condition

m Mixed

CHAPTER - I

INTRODUCTION

1.1 STRATIFIED FLUID SYSTEMS

Stagnant water in most of the reservoirs are stably stratified throughout most or all of the year. This stratification is caused primarily by temperature variation with depth, and secondarily by a variable concentration of dissolved or suspended solid. Selective withdrawal from stratified fluid system, where flow in horizontal direction is restricted and thus enables the water to be withdrawn in horizontal layers, has become a popular engineering practice in a number of engineering fields. In the following subsections, only a few examples are mentioned to demonstrate the economic necessity of large scale control of stratified flows.

1.1.1 Layering of miscible fluids

The efficiency of thermal energy system can be improved by providing for heated and/or chilled water. Water in power station cooling ponds and water in solar ponds used for power generation, are two examples in which there exists a more clearly defined layering of the water body. Cooling ponds usually have a layer consisting of warm, recently used water, above a cool denser layer. In solar ponds, heat energy is stored by building a two-layered system of cold fresh water above warm saline water; this energy may be used for power generation, heating or other purposes. The lower layer traps the solar radiation and heats up, storing the energy. Again, in stratified fluid system hot and cold fluids may are separated without physical separation, thus reduces the capital cost of the system.

Lakes and artificial reservoirs have been proposed as large heat exchangers for nuclear power plants, thereby making it necessary to design intakes to withdraw the low level cool water and to distribute the inflow of warm water near the surface. The use of thermal stratification which exists in tropical seas, as a source of energy for thermal power plants, has drawn the attention of the researchers.

Pumped sampling systems are often used by marine biologists, for example, to determine phytoplankton concentrations in stratified oceans or lakes[Fasham, 1978], and the vertical of sampling is of fundamental interest. On a larger scale the production of mixed magmas from active volcanoes is also a problem in selective withdrawal from the stratified magma chamber[Blake & Ivey, 1985] . The reduction of reservoir sedimentation by removal at the dam of water containing large amount of suspended sediment has been suggested as a means of prolonging the useful life of major structures. In the area of density variations due to dissolved salts, the control of salinity intrusion by barriers and locks separating fresh water channels from an ocean or estuary may be mentioned.

1.1.2 Layering of immiscible fluids

A common feature of the applications described above is the fact that in all cases the fluids are miscible, essentially incompressible and similar in viscosity and the density differences are small. Additional applications in cases of immiscible fluids of different viscosities might arise in the separation of petroleum products and in other liquid-liquid separation processes.

Stable stratification occurs also in the atmosphere and is important in several flow problems of engineering interest. The following are a few examples: Cooling tower and chimney plume dispersion in the lower layer of the atmosphere, flame spread near the ceiling of room fires, dense gas dispersion from chemical plant or tanker accidents, etc. The advent of low cost atomic energy source should bring a degree of atmospheric pollution control and selective withdrawal makes the cooling system of nuclear power plant more economical and more feasible.

In many of these flow situations, the density variation combines with gravity to produce body force effects (buoyancy effects) which can crucially influence the fluid dynamic behavior. These buoyancy effects are similar in many of the applications given above.

1.2 NATURE OF DENSITY VARIATION IN TWO-LAYERED FLUID SYSTEMS

Water stored in reservoirs is usually stratified into layers of different temperature or salinity, and hence density, by the action of the weather on the surface and the inflowing rivers. This stratification has a rather irregular structure, although it typically consists of a reasonably well mixed surface of several meter thickness called the epilimnion, above a sharp density interface, the thermocline (or pycnocline), which in turn lies above a weakly stratified lower layer, the hypolimnion, reaching down to the bottom. This naturally occurring stratification is of stable type (lighter fluid overlying denser fluid) and is sometimes enhanced by inflow of warm water from some external sources. In such cases, it is usually permissible to treat the fluid as a simple two-layered system. The detailed nature of the stratification may vary widely depending on many physical factors such as cyclic variation of solar radiation, wind shear, tidal motion, quality and quantity of inflow and outflow of water etc. In laboratories, this wide range is simulated generally in terms of various types of profiles suited to different types of field situations (Fig. 1.1); for example:

a. linear stratification; density increases linearly with depth. This type of density profile simulates the nearly linear stable temperature gradient in deep water when the surface is heated mainly due to solar radiation (Imberger & Fischer, 1970; Ho, 1973; Rahman, 1978).

b. two-layered stratification; a homogeneous layer of lower density fluid lies atop another homogeneous layer of higher density fluid. Ideally, this type of profile simulates the layers of two immiscible fluids.

c. two-layered stratification; a homogeneous epilimnion, overlies a linearly stratified hypolimnion. Lawrence and Imberger [1979] claimed that the impounded water of some reservoirs may be represented by this type of profile with a sharp pycnocline or without any pycnocline between the two layers.

d. two-layered stratification; a mixed steep gradient interfacial region known as thermocline or pycnocline exists between the two homogeneous layers namely epilimnion and hypolimnion. This mode simulates the density variation occurring in shallow water bodies or the near surface zone of large water bodies (Islam, 1988). A two-layered fluid system of this type of density profile has been studied in this thesis.

1.3 EFFECT OF STRATIFICATION OF WATER ON THE ENVIRONMENT OF LARGE LAKES OR IMPOUNDED POOLS

Water of large lakes or reservoir are density stratified. Seasonal variation in solar radiation and surface wind conditions causes changes in the location and dimension of several layers of a density stratified fluid system. This has effect on the life of under water species. It has been reported (Sport Fishing U. S. A., 1971, Government Printing Press) that the population of some warm-water species declines drastically after the introduction of a dam, which causes the water to be stratified and begins to release cold water from the lower layers of the reservoir. Furthermore quality of water in the down stream of a hydroelectric power plant may undergo periodic variation and thus effect the aquatic life on the down stream of the concerned river.

1.4 SELECTIVE WITHDRAWAL

Selective withdrawal is one, where one can select the strata of fluid of a stratified fluid system at the sink level. It is a technique of water quality management which is extensively used in power plants. `Selective withdrawal' is a term associated with a specific (usually desirable) phenomenon in buoyant flows whereby fluid, withdrawn at the boundaries of a fluid body, flows predominantly from a spatially limited selective layer (or region) of a stratified environment (Islam, 1988).

Selective withdrawal has been used in cooling ponds where withdrawal of coolest possible water implies considerable fuel savings. Harlem [1958] studied the withdrawal from ponds normally consists of two relatively distinct layers. His study involved a canal leading from the cooling pond, withdrawal being from a slot under a skimmer wall. The skimmer wall was at sufficient depth that it occupied a significant portion of the lower cold layer depth. This type of control has been use in Australia, the United States, Sweden, and Japan, and it presents the designer with particular problem of predicting the temperature of the inflow water. Again in many parts of the world there is a need for alternating heating and cooling over the 24 hour night/day cycle, that is, there is a need for chilled water during the daytime and heated water at night. By storing the water that is chilled partially by heating the building at night and hot water in the same reservoir, the efficiency of the system can be improved to a large extent by using 'Selective Withdrawal'.

This phenomenon has been applied for better performance in condenser cooling water, where the design of intake has a great influence on the performance of water quality. A common practice for the condenser cooling system of thermal and nuclear power stations is to withdraw cold water from a neighboring large water body, pass it through the condensers and discharge it again into the same water body with a raised temperature. Power plants are therefore conveniently located near the coast or a large river. The discharged warm water forms a floating surface layer and may be transported by the tidal velocity into the vicinity of the cooling water intake (Fig. 1.2). A poorly designed intake system may then withdraw at least partially from the upper warm water layer, which then results in a higher than the desired temperature of the heat sink and thereby a reduction of power plant efficiency. Engineers are constantly trying to solve this problem by choosing the optimum design criteria for the intake system through proper understanding of the associated flow pattern. In recent years, single or multiple round intakes have been used to selectively withdraw the cold water for condenser cooling systems from a thermally stratified water body. Furthermore, the effect of a cap or hood over the intake hole is still under investigation (Islam, 1988).

1.5 CRITICAL DISCHARGE

A critical discharge, Q_c is defined such that for $Q \leq Q_c$ flow is restricted to the lower layer, and for $Q > Q_c$, flow is from both layers. The flow condition $Q < Q_c$ is termed as subcritical and the condition $Q > Q_c$ is termed as supercritical in the literature.

1.6 AIM OF THE STUDY

Selective withdrawal is very useful for water quality management in large reservoirs, lakes, cooling pools etc.. If one can know the mechanism of withdrawal, he can design efficient withdrawal system. For subcritical flow, the flow is restricted to the lower layer but for super critical flow water from both layers flows through the sink. Location of sink plays an important role in percentage drawdown from stratified fluid system. The present work is aimed at to investigate the drawdown history and the effect on drawdown of the location of sink.

1.7 SIMPLIFICATION OF THE PROBLEM UNDER CONSIDERATION

A cooling water intake from a shallow water body is in general a three-dimensional time dependent problem. Three-dimensionally is introduced firstly by the spatially varying background velocity field of the water body (e.g. the main stream velocity of a river or the coastal currents). The intake geometry may also induce local three-dimensional flow in its vicinity. The main river velocity or the near coast currents also vary with time and this variation makes the problem time dependent. Further time-dependency is associated with the changing cycle of ambient parameters on both daily and seasonal time-scales. Finally, as mentioned above, warm water discharge near the intake produces a buoyant floating layer over the cold layer of water. The depth of this layer and the associated stratification may be influenced by additional mixing caused by wind shear on the free surface and by heat loss to the atmosphere.

Although all the above complexities certainly influence the real life problem, in this study it is considered appropriate to examine initially the more fundamental case of the near-field flow pattern in the withdrawal through a single intake from a stable two-layered system. Phenomena excluded from the current work are time-dependent ambient effects, all three-dimensional effects and all free surface effects such as wind shear and heat loss. In spite of all these neglected factors, the problem which remains is sufficient to represent the real case to provide an understanding about the phenomena which occur at the full scale.

1.8 OUTLINE OF THE THESIS

The objective of this work is to find the effect of sink location on percentage drawdown. This thesis is divided into five chapters. Chapter - I of this thesis consists of aim of the current work and several examples of selective withdrawal. A comprehensive literature review is provided in Chapter - II. In Chapter - III a brief description of the experimental setup and procedure is described. Chapter - IV is the most important chapter of this thesis, in this chapter experimental results are summarized and all the findings are noted. The findings of the current experimental work and the guideline for future modification is noted in Chapter -V. Uncertainty analysis and thermometry are described in the appendices.

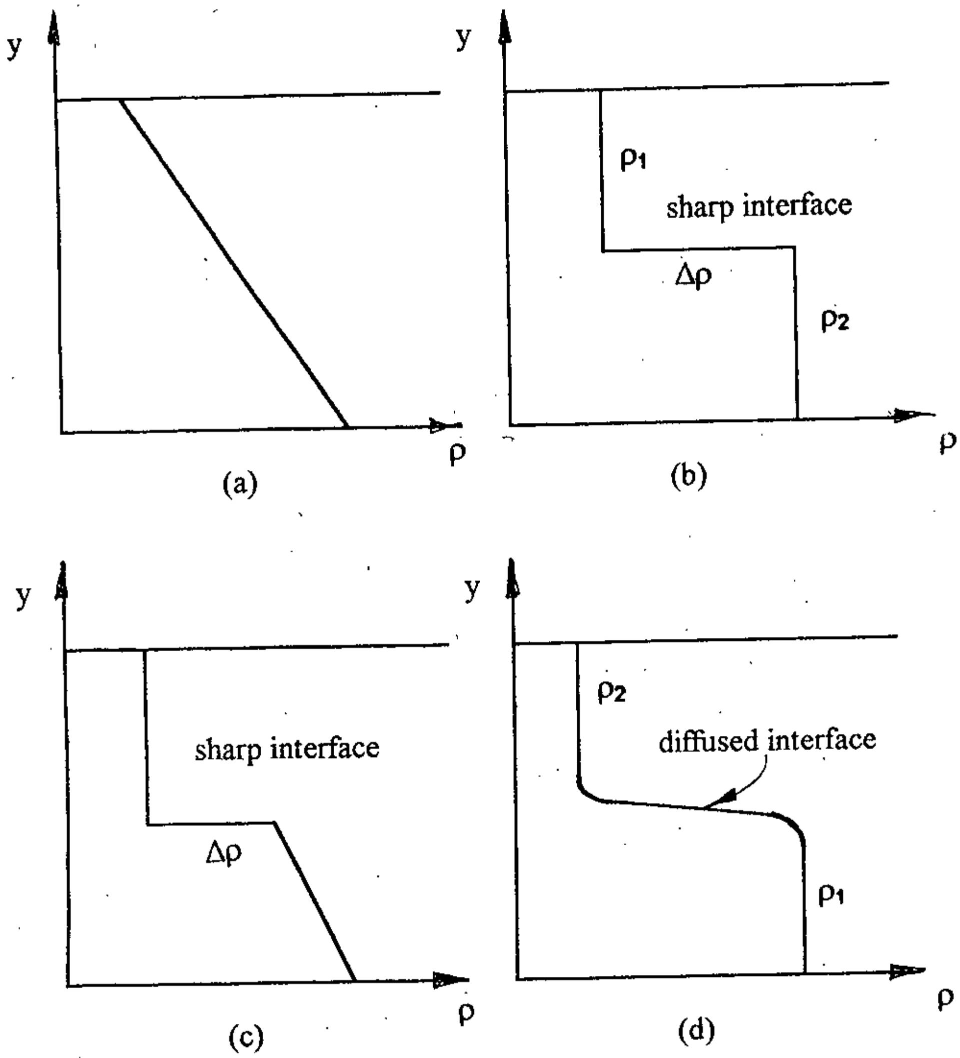

Fig. 1.1 Typical stratification (a) linear , (b) two homogeneous layers with a sharp interface, (c) upper layer homogeneous & lower layer linearly stratified with a sharp interface, and (d) two homogeneous layers with a diffused interface

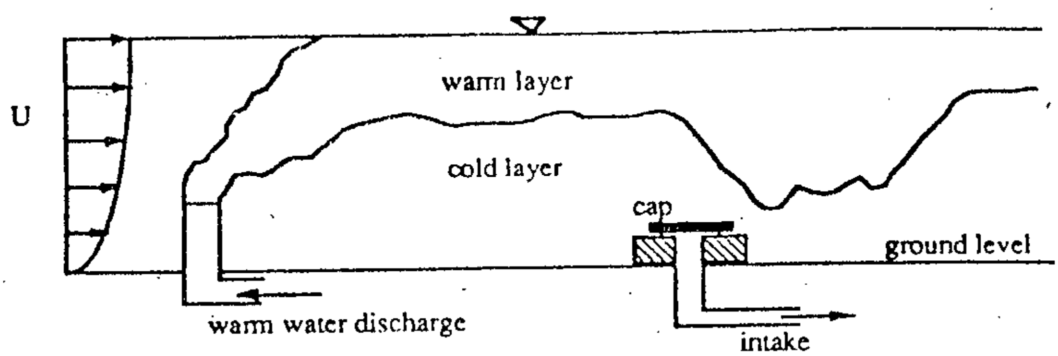

Fig. 1.2 A typical cooling water intake in cross flowing stream.

CHAPTER - II

LITERATURE REVIEW

2.1 INTRODUCTION

'Selective Withdrawal' from stratified fluid system has been discussed in many journals since 1950. Islam [1988] and Imberger [1980] have provided a comprehensive review on this topic. Recently Razzaque[1994] investigated vertical axisymmetric selective withdrawal phenomena from a two layered stably stratified ambiance due to temperature variation. He [Razzaque] investigated affects of intake and intake Froude number on drawdown. The following subsections contain a review of previous work on selective withdrawal from a stably stratified environment.

2.1.1 Name of a few parameters governing the flow of interest

Imberger and Fischer [1970] have described a detailed parametric analysis of selective withdrawal problem from stably stratified media (Islam, 1988). If in a stratified flow field, ρ_o is the mean density over depth and $\rho_a(y)$ is the density above ρ_o at rest, then a length scale for the ambient density gradient is related to,

$$\gamma = -\frac{1}{\rho_o}\frac{\partial \rho_a}{\partial y} \tag{2.1}$$

The variable density introduces a body force which can cause a principal modification of flow. For example, in a stagnant environment, if a fluid element of volume δv is displaced vertically by an amount δy, then it experiences a body force equivalent to $-\rho_o \gamma g \delta y \delta v$ in the direction of its original level. This body force or buoyancy force plays an important role in the vertical momentum balance in a flow field and tends to inhibit vertical motion. For higher γ (i.e. when the stratification is strong) this buoyancy force dominates over the other prevailing forces and the flow becomes horizontally layered.

In an unsteady flow driven or influenced by the above buoyancy force, a time scale is fixed by the natural period of oscillation of an elementary particle in the gravitational field and is given by,

$$\tau = \frac{1}{N} \tag{2.2}$$

where, $N = (\gamma g)^{1/2}$ is the natural frequency of oscillation and is known as the "buoyancy frequency" or "Brunt-Vaisalla" frequency.

The sudden initiation of withdrawal from a stratified environment through a sink induces a pressure gradient which is counteracted in the vertical direction by the buoyancy forces. As the buoyancy forces inhibit vertical motion, the flow becomes concentrated within a narrow withdrawal layer. As the fluid moves towards the sink, a balance must be set up between pressure, buoyancy, inertia and viscous forces. For an inviscid buoyancy layer, the scaling parameter characterizing the flow is the ratio of inertia to buoyancy forces and can be written as:

$$\frac{\text{inertia}}{\text{buoyancy}} - - \frac{\text{forces}}{\text{forces}} = \frac{U^2}{N^2 l^2} = F^2 \qquad (2.3)$$

where, l is a characteristic length scale for the motion and F is the densimetric Froude number in cross flow. Similarly, for creeping flow the scaling parameter is the ratio of viscous to buoyancy forces and is given by,

$$\frac{\text{viscous}}{\text{buoyancy}} - - \frac{\text{forces}}{\text{forces}} = \frac{\nu U}{N^2 l^3} = \frac{F^2}{R_e} \qquad (2.4)$$

where, $R_e = Ul/\nu$ is the Reynolds number of the flow (ratio of inertia to viscous forces). For a diffusive fluid, Peclet number, Pe, measures the relative strength of convective to diffusive transport of the species and is given by,

$$\frac{\text{convective}}{\text{diffusive}} - - \frac{\text{transport}}{\text{transport}} = \frac{Ul}{D} = P_e \qquad (2.5)$$

Although these three independent parameters(F, R_e and P_e) are in principle required in the study of withdrawal from a stratified environment, other combinations are possible and sometimes found in the literature, e.g.:

Schmidt number, $Sc = \nu/D = Pe/R_e$

Rayleigh number, $Ra = (R_e.P_e)^{-1/2}.F$

2.2 WITHDRAWAL THROUGH TWO DIMENSIONAL LINE SINKS

Most of the axisymmetic withdrawal phenomenon may be simplified into 2-D plane flow. If it is assumed that the reservoir depth is sufficiently great i.e. densimetric Froude number is very very small ($F<<1$) so that at large distances from the sink the flow will be very slow its development into a layered structure will not be influenced by inertia forces. In such cases the fluid will undergo three distinct flow transitions as it moves towards the sink. Very far upstream the flow is laminar. This slow flow then becomes layered by the action of buoyancy. As this layer approaches the sink it becomes thinner, and at some critical distance from the sink inertia forces become comparable to the buoyancy forces. The subsequent flow in the layer will be governed by the balance of inertia, buoyancy and viscous forces.

2.2.1 Linear stratification

Weak motion of a density-stratified fluid in a gravitational field often exhibit large departures from the motion of homogeneous fluids. Physically, in a stably stratified fluid work must be done to displace any fluid particle vertically since there is a force due to the gravity field always tending to oppose the displacement. Vertical motions are therefore inhibited in favour of horizontal motion. Stratified flows are common in the oceans and in the atmosphere.

The problem of linearly stratified flow towards a sink was first investigated by Yih [1958]. He investigated this problem analytically with linearly stratified fluid flowing towards a line sink placed at the bottom right hand corner of a channel (Fig. 2.1); a solution for the normalized stream function was obtained which demonstrated the way in which buoyancy modifies the flow. Froude number was defined as $F = \frac{U}{NH}$ where, U is the cross flow velocity, H is the channel depth and N is the buoyancy frequency. At $F = 1/\pi$, it was predicted that the eddy (recirculating zone) extended to infinity and this was interpreted as the onset of a selective withdrawal layer. The infinite size of the eddy violated the upstream boundary conditions used by Yih, and the mathematical approach adopted was incapable of providing solutions for less than the critical value ($F_c = 1/\pi$). Yih assumed the velocity and density to be undisturbed far upstream, so that no solution was obtained for $F < \pi^{-1}$. An exactly analogous experimental investigation was conducted by Debler [1959], using a long finite sized channel. He[Debler] showed by experiment that $F \sim \pi^{-1}$ is indeed a critical Froude number, above which Yih's solution is valid, and below which the flow separates into a flowing region near the level of the sink, the fluid remaining essentially stagnant elsewhere (i.e. selective withdrawal occurs). The experimental results indicated the critical Froude number, $F_c = 0.28$. The Reynolds number, $Re = UH/\nu$ in this case was sufficiently high [$O(10^4)$] and the Peclet number, $Pe = UH/D$ was of the order 10^7, so that the results might be considered to be a first approximation for the inviscid and non-diffusive case.

For flows with $F < 1/\pi$, Kao [1965, 1970] proposed an inverse trial-and-error method of solution for this problem using a fictitious distributed sink on the vertical wall(Fig. 2.2). The flow field would then possess a dividing streamline above which the fluid leaves by way of the distributed sink and below which the fluid comes out of the bottom sink. By requiring that the pressure variation on this dividing streamline be equivalent to the hydrostatic pressure (assuming dP/dx=0) due to the fluid above it, the flow above the dividing streamline may be replaced by stagnant fluid with a vortex sheet at the dividing streamline. That is the velocity above it remained constant and this fluid is therefore discharged through the fictitious sinks; the fluid below the dividing streamline was discharged through the physical line sink. In this way the sum of the individual Froude numbers of the fictitious sink and the physical sink was greater than $1/\pi$ and Yih's solution could be applied to the entire channel. This analysis led to a unique Froude number based on the depth of the flowing layer, Fr_δ (=$U/N\delta$) = 0.33 for all withdrawal rates below F_c whereas the experimental results of Debler [1959] indicated Fr_δ = 0.2 to 0.28 when the ratio of the flowing layer to the total depth (δ/H) varied from 0.3 to 1.0.

2.2.2 Effect of viscosity and diffusivity

The effect of viscosity and diffusivity in stratified fluid flow towards a line sink were studied by Koh [1966a], Imberger and Fischer [1970], Imberger [1972] and Pao and Kao [1974]. For fluid with Schmidt numbers, Sc, of order unity, the withdrawal layer is composed of distinct regions, in each of which a definite force balance prevails (Imberger and Fischer, 1970). If the channel depth is sufficiently large, then at very far upstream the flow will be slow and parallel (Fig. 2.3). This slow parallel flow then becomes layered by the action of buoyancy in the outer region where both viscous and buoyancy forces are significant. As the flow approaches the sink, the withdrawal layer becomes thinner and at some critical distance $x_c = (2F_r)^{3/2}$ H/Ra (Imberger and Fischer, 1970) [$F_r = q_o/2NH$, $Ra = (\nu D)^{1/2}/NH^2$] from the sink, inertia forces become comparable to the viscous and buoyancy forces (the inner region). Very close to the sink [$(x/x_c)^{1/3} < 0.05$; Pao and Kao, 1974], sink inertia becomes dominating and the flow becomes inviscid and buoyant.

Koh [1966a] investigated this problem with a diffusive linearly stratified fluid for an infinite medium. He obtained a solution neglecting the non-linear inertia terms, which predicted a self similar velocity profile with a peak at the level of the sink and a velocity which decays rapidly in an oscillatory manner above and below the x-axis (symmetry axis in Fig. 2.3). In addition, the thickness of the withdrawal layer, δ (Fig. 2.3) increased at a rate of $x^{1/3}$ where x is the distance from the sink and δ/H was proportional to $Ra^{1/3}$. Imberger and Fischer [1970] and Imberger [1972] analyzed the same problem as Koh did but with a finite depth. Using the results from Koh's method for the outer region (Fig. 2.3) as the upstream boundary condition, they obtained an integral solution for the inner region incorporating the inertia terms. This prediction also indicated a self similar velocity profile and withdrawal layer growth of order $x^{1/3}$ but added a viscous layer to the inviscid result obtained analytically by Kao [1970] ($\delta = 0.33N/U$) and experimentally by Debler [1959] [$\delta = (0.24 \pm 0.04)$ N/U] (in Debler's experiment, x_c was of the order 10^5m, confirming that all measurements belong to the inviscid core).

Koh [1966a] and Imberger [1972] also reported experimental data to support their analytical solutions. These experimental studies were carried out with very low Reynolds and Froude numbers [$Re = O(10)$ and $F_r = O(10^{-4})$]. The value of x_c was varied from 2cm to 2m in Imberger's experiments whereas his flume length was 13m. Koh's experimental flume was much shorter (50cm effective length), but x_c varied from 0.7cm to 4m. In both studies, the measurement locations belong to the inner and outer regions. The data for velocity profiles in both experiments showed a self similar shape in both inner and outer regions, validating the analytical solutions. However, in Imberger's experiments, the reverse flow above and below the withdrawal layer increased with $(x/x_c)^{1/3}$, while his analytical solution predicted only the forward flow within the withdrawal layer. The measured growth of the thickness of the withdrawal layer, δ with x was predicted better by Imberger than Koh, since the first method considered the inertial effects in the flowing layer.

In his paper, Koh [1966a] also presented photographs showing the flow development at the level of the sink with time (measured from the moment withdrawal was begun) and these clearly indicated the presence of propagating waves. In the course of his experiments, Debler [1959] also observed some wave motions in the flow field. All these observations indicate some transitional behavior towards the steady state. Koh [1966b] reported some calculations (for the unsteady flow) for an linearised initial value problem appropriate to a sink in an infinite medium with linear stratification. His solution predicted an increase in the horizontal velocity towards the sink with time, but this increase was felt instantaneously at all distances away from the sink by an amount inversely proportional to the radial distance from the sink, which is physically unrealistic (Pao and Kao, 1974). The detailed transient behavior of this problem was first analyzed by Pao and Kao [1974] who again studied the linearised initial value problem. The sudden sink opening disturbs the fluid particles very close to the sink which due to the presence of the linear density stratification, start to oscillate at the natural frequency N. But the buoyancy force wants to restore the particles to their original positions and the oscillation and restoring process gives birth to harmonics which eventually produce an infinite number of internal waves with progressively decreasing vertical wave length. These waves propagate upstream with a speed of $C_n = NH/n\pi$, where the mode number $n = 1,2,3....\infty$ and are continuously attenuated by the viscous/diffusive action. The waves propagate against the induced upstream velocity, $U = q/2H$ (H = half depth of fluid). If the propagation speed C_n is greater than the upstream velocity, U, then the flow field is modified by the internal waves and selective withdrawal prevails (Fig. 2.4). At (or above) a critical Froude number ($F_{rc} = 1/\pi$), the fastest wave speed is the same as (or less than) the induced upstream velocity, U, thus no waves can propagate upstream and hence no selective withdrawal occurs. Below the critical Froude number ($F_{rc} < 1/\pi$), n modes can propagate when $C_n > U$.

Pao and Kao [1974] also presented a numerical solution of the unsteady, two-dimensional non-linear partial differential equations governing the flow. Kao, Pao and Wei [1974] obtained experimental data which give excellent support to their numerical results in terms of existence and speed of propagation of internal waves for a wide range of Reynolds and Froude number ($Re = 627 - 3380$ and $F_r = 0.0143 - 0.106$). Their experimental data belong to the inviscid core and to the inner region [$x_c \approx O(10^3 m)$]. In the numerical calculations, the experimental setup was not simulated exactly, instead a constant depth and infinite length channel was used with slip conditions at all solid boundaries to avoid viscous action on the wall. The full Navier-Stokes equations were transformed into a stream function/vorticity formulation which was discretised and solved numerically using an explicit time marching method, upwind differencing for convection terms and central differencing for all other terms. By a suitable coordinate transformation ($x' = 1-e^{-ax}$) the infinite length was reduced to a computational domain of unit length in which the upstream boundary condition was specified from potential flow equations and remained the same at all times. Numerical calculations were presented for various Reynolds and Schmidt numbers to account for the effect of viscosity and diffusivity on the flow development. Pao and Kao [1974] concluded that the establishment of flow and density fields was essentially inviscid and non-diffusive for the range $F_r > 0.07$ and $Re > 10^4$ when $Sc > 1$. The steady state velocity profiles from the numerical and experimental studies were also compared with the analytical solutions of Koh [1966a] and Imberger [1972]. Koh's self similar velocity profile agrees quite well with the results and is better than Imberger's. Computed and measured steady state withdrawal layer thicknesses were also compared with Koh's and Imberger's solution. For this parameter, Imberger's solution indicated a better agreement with the experiments than Koh's.

2.2.3 End wall effect

In any experimental study, there exists an end wall which blocks the horizontal velocity far upstream; this can affect the whole flow field at later times if the internal waves are reflected from the end wall, before being attenuated by viscous action. Silvester [1980] provided an experimental study on the evolution, propagation and reflection of the internal waves in a linearly stratified fluid and its effect on the flow field. From the observation of his experimental results, Silvester concluded that each mode can travel a distance proportional to n^{-3} before attenuation. For a long channel, symmetric velocity profiles were observed, even at the time of first mode reflection. For a shorter tank, however, for times when several modes has been reflected from both walls, a marked asymmetry in the velocity field was produced.

2.2.4 Initial Motion

Pao & Kao [1974] have studied the dynamics of initial motion of the withdrawal of fluid from stratified container through a line sink. Immediately after the sink is turned on a nearly horizontal potential flow is created. This flow is then progressively modified by discrete spectrum of planar shear waves that travel out from the sink against the induced uniform upstream velocity. As McEwan & Baines [1974] found, each shear front travels with a speed

c_n = NH/nπ, where n is the modal number and H the depth, and has a frontal width w_n = $H(NT)^{1/2}/n$, where T is the time. The modification of the potential flow by these shear waves dominates the initial dynamics of flow.

2.2.5 Inflow

G. N. Ivey and S. Blake [1985] studied effect of inflow into a continuously stratified environment. While analysing the axisymmetric inflow of a homogeneous fluid into a stratified container, attention is here on the case of neutrally buoyant inflow at constant discharge Q with low momentum such that there are no entrance mixing effects. They obtained a transition parameter denoted as 'S ', where $S = \left(\frac{Q^2 N}{\nu^3}\right)^{\frac{1}{15}}$. If S is very large, viscosity is unimportant and thickness of the inflow $\delta \sim (Q/N)^{1/3}$ and spreading law;

$$l_r \sim \left(\frac{Q^3 N}{(\nu D)^{1/2}}\right)^{1/7} t^{3/7} \tag{2.6}$$

where, l_r is the radial extent of the spreading intrusion, D is the diffusivity of fluid, t is time. Again, when S is small then viscous forces are important throughout the flow field, the initial intrusion thickness $\delta \sim (\nu Q/N^2)^{1/5}$ and the spreading law

$$l_r \sim \left(\frac{Q^4 N^2}{\nu}\right)^{1/10} t^{1/2} \tag{2.7}$$

Chen [1980] used similarity technique to evaluate the constants of equation (2.7). Zatsepin & Shapiro (1982) conducted a number of laboratory experiments in the same flow regime and found good agreement with the predicted spreading law.

2.2.6 Computational verification

Islam [1988] did the computational study of the experimental works of Debler [1959], Kao, Pao and Wei [1974] and Silvester [1980]. The experimental set up for these three cases considered differ only in that in Debler's experimental studies, the sink for withdrawal was at the bottom corner of the tank while in other cases, it was at mid-depth. In all cases, salt was used as the stratifying agent and a linear vertical profile of concentration was ensured throughout the tank before the initiation of flow. Photographic techniques were employed for quantitative measurements.

To obtain the numerical predictions of these experimental studies, calculation domains were simulated using exactly the same physical dimensions as in the experiments. Calculation proceeded from time t = 0 when the sink was opened. A uniform velocity profile was assumed at the sink and as a consequence of these approximations the free surface dropped at a uniform velocity as discharge continued. To adjust the calculation domain to always match the physical domain size the governing equations were transformed into a moving boundary Eulerian co-ordinate frame. A linear stratification at a gradient fixed by the experimental condition was assumed in the stagnant water prior to the start of calculation. Zero gradient conditions were applied at the free surface which was otherwise treated as a "rigid lid" in the usual way. No-slip conditions were used along all solid surfaces for velocities and zero gradients for the concentration field.

The main experimental outcome of the Debler's study was the determination of the withdrawal layer thickness as a function of Froude number; flow visualization was used to determine this thickness by observing the motion of lines of dyed fluid introduced into the tank during the establishment of the initial linear density gradient. Fifteen layers (each approximately 40 mm thick) were used with alternate layers dyed. As time progressed after the start of withdrawal, a number of layers would bend down from their originally horizontal locations towards the sink exit, on the other hand, those layers in the stagnant upper layer would remain essentially horizontal; the existence of a dividing streamline (below the critical Froude number) could therefore be noted and quantified.

This experimental technique was simulated computationally by tracking the location of a number of neutrally buoyant particles placed along originally horizontal and vertical lines within the calculation domain. As the calculation proceeded, the particles were moved to new positions as demanded by the predicted flow field and at any instant the lines obtained by joining the new particles positions represented the time lines for that instant. The withdrawal depth was then evaluated from the computation as the height of the last time-line (above the tank bottom) which curved monotonically towards the sink exit.

Ten experimental cases were considered covering a Reynolds number range from 70 to 42,200. One run provided data for the additional effects in the flow field due to waves reflected from an end wall and finally another test considered the special case of a two-layered system.

The existence of internal wave motions in the fluid could be clearly seen from the predicted time-line patterns, leading to a quite complex flow structure in the vicinity of the sink at the later times. The predicted withdrawal layer depth over the whole Froude number (instantaneous) range of Debler's experiment was compared with the experimental results. Excellent agreement was found at lower Froude number but there was some deviations at higher values of Froude numbers. The measurements indicated a critical value of Froude number, F_C of 0.289, whereas the numerical predictions implied 0.33 in agreement with the inviscid theory of Yih [1958].

Streamline patterns for finite and semi infinite tank for an initial Froude number, $F_O = 0.112$ at different time lines were predicted and the propagation of internal waves in the form of a corner eddy was found to be very much similar in both the cases. History of propagation of wave modes and the reflection of internal waves were investigated in details. Velocity and concentration profiles obtained by prediction were compared with experimental results and a good agreement was found.

2.2.7 Two-layered stratification

For the case of two-layered stratification, Froude number is still the primary governing parameter which characterizes the flow. Craya [1949] (Brooks and Koh, 1969, Islam, 1988) investigated this problem for an inviscid and non-diffusive fluid unbounded in the vertical direction with the sink placed in the vertical wall at a certain height, h away from the interface between the two fluids [Fig. 2.5(a)]. He found the critical Froude number above which both layers flow to be:

$$F_{r_c} = \frac{q_o}{\sqrt{g'h^3}} = 1.52 \qquad (2.8)$$

Huber [1960] studied this problem but with slightly different geometry [Fig. 2.5(b)] and obtained the value of the critical Froude number to be:

$$F_{rc} = \frac{q_o}{\sqrt{g'h^3}} = 1.66 \qquad (2.9)$$

The differences in the values of the critical Froude numbers for these two configurations are presumably due to the different boundary conditions. Kao [1976] analyzed this problem with two homogeneous fluid with the aid of wave theory. The disturbance experienced at the interface by the intake flow is also influenced by the boundary conditions and thus provides different results. He extended his analysis to the thermocline type of stratification with the line sink located at the middle of the thermocline. The critical Froude number, he obtained for this case is:

$$F_{i_c} = \frac{q_o}{\sqrt{g'\beta b}} = \frac{1}{\sqrt{2}} \quad (2.10)$$

where $\beta = \Delta\rho/(\rho_1 + \rho_2)$, b is the half thickness of the thermocline .

2.2.8 Interface shape: Analytical and experimental work

The shape of interface during drawdown plays important role in water quality management. The interface shape during the flow of two-layered fluid system into a line sink was studied by Ingber and Munson [1986] both analytically and experimentally. They identified that three essential distinct, steady state flow topologies exists (Fig: 2.6). In the first flow toplogy, a stagnation point exists in the interface directly above (below) the sink. In this case, the layer with the sink is flowing, while the other is essentially stagnant outside a thin shear layer. In the second flow topology, the interface between the two fluids cusps down toward the sink but does not enter into it. Again, one layer flows, while the other is essentially stagnant. In the third flow topology, the interface is drawn down into the sink. In this case both layers are flowing.

The range of Froude number over which each flow topology exists was determined experimentally. Experimental results where viscous effects were taken into account, are shown in Fig. 2.7. Froude number was defined as $Fi = [q^2/2g'h^3]^{1/2}$. For flows with $Fi \le 0.36$, the stagnation point interface was obtained. The horizontal extent of the deflected surface was approximately one and a half times the depth of the lower fluid independent of the Froude number. For flows with $Fi \ge 0.38$, the interface was drawn down into the sink. With considerable care it was possible to adjust the flow rate to produce the interfacial position shown in Fig. 2.7 with Froude number, $Fi = 0.37$. This condition is essentially like the cusp down flow where the interface cusps down toward the sink but does not enter into it. The region above the sink ($0 < x/h_c < 0.4$; dashed portion of the curve) was observed to be quite unsteady with apparently considerable viscous and surface tension effects. However, a slight change in flow rate changed this type of flow into either a drawdown or a stagnation point flow.

For the problem of withdrawing water through a line sink from a region containing two distinct homogeneous layers of different densities separated by a very sharp interface, Tuck and Vanden-Broeck [1984] showed that only two types of solution are possible beneath the critical Froude number, i.e. when only a single layer is flowing out through the sink. The first solution type involves a stagnation point on the interface directly above the sink. Peregrine [1972], Vanden-Broeck, Schwartz and Tuck [1978] and Tuck and Vanden-Broeck [1984], all computed solutions of this type for the case of a line sink but had limited success as the Froude number $F_r = (q^2/g'h^3)^{1/2}$, was increased (Here, h is the depth of lower layer). Hocking and Forbes [1991] computed solution with a stagnation point for the case of a layer of infinite depth for values of Froude number, $F_r = (q^2/g'h^3)^{1/2}$, upto 1.4 where h is the depth of the sink beneath the level of the interface.

The second solution type characterizes the critical Froude number above which water in the layer above the interface begins to be drawn out through the sink. In this flow, a downward cusp forms in the interface directly above the sink, as the interface is drawn down to enter the sink vertically.

There was a gap between the works of Hocking and Forbes [1991] and Tuck and Vanden-Broeck [1984] in the range $1.4 < F_r < 3.54$ in case of infinite depth. Hocking [1991] derived and solved an integral equation for this case which verified all the results of Vanden-Broeck and Keller [1987] and extended to the branch of solution in which the interface contained a hump above the sink as the sink depth approached zero, even upto the region where the sink rises above the level of the interface in the far field. He attempted but failed to compute solutions with a cusp for values of Froude number less than unity.

2.2.9 Effect of sink location

When water is withdrawn from a fluid consisting of two or more homogeneous layers of different density separated by an interface, the withdrawn water will come from the layer adjacent to the point of removal untilsome threshold in flow rate is reached, after which the other two layers will begin to flow out through the sink. This threshold can be described most easily in terms of a dimensionless parameter the Froude number $F = (q^2/g'h_b^3)^{1/2}$, where h_b is the depth of the lower layer of fluid. Hocking [1991] studied effect of the location of on the rate of withdrawal from both layer. He found that the interface between two layers rises up and then enters the sink vertically from above even when the sink is located above the undisturbed level of the interface. He redefined Froude number as $F = (q^2/g'h_s^3)^{1/2}$, where h_s is the depth of the sink beneath the level of the interface. He developed a mathematical model and solved the problem numerically. In his solution he found that the interface contained a hump above the sink as the sink depth approaches zero. His numerical method was capable of producing solution in the region where the sink rises above the interface level in the far field (Fig: 2.8).

2.2.10 Drawdown history

Hocking [1991], in a technical note presented the results of a series of experiments in which the critical value of densimetric Froude number was obtained for the case of a line sink in the bottom corner of a rectangular tank containing two layers of fluid of different densities over a range of different interface thickness. The experiments were performed in a double-glazed glass tank, 5.5m long, 0.5m wide and 0.6m deep. A two-electrode conductivity probe was used to continuously monitor the density of the out flowing water. A four electrode conductivity probe mounted on a step motor traversing gear mechanism was used to determine the density profile and the interface thickness 'l', defined as the distance between 10% and 90% of the density difference between the layers. Sodium Chloride solution beneath a layer of fresh water was used and $\Delta\rho/\rho$ was of the order of 0.001. Interface thickness was measured before the initiation of the sink flow. The time of the drawdown was computed from the plot of conductivity against time measured behind the sink (Fig. 2.9). The moment at which drawdown occurred was identified by a drop in conductivity indicating the initiation of the flow from the fresh water layer.

A best fit curve was drawn through the data, the equation of which is given by, $\log F = -0.71 - 0.51 \log F_l^{-1}$; where, $F = [q^2/g'h^3]^{1/2}$ (Froude number based on the lower layer depth) and $F_l = [q^2/g'l^3]^{1/2}$ (Froude number based on interface thickness). Given relationship indicates that $F \propto F_l^{1/2}$ which is in contrast with the linear relationship obtained by Jirka and Katavola [1979] for a point sink. A lower bound for the critical value of Froude number F was determined approximately to be 0.46, which is close to the theoretical value of $F_c = (2/3)^{3/2} = 0.54$ given by Jirka and Katavola [1979]. The finding that it is a lower bound suggests that the actual critical value of Froude number with an infinitesimal interface may be larger.

2.3 AXISYMMETRIC WITHDRAWAL THROUGH POINT SINKS

Works on vertical withdrawal through a round hole (point sink) are described in this subsection. Vertical withdrawal is the situation most similar to the cooling water intake problem. Davidian and Glover [1956], Harleman, Morgan and Purple [1959], Hino and Onishi [1969], Ho [1973], Lawrence and Imberger [1979], Goldring [1981], Onishi et. al. [1982], Ivey and Blake [1985], Islam [1988] and Zhou and Graebel [1990] and Razzaque [1991] have studied the vertical axisymmetric withdrawal. These works include both two-layered fluid system and continuous linear stratification.

2.3.1 Linear stratification

Ho [1973] provided analytical and experimental data for axisymmetric withdrawal from a linearly stratified fluid. His work yielded a self similar velocity profile and a withdrawal layer thickness growth at a rate of $r^{1/3}$, where r is the radial distance from the sink.
Lawrence and Imberger [1979] and Lawrence [1980] have demonstrated that for the case of axisymmetric withdrawal the flow field is modified and the withdrawal layer is established by the passage of internal waves in an exactly analogous manner to the 2-D line sink flow. However, in this case the waves are cylindrical with amplitude inversely proportional to the radius.

As in withdrawal through a line sink, Rayleigh number, Ra describes the relative importance between viscous, inertia and buoyancy forces in the flow field. For a linear stratification and for $F.Ra^{-2/3} > 1$ (F and Ra based on L, the distance between the sink and the upstream wall) the flow in most of the tank is governed by inertia and buoyancy forces and the withdrawal layer thickness, δ is of order $(Q_o/N)^{1/3}$. Lawrence and Imberger [1979] suggested $\delta = 0.66 (Q_o/N)^{1/3}$, Imberger [1980] quoted $\delta = 0.71 (Q_o/N)^{1/3}$ from the works of Bohan and Grace [1973]; finally Ivey and Blake [1985] reported $\delta = 0.71 (Q_o/N)^{1/3}$. For $F.Ra^{-2/3} < 1$, when most of the tank is governed by viscous and buoyancy forces, Ivey and Blake [1985] suggested that the withdrawal layer thickness, δ should be of the order of $(\nu Q_o/N^2)^{1/5}$ and quoted $\delta = 2.1 (\nu Q_o/N^2)^{1/5}$ from their experimental observations.

2.3.2 Effect of location of sink

Hino and Onishi [1969] studied this problem analytically for the performance of the location of the point sink in a linearly stratified fluid (Fig : 2.10) and defined densimetric Froude number as

$G = \dfrac{Q}{2\pi\sqrt{g\beta d^3}}$, where $\beta = \dfrac{\rho_0 - \rho_1}{\rho_0 d}$ and ρ_0 and ρ_1 are the densities at the bottom and top of the pool, respectively. They developed a mathematical model and predicted that the critical value of G_{cr} varies according to the location of the sink. To study the range of the value of G under which selective withdrawal of the stratified fluid is possible, they considered the point sink is located near by the mid depth of water. There may exist three different conditions of flow for different ranges of G.

(i) If the rate of inflow is large enough or the stratification is slight enough, the whole portion of the sink flows into the sink.

(ii) When the rate of inflow is so small and/or the stratification is so strong that the value of G is less than G_{cr}, The theoretical solution shows that the stagnation zone begins to appear in the region of fluid above the sink in the case of b < 0.5 (below the sink in the case of b > 0.5). According to the inviscid fluid flow theory, the region of stagnant layer grows in the upper portion of fluid when the sink is located below the mid depth of water (in the lower portion of fluid for the sink located above the mid depth of water). When the stagnant layer exists in the fluid, the depth of flowing portion d', can be obtained from the relation $G' = \frac{Q}{2\pi\sqrt{g\beta d'^3}}$.

where G' is equal to G_{cr}

(iii) With further decrease in the value of G, the stagnant layer increase more and more in the depth, and a second critical condition at which the value b' = bd/d' , (or 1-b'), becomes to be 0.5. Let denote the value of G at the second critical condition by a symbol of G_{cr}^* . Under the flow condition with the value of G less than G_{cr}^* the layers can exist in both the upper and lower portions of fluid. At the second critical condition, the value of G was calculated taking d'=2db for the case b <1/2 (or with d'=2(1-b)d for case b >1/2) is equal to the value of G_{cr} for b=.05. This relation is described by

$$G_{cr(atb=.05)} = \frac{Q}{2\pi\sqrt{g\beta\{2(1-b)d\}^3}} \quad \text{for} \quad b < 0.5 \tag{2.11}$$

$$= \frac{Q}{2\pi\sqrt{g\beta\{2bd\}^3}} \quad \text{for} \quad b > .05 \tag{2.12}$$

The numerical solution that they have got is shown in Fig: 2.11, it shows the relation between G_{cr} and the location of sink. When a point fixed by G and b drops in the area numbered as 1 in Fig: 2.11, the stagnation layer exists in the upper portion of fluid and it is possible to withdrawan only from the lower portion of the stratified fluid. When the point said above is in the area2, the withdrawal of water only in the upper layer of stratified fluid is possible. If the value of G and the point sink location is selected so that the above mentioned point falls in the area 3, then only the water in the mid layer of fluid can be taken in, leaving both upper and lower stagnant layers.

2.3.3 Effect of rotation on selective withdrawal

Monismith, McDonal, and J. Imberger [1993] studied the axisymmetric flow of a rotating linearly stratified fluid into a point sink. Linear analysis of the initial value problem of flow of a linearly stratified fluid into a point sink that is suddenly switched on shows that a spatially variable selective withdrawal layer is established through the outward propagation of inertial shear wave. The amplitude of this shear waves decays with distance from the sink. The flow reaches an asymptotic state, dependent on viscosity and species diffusion, in which the withdrawal layer structure only exists for distances less than the Rossby radius $R = Nh/f$, based on the wave speed of the lowest mode, where N is the buoyancy frequency, f is the Coriolis parameter and h is half depth of fluid (here $N > f$). Since there is no azimuthal pressure gradient to balance the Coriolis force associated with the radial, sinkward flow, a strong swirling flow develops. This swirl causes the withdrawal layer thickness to grow like $(ft)^{1/3}$ (t=time), such that eventually there is no withdrawal layer anywhere in the flow domain.

Robertson & Ivey [1983] who considered the possibility of selective withdrawing 4°C bottom water from Lake Ontario for use as cooling water to air conditioning Toronto in summer. But the so-called 'FREECOOL' scheme would not work because rotational effects would greatly increase the vertical extent of the withdrawal layer. The authors considered the analysis of Whitehead [1980], to simplify the analysis the considered the deceptively simple case of finite-depth, infinite-horizontal-extent fluid domain. They start looking at the inviscid, linear initial value problem associated with impulsively initiating the sink flow. The resulting solution obtained by modal expansions and Laplace transforms, shows the establishment of a withdrawal layer by long inertial-internal waves, which can be dubbed 'inertial shear waves' by analogy with their non-rotating counterparts. The asymptotic solution form taken by the transient solution is not entirely expected in that it shows that the withdrawal layer vanishes at a distance of order Nh/f.

From their analysis they found that 'Rossby radii' is very important for selective withdrawal. In order to maintain any selectivity , the withdrawal structure must be placed within one or two Rossby radii of the lowest internal wave mode of the shore. In general, in order to have the ability to produce as narrow a layer as possible and so gain the maximum degree of control of the outflow, the structure should be positioned so as to prevent the development of swirl around the structure.

2.3.4 Two-layered stratification

Harleman, Morgan and Purple [1959] investigated experimentally a two-layered system for the configuration as shown in Fig. 2.12(a). The main objective of this study was to investigate the performance of different types (sharp edge and rounded edge) of intake pipes and the results yielded a unique critical Froude number irrespective of size and shape of intake pipe when the intake diameter, d varied from 0.3h to 1.5h. But for drawup case as shown in Fig. 2.12(b), Davidian and Glover [1956] reported a critical Froude number which is dependent on the size of the intake pipe when the intake pipe diameter varied from 0.3h to 14h. These two experimental studies revealed that the size of the intake pipe will not affect the critical condition so long as the pipe diameter is small compared to the characteristic length, h.

For two-layered stratification, Ivey and Blake [1985] reported a drawdown height, (i.e. the height at which upper layer fluid is withdrawn) (Fig. 2.12) for the inertial regime ($F.Ra^{-2/3} > 1$) as $h = c_1(Q_o^2/g')^{1/5}$ and for the viscous regime ($F.Ra^{-2/3} < 1$) as $h = c_2(\_Q_o/g')^{1/4}$. The analytical solution of Craya [1949] suggested $c_1 = 0.69$, Harleman, Morgan and Purple [1959] gave $c_1 \doteq 0.826$ from their experimental results and Goldring [1981] reported $c_1 = 0.64$ from experimental studies with fresh and salt water. For the viscous dominated regime Blake and Ivey [1985] (quoted from Ivey and Blake, 1985) obtained $c_2 = 2.1$ from their experimental results.

2.3.5 Effect of intake shape

Razzaque [1994] in his M. Sc. thesis investigated the effect of shape on the percentage drawdown. He worked with three types of intakes, they are plain, rounded and protruded intakes. The results that he has got is that for the same for the same intake Froude number, rounded intakes reduces the percentage drawdown based on critical height of the mean interface measured from intake level. Sharp protrusion reduces this height further.

2.3.6 Effect of a cap

The effect of cap on a bottom withdrawal through a circular pipe has received much less attention for the case of a two-layered fluid system. Under slack water conditions, Goldring [1981] has provided the single set of experiments available in the literature, which served to demonstrate the beneficial effect of the cap on the critical withdrawal situation.

2.3:7 Computational verification: Miscible two layers

The experimental program of Goldring [1981] consisted of 4 runs for the plain hole case and 17 runs in 5 series for the capped hole case. The diameter of the cylindrical vessel containing the initially stagnant stratified fluid was 236mm and the withdrawal hole diameter (centrally located) was 18.8mm in both cases. For the capped hole runs, the cap radius, $R_c = (d_c/2)$ varied from 9.4mm to 20mm whereas the cap height, S varied from 4mm to 6.2mm. In computational work of Islam [1988], all the experimental runs were simulated in the calculations initiated at time t = 0 when the intake hole at the bottom was opened. Uniform exit velocity and approximately 2mm thick pycnocline were assumed. All the tests were carried out in the falling surface mode and hence the solution domain was also adjusted continuously to match the physical domain size.

The critical interface height was identified by observing the motion of neutrally buoyant dye spots placed at the initial interface height. When the first of these entered the intake, the experiment was terminated and the lower layer depth at the cylinder was taken as the critical interface height. Islam [1988] simulated this by tracking the locus of an originally horizontal line of neutrally buoyant particles placed at the interface height (x at $\theta = 0.5$) until one particle left the solution domain; the height of the particles far away from the intake was then taken as the predicted critical height. All the predicted and experimental data were shown to be in good agreement with the Goldring's [1981] correlation,

$$\frac{h_c}{d} = 0.64\left(\frac{Q^2}{g'd^5}\right)^{1/5} \qquad (2.13)$$

This equation reveals that the critical height is independent of hole diameter and varies linearly with the one fifth power of (Q^2/g') as was also obtained by Ivey and Blake [1985] for the inertia dominated regime. But this finding is in contrast with the Davidian and Glover's [1956] experimental correlation for the range $0.3 < d/h < 14$ showing the dependence of critical interface height on intake diameter. About 30% higher value for the constant of proportionality of equation 2.9 was reported by Harleman et. al. [1959] from there experimental studies. In Harleman's experiment the interface height was kept constant by recirculating the lower layer fluid and the critical intake flow rate corresponding to the given interface height was recorded by increasing the flow rate until the interface was pulled down to the hole (Fig. 2.13).

Numerical prediction of withdrawal ratio indicated that a smaller amount of mixed fluid is withdrawn (i.e. lower λ) as the critical height and hole diameter increases. This is due to the sharper drawdown cone for higher h_c and d.

2.3.8 Effect of a cap

The presence of the cap does exert an influence on the internal waves and acts to produce significant local distortions in the flow above the cap (Islam, 1988). The experimental data by Goldring [1981] and the numerical predictions by Islam [1988] were found to be in good accord with the semi-empirical equation by Goldring.

$$\frac{h_c}{S} = 0.26\left(\frac{S}{R_c}\frac{Q}{\sqrt{g'S^5}}\right)^{\frac{2}{3}} \qquad (2.14)$$

where S and R_c represent the cap height and cap radius respectively. According to equation (2.10), h_c is independent of S but varies inversely with two third power of R_c. But numerical predictions by Islam [1988] showed this statement to be invalid except for some limited conditions.

2.3:9 Computational verification: Immiscible Two layers

The axisymmetric withdrawal of both one and two-layered fluids from a circular tank has been studied analytically and experimentally by Lubin and Springer [1967], who found a relation between the critical height, the drain rate and the density ratio. They observed that the drain rate is nearly constant throughout the draining process until a dip is formed. The formation of the dip was so quick that it appeared to extend into the sink almost instantly. The analytic formula obtained by Lubin and Springer is in excellent agreement with their experimental data, in spite of the fact that only the Froude number based on the drain rate (assumed to be constant) and the density ratio are included.

Zhou [1989] studied this problem numerically and found for the one layer fluid case that when a dip forms, the computed critical heights agree with Lubin and Springer's analytic solution only for moderate values of the Froude number. For large Froude numbers the computed values are considerably smaller than their analytic values. The discrepancies increased with the Froude numbers and varied with the sink sizes and the initial depths of the free surface. For the two-layered fluid case the differences are even larger. It was also found that there are strong free surface oscillations as predicted theoretically by Saad and Oliver [1964] and Zhou and Graebel [1989].

For both one and two-layered fluid cases, Zhou and Graebel [1989] investigated numerically the axisymmetric evolution of a free surface and an interface in a circular tank under a constant draining rate through a concentric hole at the bottom. Froude number was defined as $F_R = (Q^2/gR^5)^{1/2}$, where R stands for the tank radius and is the normalizing parameter. In case of one layer fluid the effect of dimensionless parameters controlling the flow, i.e. Froude number, F_R, normalized initial depth of free surface, H_o, and the normalized Sink radius, **a**, was analyzed. It was found that the free surface configuration was nearly independent of initial free surface height, H_o for same F_R and a, until $H_o \geq 1$. For same a and H_o, a sufficiently large value of F_R (say larger than 1.0) can suppress the drainage initiated free surface oscillations. In the case of small mean level of the free surface, similar final surface configurations may be occurred despite different motion histories; because of the quick damping out of the existing oscillations by the dominating sink influence. For same H_o and small F_R (say = 0.1), a smaller **a** results in a greater drawdown of the free surface. Equivalently, one can say that a more concentrated drawdown force overcomes the squeezing of the near-centre surface points by the off-centre surface points and a pulling down of the centre of the free surface. Thus a sufficiently small a can give rise to a dip (Fig. 2.10) whereas if a is not sufficiently small, the squeezing together of the near-centre surface points decelerates the centre and consequently a reverse jet is formed. (Fig. 2.15). When a dip is about to form, the surface velocities near the centre are dominant while those away from the centre are small (Fig. 2.16). This is the kinematic reason why the dip develops so rapidly. But when a reverse jet appears, the maximum surface velocity occurs at the trough of the free surface. If the trough velocity is sufficiently large, the centre must be pushed upward owing to the strong compression, hence a reverse jet will form. The effect of H_0 on whether a dip or a jet forms is similar to that of a. A weak jet occurs when the initial depth H_0 is large and the drainage- initiated free surface oscillations occurs in the early stage of the motion.

For the two-layer fluid case, where only a slight stratification exists, (say density ratio = 0.9) the free surface undergoes severe oscillations when a dip forms on the interface (Fig. 2.17). But for a large stratification (say density ratio = 0.5), the free surface shows the sign of traveling waves when a reverse jet forms on the interface (Fig. 2.18). The physical mechanism as to why different values of stratification cause quite different surface motion, was explained by the interfacial vorticity. When a dip develops on the interface, the vortex strength near the centre is negative, which aids in pulling the centre of the interface into the sink. The negative vortex strength indicates that the inward (pointing toward the centreline) tangential velocity of the upper fluid on the interface is greater than that of the lower fluid on the interface. When a jet forms, the vortex strength is positive everywhere, indicating that particles of lower fluid on the interface move towards the centreline faster than do upper fluid particles on the interface. It has been assumed in simple analytic analysis (e.g. Lubin and Springer, 1967 and Harleman et. al., 1959) that the pressure on an interface is approximately hydrostatic. But numerical results showed that this assumption is no longer correct after an appreciable depression occurs on the interface.

2.3.10 Drawdown history

In case of two-layered fluid systems, Jirka and Katavola [1979], studied the supercritical withdrawal behavior including the effect of finite size intakes and finite ambient pycnocline widths. By defining pycnocline width l as the distance between the 10% and 90% value of the density difference and the interface position h as the distance between the intake center-line and the 50% value of the density difference, three independent Froude numbers were defined as,

$$Fr = \frac{Q}{\sqrt{g'h^5}}; \qquad F_D = \frac{Q}{\sqrt{g'd^5}}\left(\frac{4}{\pi}\right); \qquad \text{and} \qquad F_l = \frac{Q}{\sqrt{g'l^5}}$$

For the supercritical flow, a withdrawal ratio λ was defined as, $\lambda = (Q_1/Q)$, where Q = total flow and Q_1 is the flow from upper layer. The tests were conducted in a temperature insulated tank 1.52 m long, 1.32 m wide and 0.91m deep. The intake opening was located 0.30m above the tank bottom on the centreline of one of the tank walls. Variable intake openings from 5.3mm to 37.2mm wide were used. The intake flow rate was measured with precision rotameters and varied between 3.6 lpm to 27 lpm. The density stratification was produced with heated water. Temperature differences between upper and lower layer ranged from 14.3°C to 23.3°C which represents values of $\Delta\rho/\rho$ from 0.0032 to 0.0063. The thickness of the thermocline region, l, varied between 8.6cm and 16.3cm. The temperature distribution within the tank and the intake was measured by 66 thermistor probes with ± 0.05°C accuracy and 7 sec time constant. The entire probe set was connected to a fast-scanning digital recording system with a scanning rate of about 0.7 sec per probe.

All experiments were in falling interface mode while the total water depth stayed constant by an inflow of warm water at the same rate of discharge. Temperatures were monitored continuously throughout the experiment to determine the instantaneous withdrawal ratio $\lambda(t) = (T_i - T_2)/(T_1 - T_2)$, where T_1 and T_2 are the average upper and lower layer temperatures respectively and T_i being the instantaneous temperature at the intake.

Sixteen withdrawal experiments were carried out with the ranges of $F_D \sim 1$ to 437 and $F_l \sim 0.05 - 0.33$. In all experiments it was found that a small degree of withdrawal ($\Lambda < 3\%$) consistently occurred even at values of Fr well below the incipient condition. Interfacial viscous effects and ambient diffused interface were suspected to be responsible for it. The withdrawal curves (λ vs. Fr) provided the value of critical Froude number Fr_c and these curves are approximately symmetrical about the $\lambda = 0.50$ axis (Fig: 2.19). It was found that increasing values of either F_l or F_D increases the value of Fr_c. The observed values of Fr_c ranged from 0.05 to 0.27 which are much less than Craya's theoretical limiting ($F_D \to \infty$, $F_l \to \infty$) value of $Fr_c = 2.54$. This deviation was perhaps due to the lower value of F_l (i.e. the diffused interface) in the order of 10^{-1}, which was in the order of 10^3 in Gariel's experiment. A best- fit expression for approximation of Fr_c values in the experimental range was determined to be $Fr_c = 0.06 \log F_D + 0.64 F_l - 0.05$ which was in moderate agreement with the experimental data. $\lambda = f(Fr/Fr_c)$ plot of all experimental data having a moderate amount of scatter suggested that the withdrawal characteristics in the supercritical range can be represented by a unique empirical curve independent of geometric effects. The equation of this curve is given by,

$$\lambda = 0.142 \log (Fr/Fr_c) \quad \text{for} \quad Fr/Fr_c < 300 \qquad 2.(16)$$

$$\lambda = 0.50 (1-Fr/Fr_c)^{-0.22} \quad \text{for} \quad Fr/Fr_c > 300 \qquad 2.(17)$$

Wood [1978] presented an elegant theory giving the relationship between Fr and λ. Lawrence [1980] extended wood's theory to the case of two-layered fluid with a linearly stratified lower layer withdrawn through a special type of point sink. Experimental verification provided the drawdown history data without giving any satisfactory proof to the proposed specific demarcation of the flowing zones as a function of Froude number.

2.4 AXISYMMETRIC WITHDRAWAL FROM A TWO-LAYERED SYSTEM WITH CROSS-FLOW

A 3-D version of a real life cooling water intake system was simulated experimentally by Goldring [1984] (quoted from Islam,1988) for withdrawal from a thermally stratified two-layered fluid in a unidirectional cross-flow without any wind shear on the free surface. Goldring [1984] has however provided only data on critical heights and drawdown behavior under these conditions. The Reynolds number of the cross-flow was high [O(1000)] so that it became turbulent and drawdown behavior was observed to be dependent also on the inlet (cross-flow) Froude number defined as $F = U/(g'H^5)^{1/2}$, where U is the cross-flow velocity and H is the total depth of flow. Computational predictions and their verifications are available in Islam [1988].

2.5 CONCLUSION

Starting from the middle of this century, still today, a lot of analytical and experimental work has been done on 'Selective Withdrawal' from stratified fluid system. Scientists and engineers has worked on the effects of intake geometry, nature of stratification, thickness of pycnocline, rotation, location of sink and many other parameters on the 'Selective Withdrawal'. Location of sink plays an important role on quality of fluid in the outlet , but this field is yet to be excavated. The knowledge of the effect of sink location on the drawdown will definitely help one in selecting the 'strata' of fluid at the sink level more efficiently and more precisely.

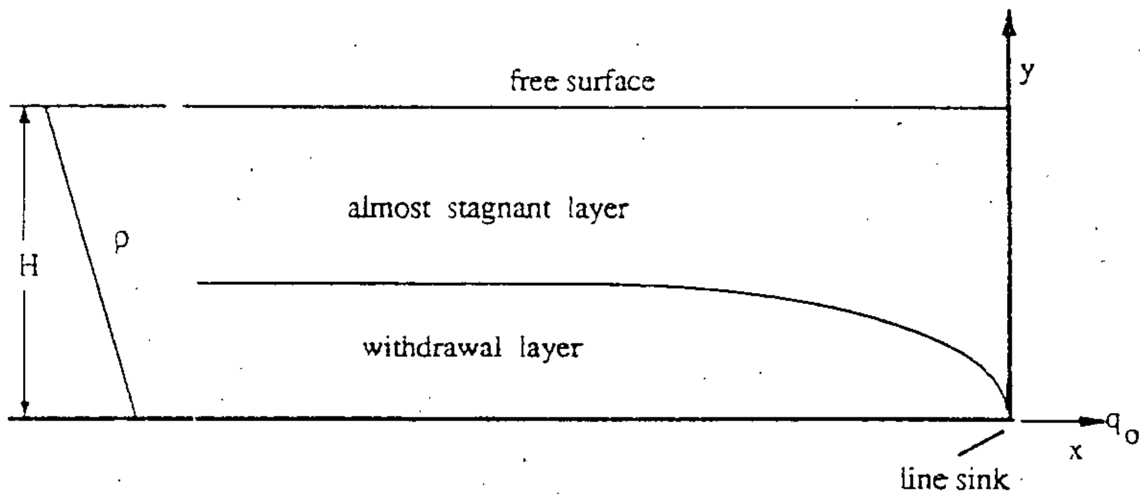

Fig. 2.1 Two-dimensional flow into a line sink.

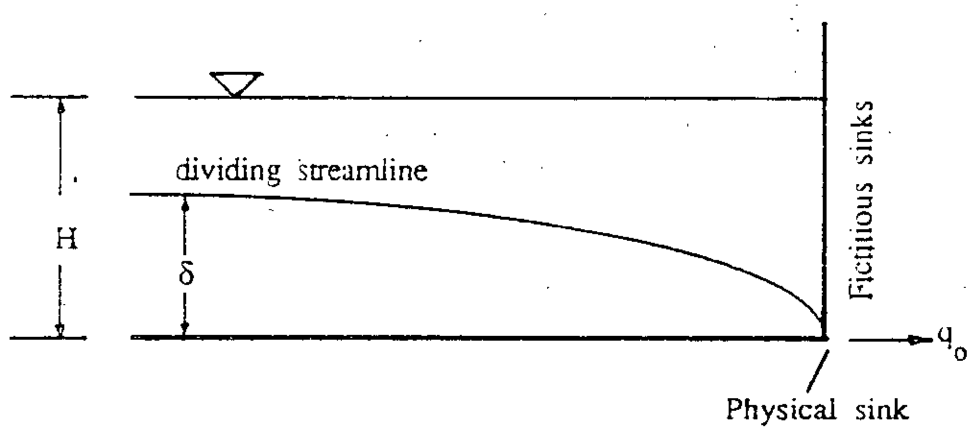

Fig. 2.2 – Definition sketch of Kao's (1970) analytical solution for 2-D line sink flow.

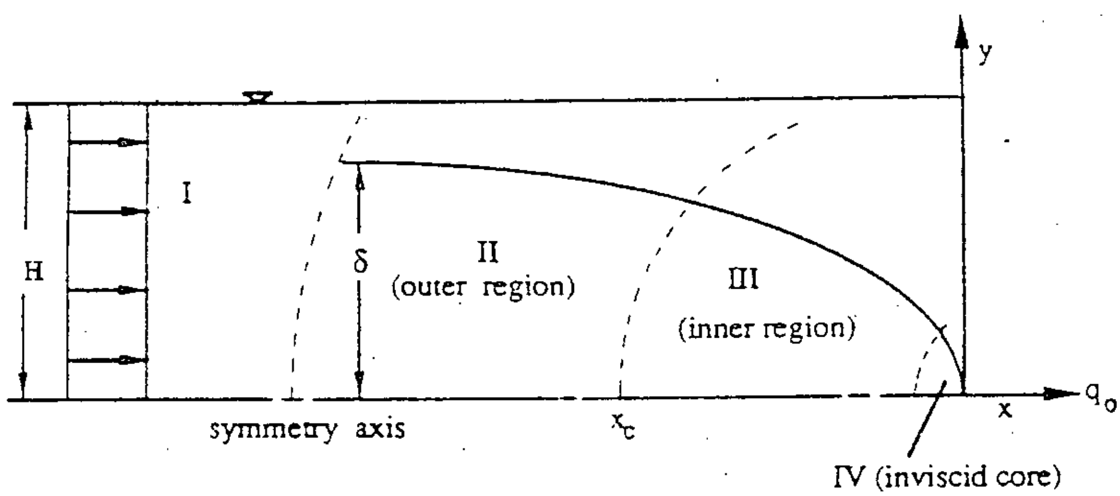

Region: I uniform upstream flow (inviscid & non-buoyant)

II outer region (negligible inertia but viscous & buoyancy important)

III inner region (inertia, viscous & buoyancy important)

IV inviscid core (inertia & buoyancy important)

Fig. 2.3 Different regions of flow towards a 2-D line sink (after Imberger & Fischer, 1970).

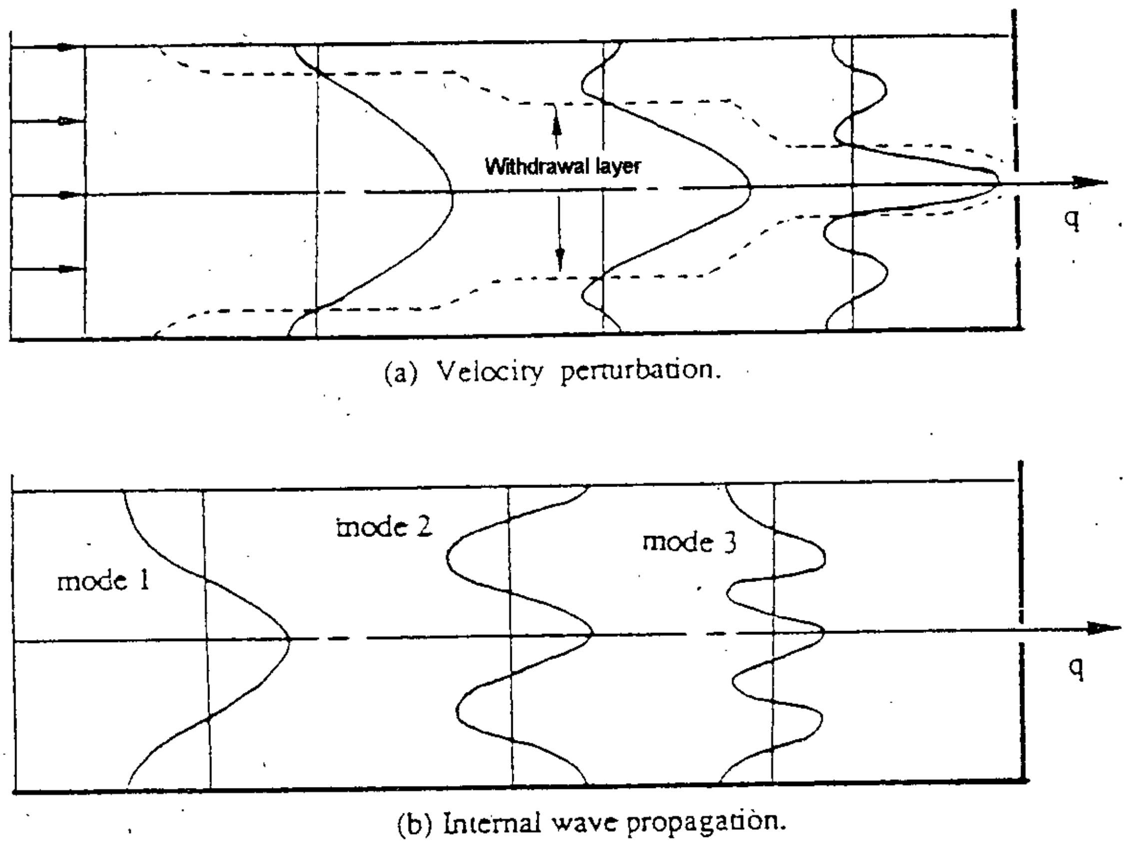

Fig. 2.4 Schematic diagram showing the effect of internal wave propagation on the velocity field. (Islam, 1988)

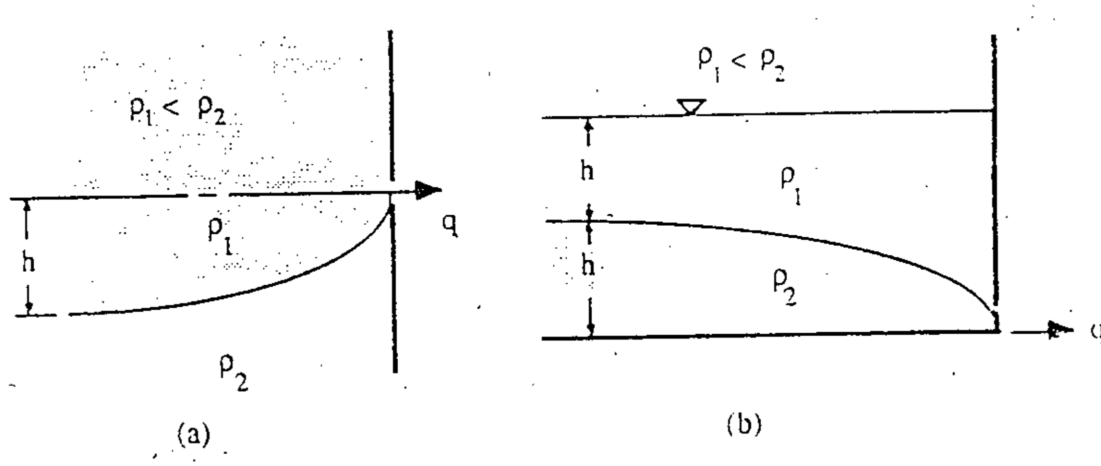

Fig : 2.5 Critical flows from two layer fluid system into a line sink; a) after Craya(1949), and b) after Huber(1960)

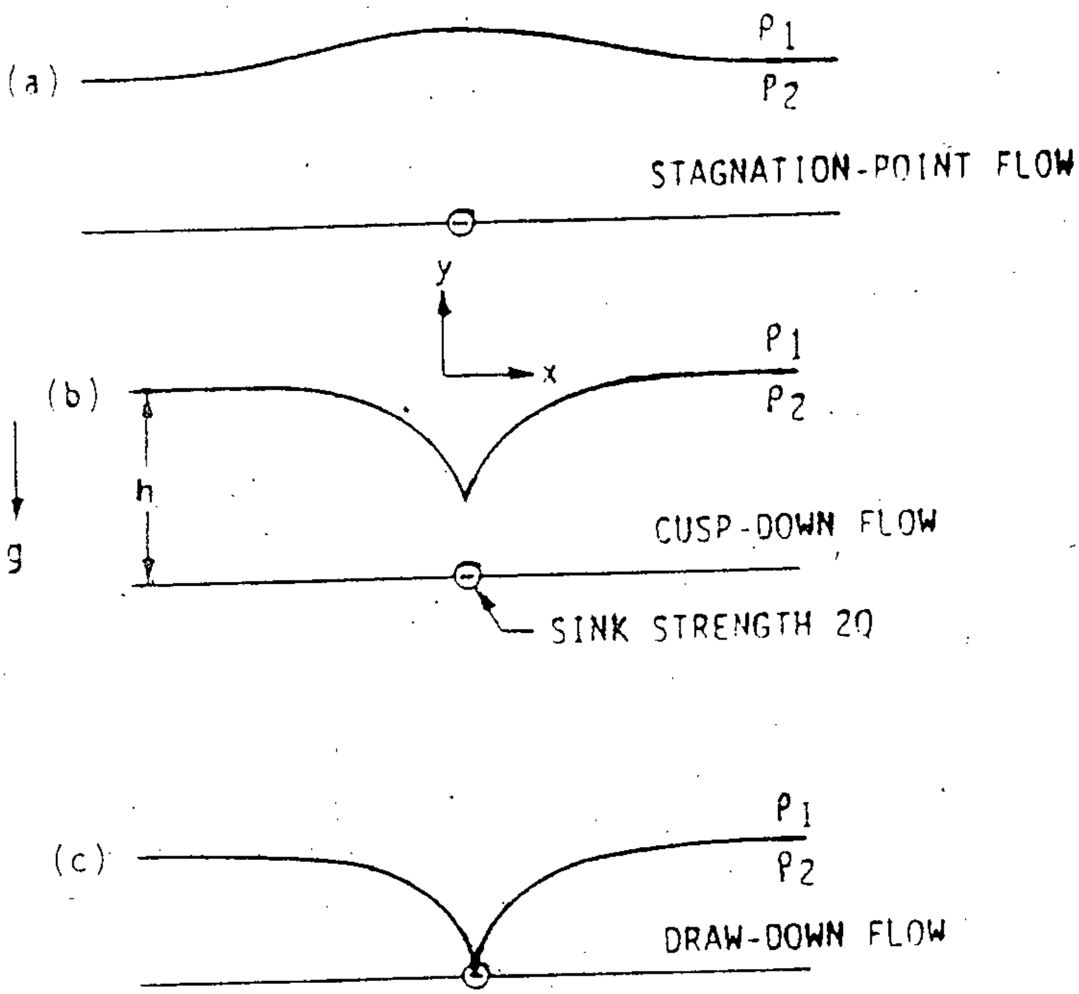

Fig: 2.6 Possible steady-state flow configeration (Ingber and Munson, 1986)

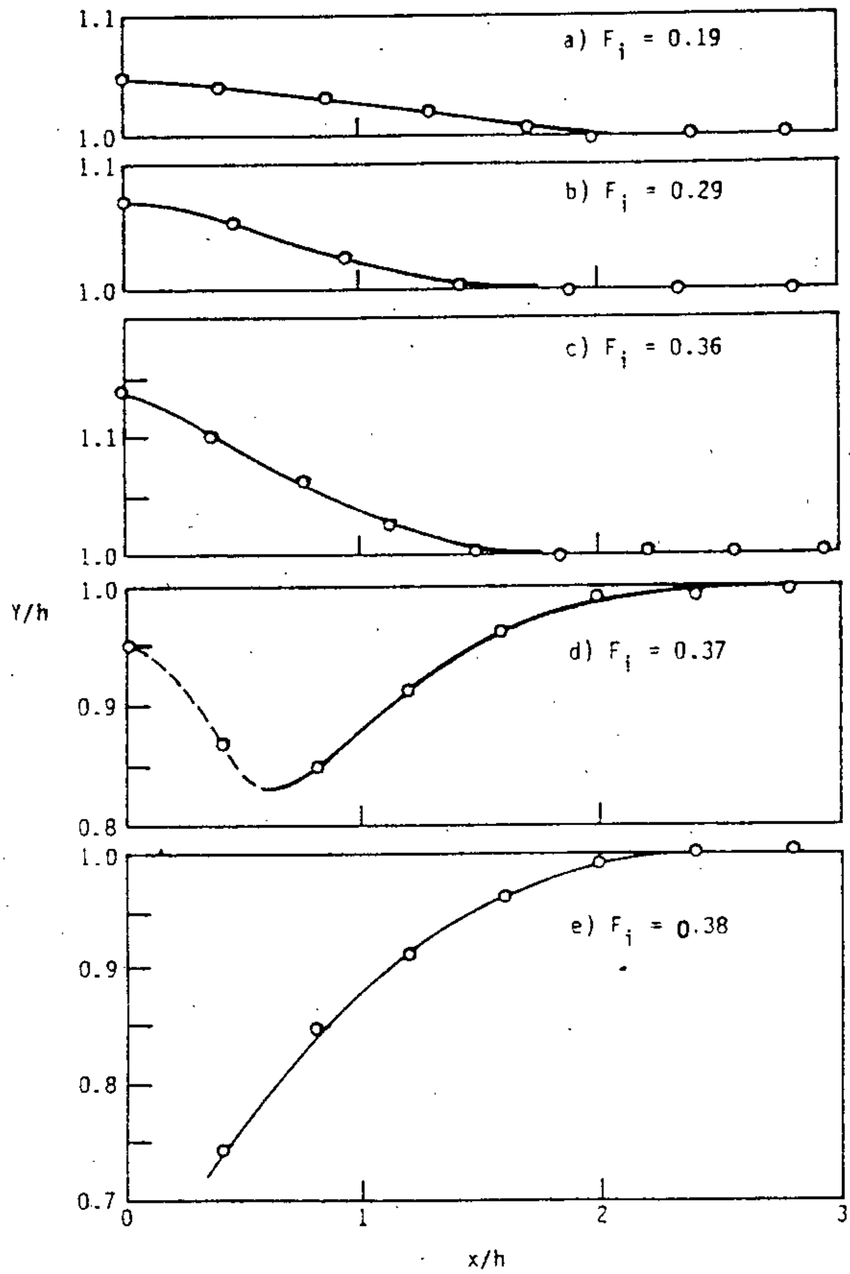

Fig:2.7 Interface shape as a function of Froude number when isolated of viscous effects (Ingber and Munson, 1986)

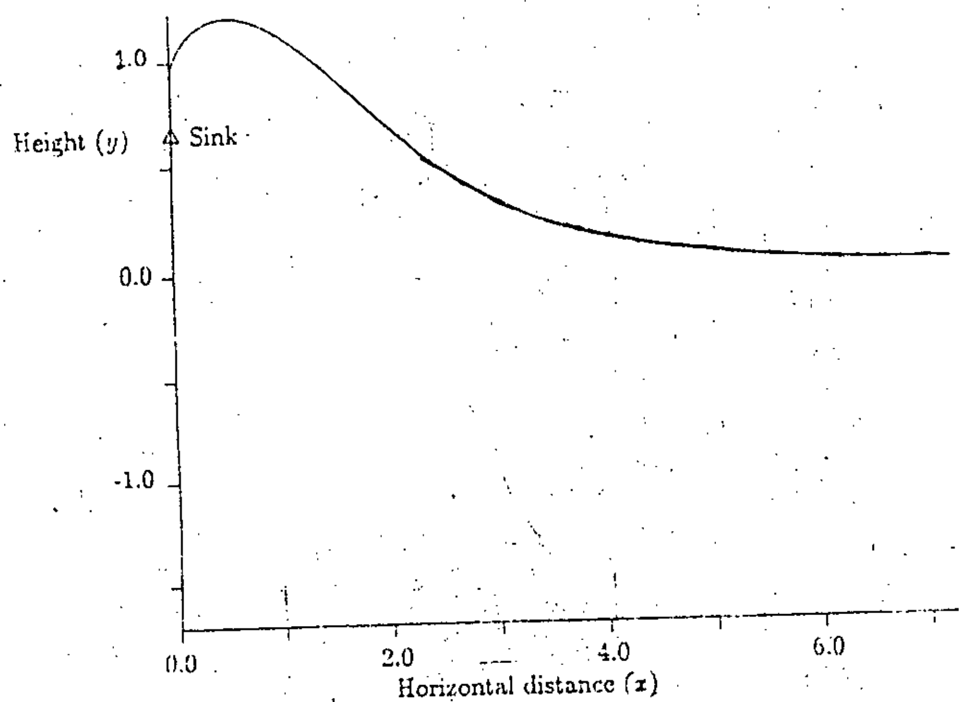

Fig: 2.8 Diagram showing the interface shape for a situation in which the sink is above the level of the interface away from the sink(Hocking, 1990)

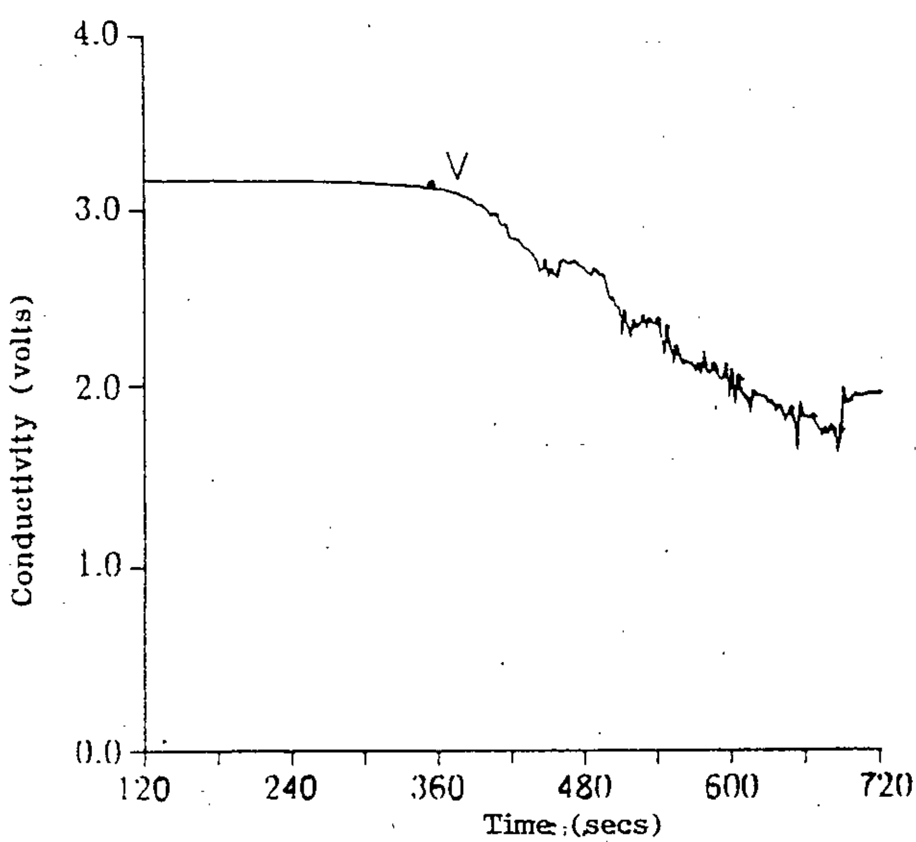

Fig: 2.9 Hocking's (1991) technique to identify the initiation of withdrawal

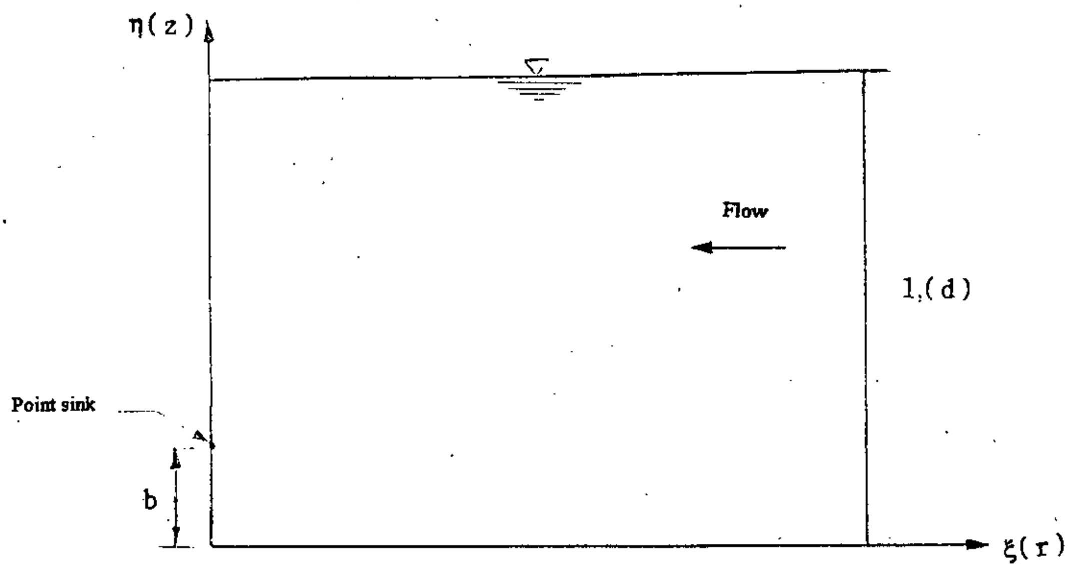

Fig: 2.10 Cylindrical coordinate for flow system (Hino and Onishi, 1969)

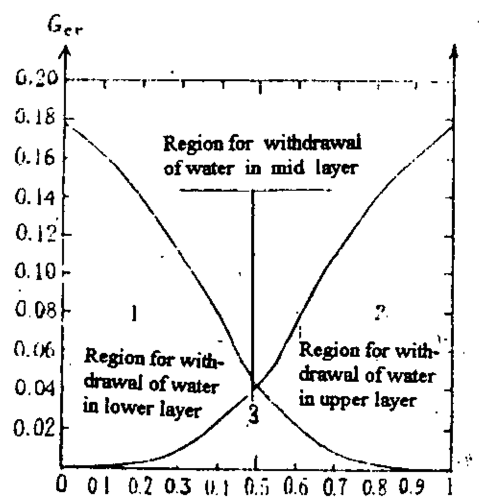

Fig: 2.11 Relation of Gcr to the location of sink and the conditions of selective withdrawal((Hino and Onishi, 1969)

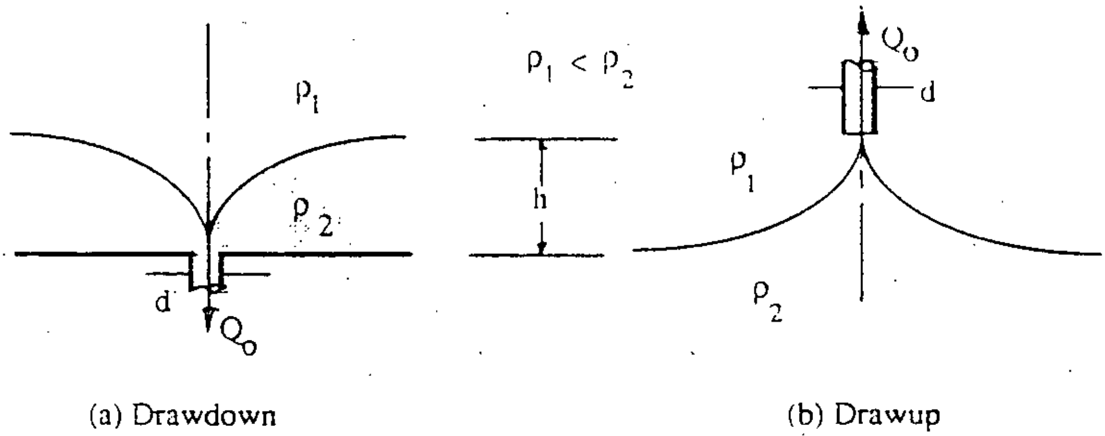

Fig:2.12 Vertical axisymmertic withdrawal through a round hole from a two layer fluid system.

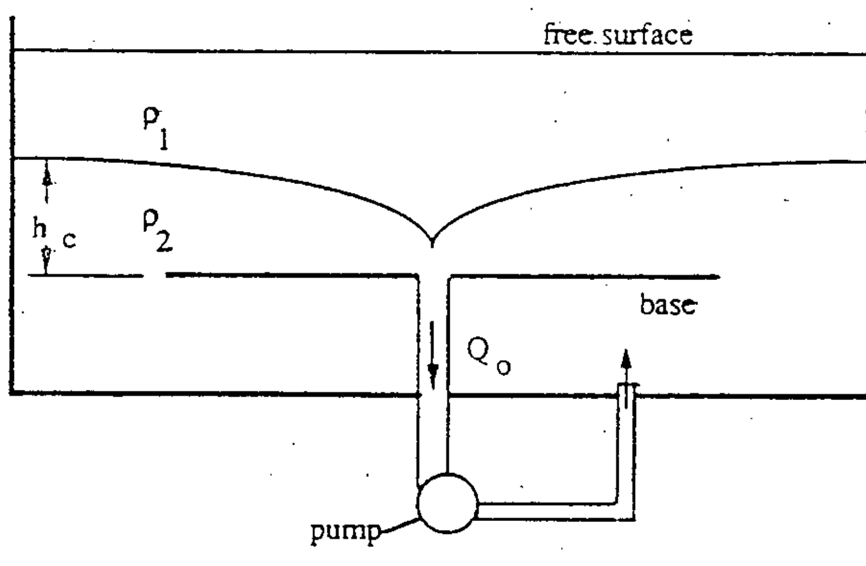

Fig:2.13 Flow configuration of Harleman et al's (1959) experiment.

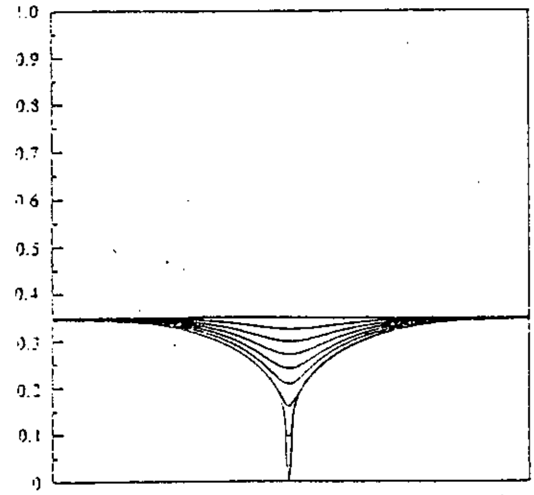

Fig:2.14 Time development of the free surface; F = 0.1, h_o = 0.35, a = 0.05 at t = 0.01, 0.02, 0.03, 0.04, 0.05, 0.06, 0.065, 0.06625. (Zhou, 1990)

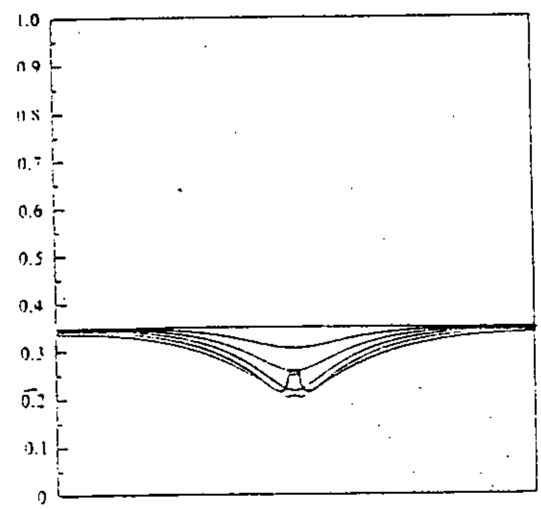

Fig:2.15 Time development of the free surface; F = 0.1, h_o = 0.35, a = 0.2 at t = 0.02, 0.04, 0.06, 0.08, 0.1, 0.102, 0.104, 0.106. (Zhou, 1990)

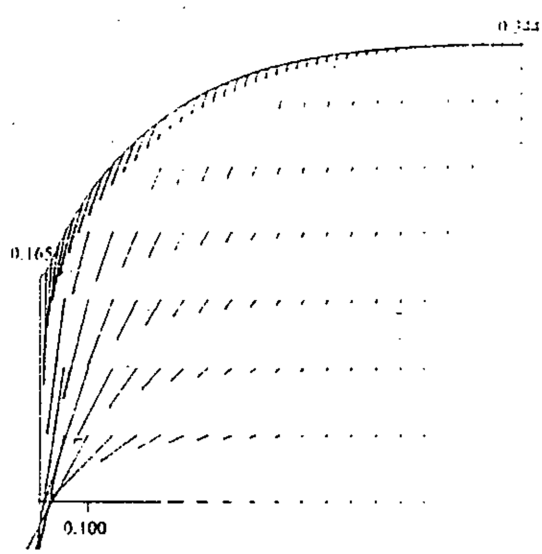

Fig:2.16 Velocity field when a dip forms; F= 0.1 h_o = 0.35, a = 0.1 at t = 0.64. (Zhou, 1990)

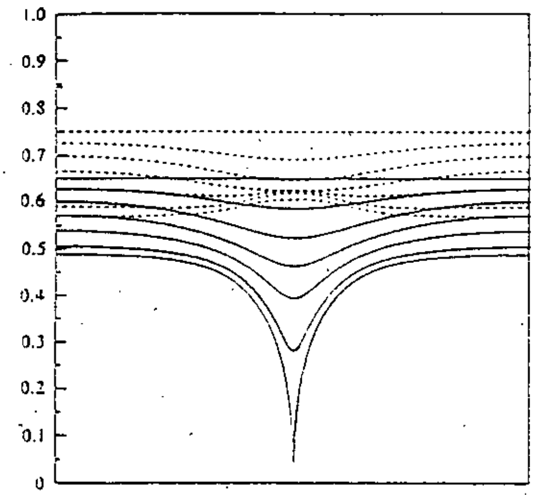

Fig:2.17 Time development of —, the free surface and —, the interface: F = 0.25, a = 0.1, β = 0.5, h_i = 0.65 and h_0 =0.1 at time t = 0.1, 0.2, 0.3, 0.4, 0.5, 0.553. (Zhou, 1990)

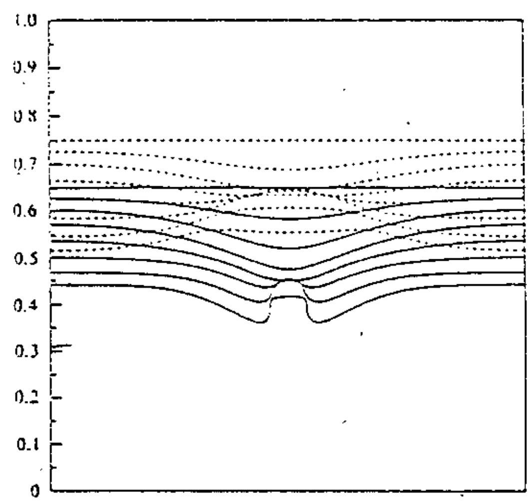

Fig:2:18 Time development of —, the free surface and —, the interface: F = 0.25, a = 0.1, β = 0.5, h_i = 0.65 and h_0 =0.1 at time t = 0.3, 0.5, 0.69. (Zhou, 1990)

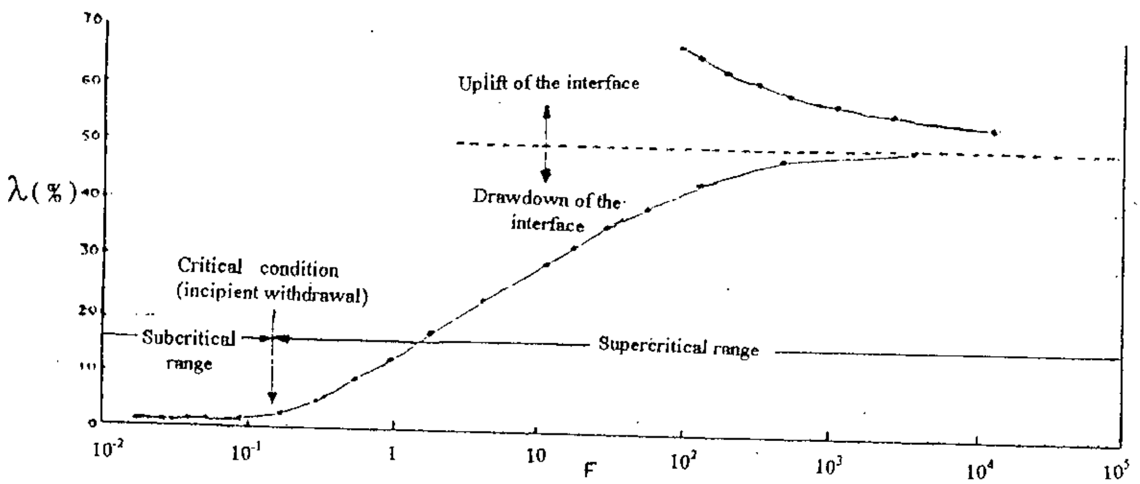

Fig: 2.19 Withdrawal curve as a function of F
(Jirka and Katavola, 1979)

CHAPTER - III

EXPERIMENTAL SET-UP AND PROCEDURE

3.1 INTRODUCTION

The objective of this experimental work is to investigate the effect of sink location on the draw down of water from stratified hot and cold water system. Most recently Razzaque [1994], has worked on a similar field, he investigated the effect of intake geometry on the drawdown. The experimental tank which he used was rectangular type and the feeder tank was attached to the tank. The experimental setup of Razzaque is not convenient for this work. Thus a new set is made and a lot of changes is done in the instrumentation. The procedure of calculation remained the same. In the following subsections a brief description of the experimental setup and procedure is provided.

3.2 THE TEST RIG

The test rig consists of experimental tank, feeder tank, mechanism for hot water supply, provision for withdrawal of water, temperature measuring devices. A brief description of these items are given below.

3.2.1 Experimental tank

A square tank (Fig: 3.1 & Fig: 3.2) of size 1210mmx1210mmx530mm is made by perspex sheet and all the experiments is performed in this setup. The perspex sheet which is used is 6 mm thick and the sheets are joined by chloroform and silicon glue. The tank is further reinforced by steel frame. The tank is placed 1700mm above the ground on a rigid steel frame. The outlet of size 38mm is placed at the middle on the ground level of the square tank. The middle point is chosen to avoid the effect of the side walls and the tank is made square so that it may be assumed to be round, thus the methods of calculation in polar coordinate may be possible. The round hole at the ground level of the tank, where the intake is placed, is encircled by a cast iron ring, so that the base is free from all possible cracks. The intakes those are used for experiments is inserted into this intake (attached with the tank) with some special attachment, which is discussed later. A measuring scale is attached on one vertical side of the wall to measure the vertical height of the water in the tank. Water is drained out through a 42mm diameter pipe. Outflow of water from the tank is controlled by a globe valve placed on the draining pipe. This draining pipe also contains the three thermocouple sets, placed at a distance of 400mm from the bottom of the tank.

3.2.2 Feeder tank

To ensure laminar and uniform flow of hot water into the experimental tank,a feeder tank (Fig: 3.1 & Fig: 3.2) of size 1115mmx38mmx64mm is used. It is placed into the tank at a desired height by hanging it from a steel bar placed on the main tank. Since the height of the feeder tank may be varied, thus one may attain numerous interface height within the tank. A number of round small sized glass marble is kept into the feeder tank so that any turbulence in the water from the hot water reservoir is damped out. Water is fed in to the feeder tank from a hot water tank placed at a height of 600mm from the bottom of the experimental tank , through four flexible pipes. These four pipes are equally spaced so that uniform flow of water prevails along the feeder tank.

3.3.3 Hot and cold water supply

Hot and cold water supply are required to make two layered fluid system. Cold water is supplied from the 'supply water' line, i.e. the cold water is at ambient temperature. For hot water, a 'water heater' is used to heat the water. The 'water heater' has four 2 kW immersion heaters, placed at the bottom of the water heater. These heaters heats the water and for intimate mixing of hot water, a pump is used for recirculating the water in the 'water heater'. The heater raises the water temperature by 8°C to 15°C above ambient condition. After attaining the desired water temperature, the water is pumped to the 'hot water reservoir' at a height of 2300mm from the ground.

3.2.4 Selection of sink

During the entire experimental work point sink is placed at eight different height of the tank, starting from the bottom of the tank and the heights are 00mm, 13mm, 19mm, 42mm, 56mm, 76mm, 100mm and 120mm. Round PVC(Poly Vinyl Chloride) pipe with sharp edge is used as sink and the diameter (19mm) of the sink is kept more or less same through out this investigation.

3.2.5 Formation of two-layered system

Formation of two layer is one of the most important work of every experiment. In all the experiments two layer system is developed by using hot and cold water. Hot and cold water have a temperature of about 8°C to 15°C and thus these two fluids have density difference, as a result they form two layer. Initially, cold water is pumped into the experimental tank up to the height of the feeder tank, the heater is turned on and it takes several hours for the heater to attain the desired temperature and during this long time water in the experimental tank becomes free from all sorts or circulation, vibrations or rather in short, from all sorts of disturbances. When heater temperature rises to a desired level hot water is pumped to the hot water reservoir. Hot water of uniform temperature is delivered to the feeder tank and is allowed to overflow slowly to form two layers with minimum interface thickness between them. Warm water from an hot water reservoir is discharged at four locations into marble layers of the feeder tank by means of four flexible PVC pipes and as a result the disturbances are damped out. Flow rate is kept low when the warm water is just overflowing the partition and it is done to ensure the minimum mixing with the cold water.

3.3 Measuring Devices and measurement procedure

3.3.1 Water flow measurement

In all the calculations for several runs average water flow rate is used. This is done by measuring the time of fall of water column from the constant volume tank. One might argue that water flow rate might vary due fall of the height of water. But here the tank is located at sufficiently high elevation and gravitational force is the driving force for the water fall. Water in all the experiments fall about 200mm only and for such little fall in water column, the variation of water flow rate with respect to the average water flow rate is less than 5%. Error of this order may be neglected for this kind of experimental work.

3.3.2 Temperature measurement

Water temperature is measured by means of Copper-Constantan (T-type) thermocouple (bead dia. ≈ 1.5mm). A digital millivoltmeter and data logger is used for recording the temperature measured by the thermocouple. Each of the above mentioned instruments is used for different purposes. They are:

a) Measurement of interface thickness : Most of the recent works (Jirka & Katavola [1979]) suggests that pycnoclinic region of width 'l' is the height difference between 10% and

90% value of the density difference and the interface position 'h' is defined as the height difference between the intake center line and the 50% value of the density difference. Researchers around the world measured this density difference in many ways and some of them are conductivity measurement, temperature measurement etc.. For this work temperature measurement technique is used for density measurement of water at different location of the tank. The reason for selecting the temperature measurement technique is that temperature measurement is very easy, and the temperature of the fluid has linear relationship within the maximum and minimum temperature of this work (temperature range of this work is 20°C to 45°C). Density of water is related to the temperature via. the following polynomial:

$$\rho = 266.5 + 6.466\,(T+273) - 0.01788\,(T+273)^2 + 0.0000148\,(T+273)^3 \qquad (3.1)$$

where , T is the temperature in Celsius and ρ is the density in kg/m^3 . Equation 3.1 is a curve-fit to the $\rho(T)$ data given in Batchelor[1980] and Islam [1988]. This is plotted in Fig: 3.3, and from the figure it is clear that within the working range of temperature of this work, the density profile is linear with temperature.

A digital millivoltmeter is used to record the temperature measured by the T-type thermocouple. The thermocouple is mounted on a traversing unit with precision ±0.1 inches and the temperature profile is measured by recording the millivolt reading of the thermocouple at different vertical locations. The normalized temperature ratio, θ, is plotted against vertical location and it is defined by the following equation,

$$\theta = \frac{T - T_2}{T_1 - T_2} \qquad (3.2)$$

where subscript 1 and 2 corresponds to upper and lower layers respectively and T denotes the local temperature. As it is assumed that temperature varies linearly with millivolt (Fig. 3.3), equation (3.3) becomes,

$$\theta = \frac{mv - mv_2}{mv_1 - mv_2} \qquad (3.3)$$

where, mv is the millivolt reading at different vertical locations and mv_1 and mv_2 are the mv(millivolt) readings corresponding to the upper and lower layer temperatures respectively. Fig. 3.4 shows a typical temperature profile. The height corresponding to $\theta = 0.5$ was taken as the mean interface height (h) and the interface thickness(l) is determined by taking the difference between the elevations corresponding to $\theta = 0.1$ and 0.9.

b) Measurement of drawdown fraction (λ) and percentage drawdown (Λ) :

Drawdown fraction is defined as the ratio of fluid volume drawn from the upper layer to the total volume flow and is represented by λ, i.e.

$$\lambda = (Q_1/Q) = Q_1/(Q_1 + Q_2) \qquad (3.4)$$

Where Q_1 and Q_2 are the inflow from the upper and lower layer respectively. If the discharged fluid can be mixed sufficiently so that it may be considered as a homogeneous fluid, its density would be in between the densities of both layers. It is obvious that this density will be an indication of the proportion of the fluid volume drawn from the upper layer. If the density of the mixed fluid past the intake is ρ_m then,

$$\lambda = (\rho_m - \rho_2)/(\rho_1 - \rho_2) \qquad (3.5)$$

Now for the small temperature range (25^o - 45^oC) of the present experiments, the relationship between density and temperature may be assumed approximately linear (Fig. 3.5) and the equation (3.5) takes the following form,

$$\lambda = \frac{T_m - T_2}{T_1 - T_2} \quad \text{and} \quad \Lambda = 100\,\lambda \qquad (3.6)$$

Where T_m is the temperature of the mixture T_m is the mean temperature of outflow, T_1 and T_2 are average temperature of fluid of top and bottom layer respectively.

Three T-type thermocouples are placed at approximately 400mm below the intake. The middle one is used while recording the actual reading and the rest two are used only for checking if the mixing of the outgoing fluid is adequate or not. To ensure proper mixing the discharge is passed through two inclined filter nets and then through a funnel before the temperature is sensed by the thermocouple (Fig. 3.6). The inclined net on both sides of the filter and the funnel helps in creating disturbances for proper mixing of the fluid. Comparison of the thermocouple readings confirms the attainment of adequate homogeneity in temperature of the fluid at the location of measurement.

Measurement of temperature of outgoing water is done by a datalogger (Fig: 3.7). The datalogger records the temperature in its buffer. After every run data from the data logger is down loaded by a computer with the help of a data accusation software. The data logger is programmable and one can choose the interval of unit of temperature, logging, type of datalogger etc.. Minimum possible reading which may be obtained from the data logger in Celsius unit is 0.1°C. The data logger and the sink is turned on simultaneously and the data logger is turned off when top of water surface reaches the sink.

Selection of logging interval is very important. The thermocouple itself has a time lag of 1sec (Appendix, Fig: A2 to Fig: A4) and the termocouple which is measuring the temperature is about 400mm away from the intake. For the current work the maximum possible time, which the water requires to reach the thermocouple is around 2.5 seconds. Thus the total lag time is 3.5 seconds. So we should select an interval greater than 3.5 sec. In all the experimental runs the interval is kept at 5 sec.

3.4 Experimental procedure

Initially a point sink is placed at a desired location of the tank and then the tank is filled with isothermal water at temperature T_2 and hot water is introduced at temperature T_1 in the tank as mentioned in section 3.2.4 to form two layers. After formation of two layers, the interface thickness and the height of interface are measured according to the procedure described in section 3.3.2 a. Next, the sink and the datalogger are turned on simultaneously to record the temperatures of the water at outflow. The value of λ and Λ are calculated according to the section 3.3.2 b and then the instantaneous mean height of interface is measured.

3.5 Calculation of F_r, F_d, F_l

The literature review follows that the Froude number emerges as the primary similitude parameter for this type of flow. Three types of Froude number were used in calculation and they are defined as,

densimetric Froude number, $$Fr = \frac{Q}{\sqrt{g'h^5}} \qquad (3.7)$$

intake Froude number, $$F_d = \frac{Q}{\sqrt{g'd^5}} \qquad (3.8)$$

and interface Froude number, $$F_l = \frac{Q}{\sqrt{g'l^5}} \qquad (3.9)$$

where,

	Q	=	flow rate at the initial stage of the withdrawal
	h	=	instantaneous interface height from the intake level
	d	=	intake diameter
	l	=	interface thickness measured just before the onset of the withdrawal

The value of g' indicates the effect of gravity. A heavier fluid flowing beneath a lighter fluid will be subjected to gravitational effects which depend upon the difference between the two specific weights rather than upon the absolute magnitude of the specific weight of the heavier fluid. The less dense fluid may then be regarded as if it were weightless and the more dense as if it were subjected to a reduced gravitational acceleration of magnitude

$$g' = \frac{\rho_2 - \rho_1}{\rho_2} g = \frac{\Delta\rho}{\rho_2} g \tag{3.10}$$

This effective gravitational acceleration was used in all calculations and the value of ρ was determined from equation (3.5). The magnitude of g was assumed to be 9810 mm/sec^2.

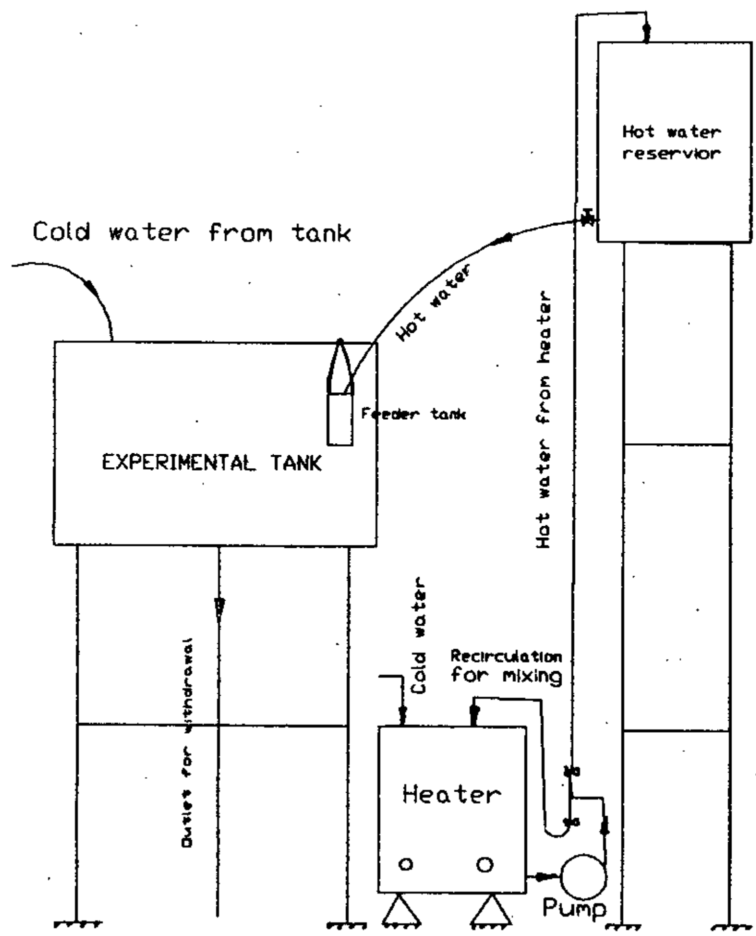

Fig: 3.1 Schematic Diagram of Experimental Setup

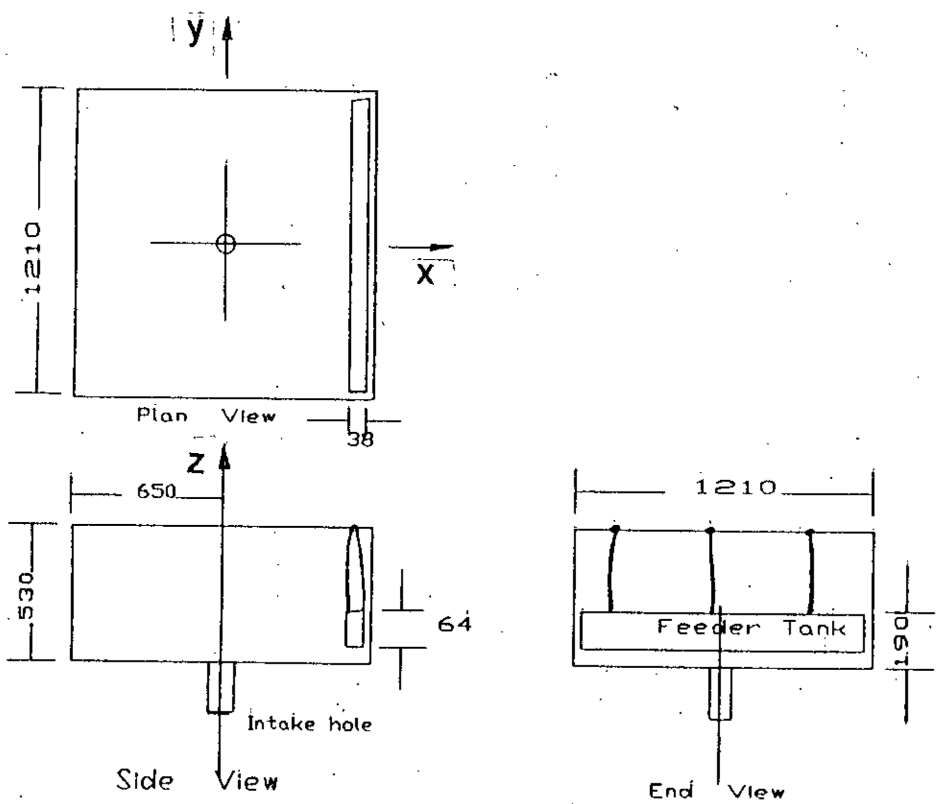

Fig: 3.2. Experimental Tank (Dim: mm)

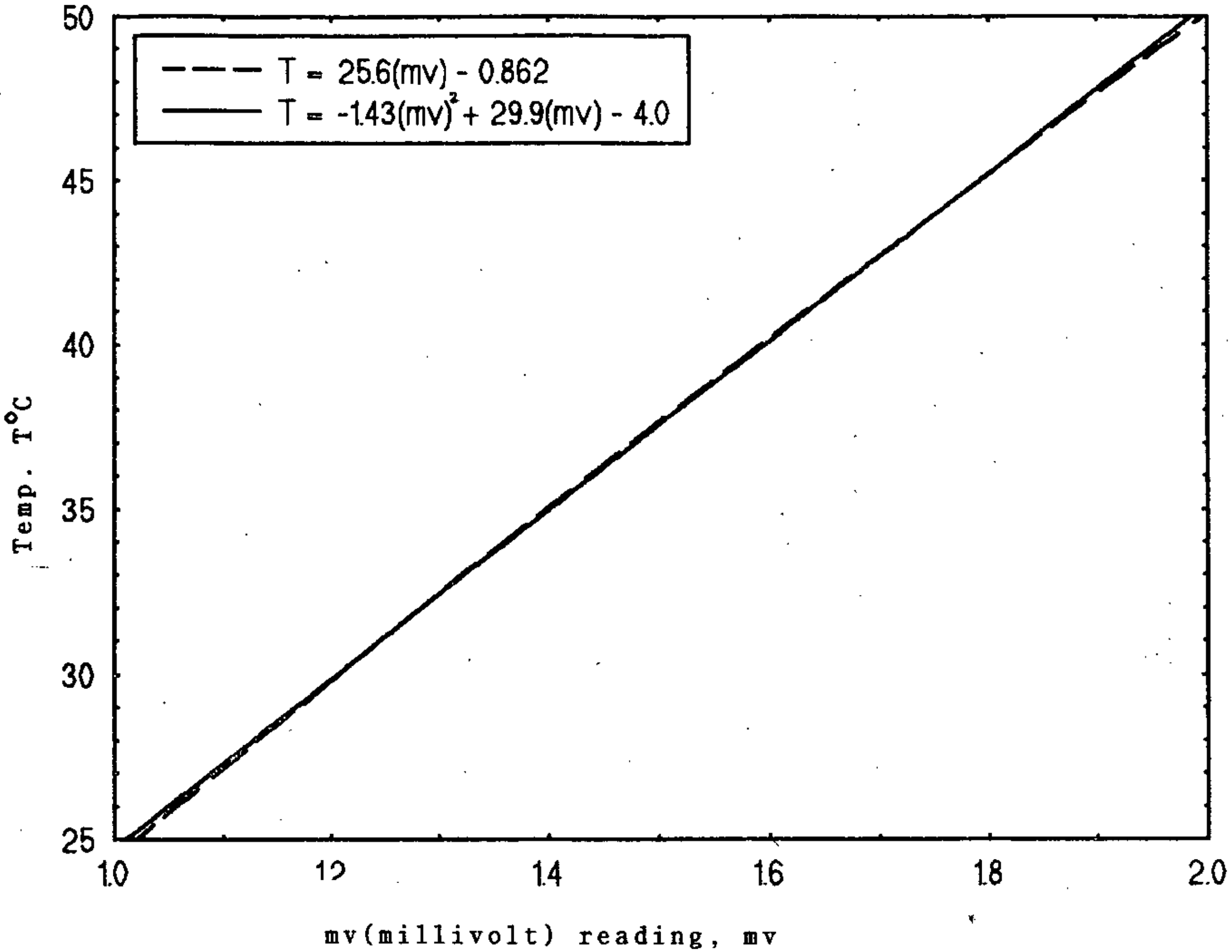

Fig: 3.3 Temperature millivolt relationship of T-type thermocouple

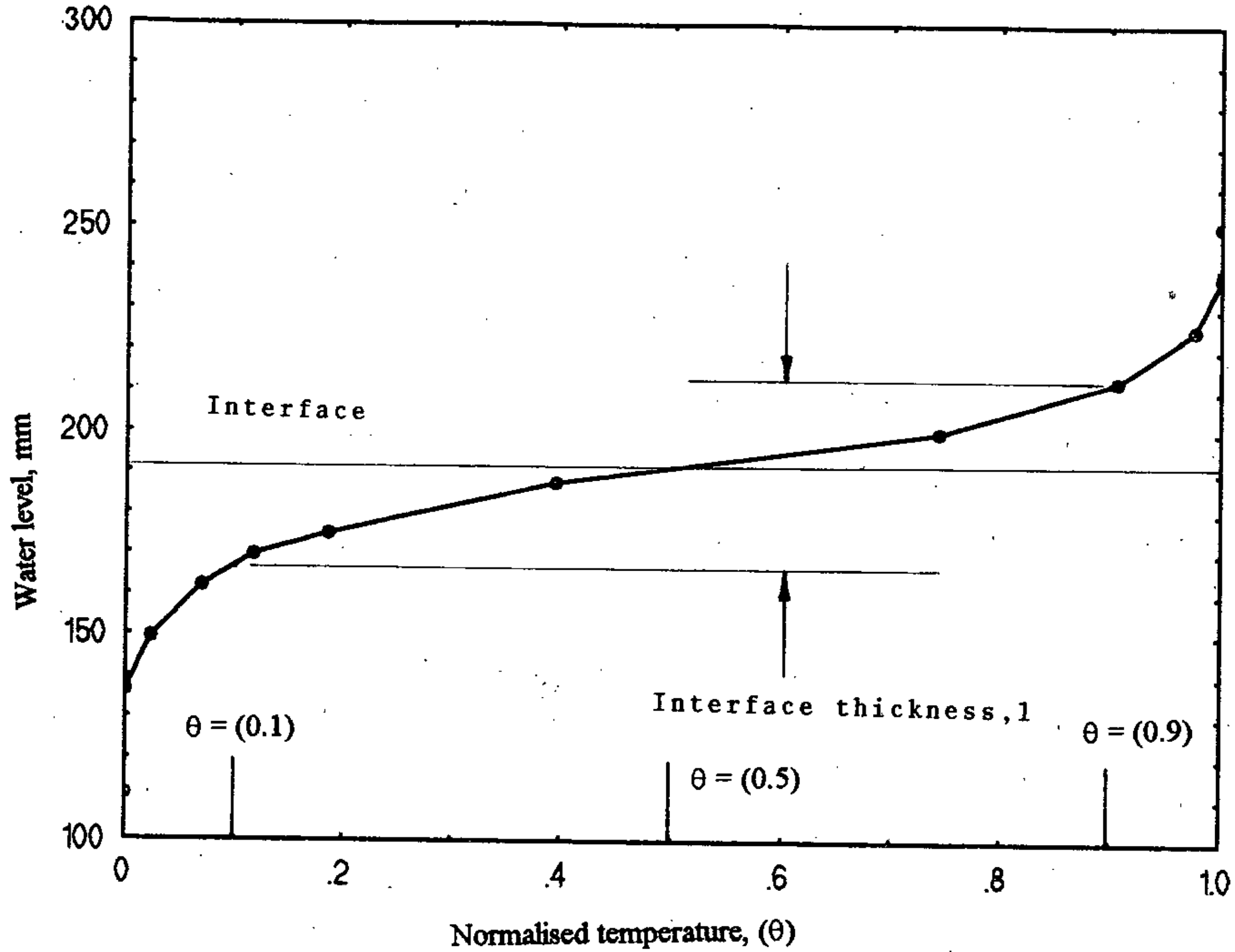

Fig: 3.4 A typical temperature (density) profile

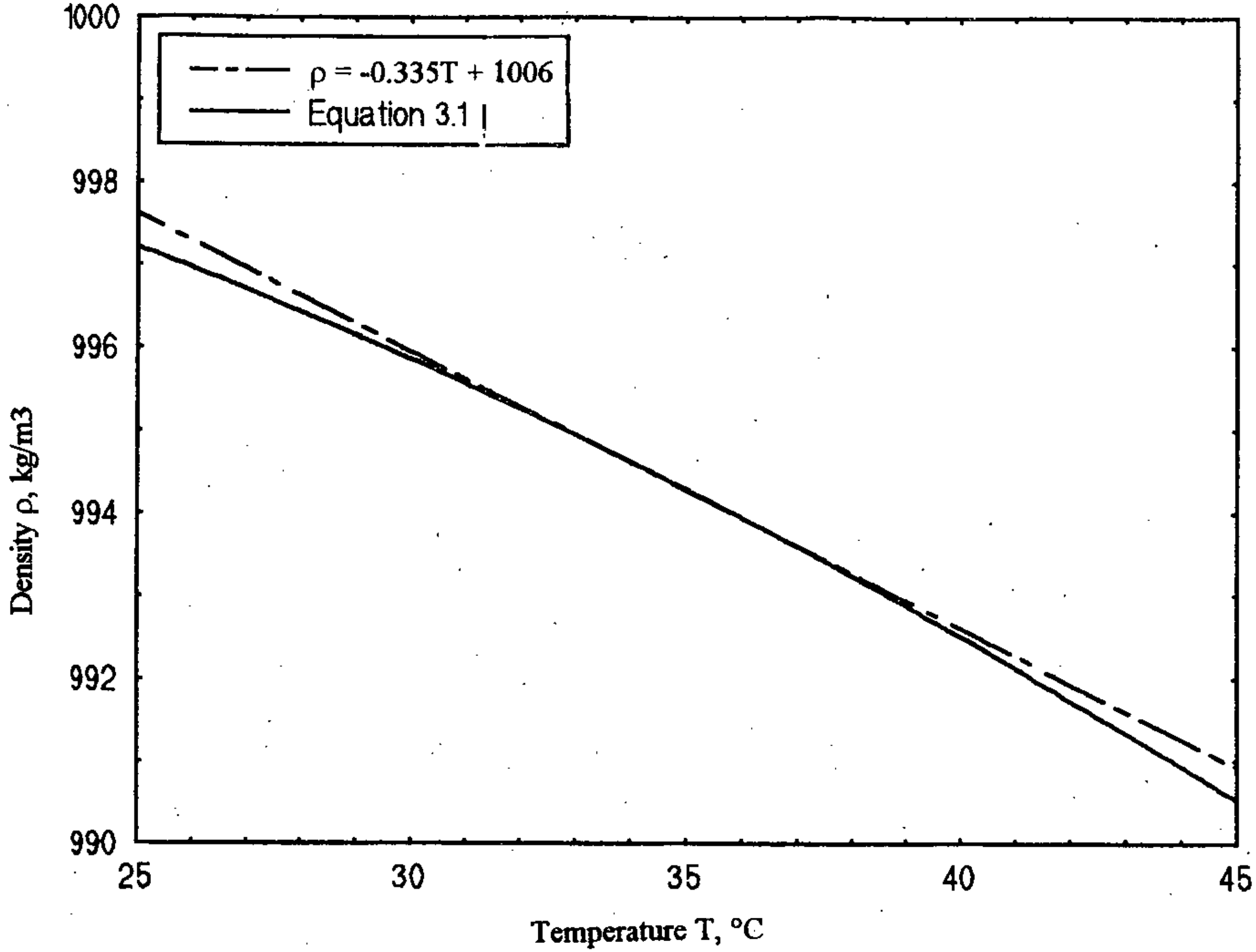

Fig: 3.5 Variation of water density with temperature

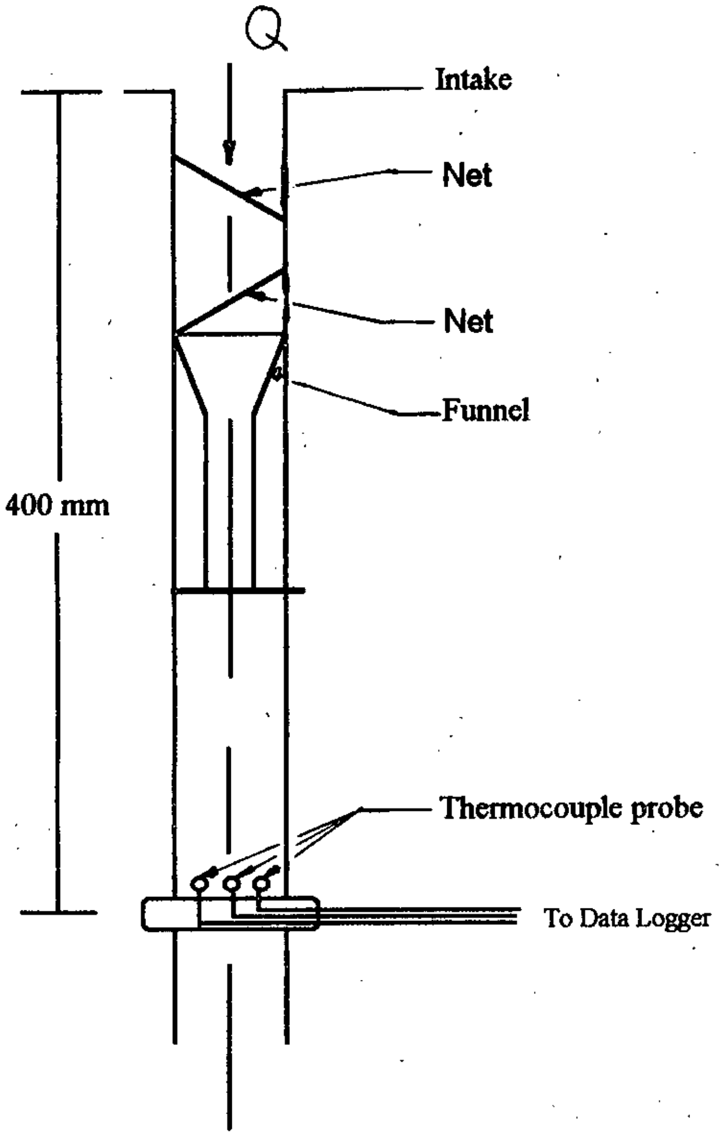

Fig. 3.6 Arrangement of filter, funnel and thermopcuople probe in the discharge pipe

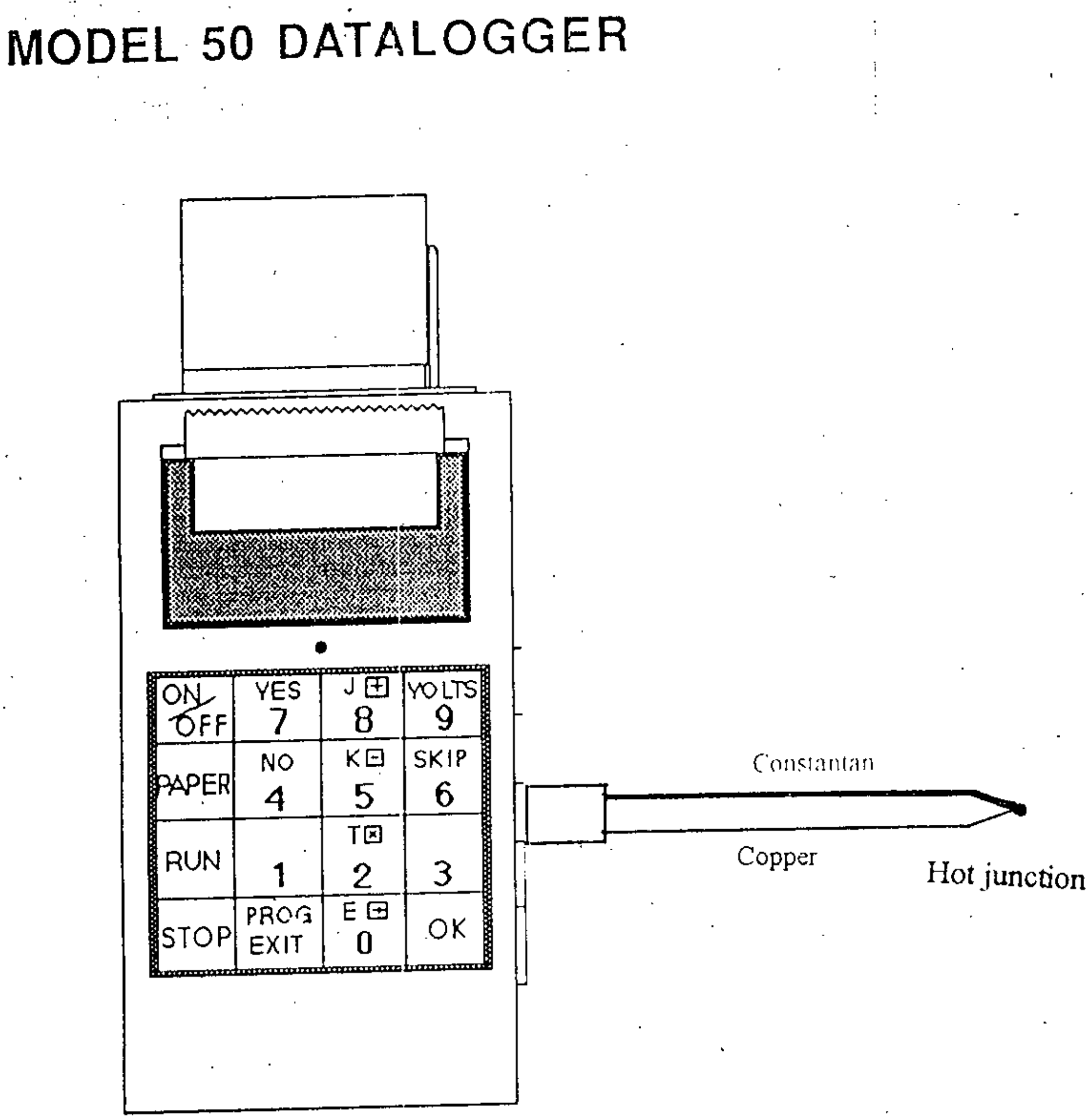

Fig. 3.7 Themocouple circuit of datalogger

CHAPTER - IV

EXPERIMENTAL RESULTS

4.1 INTRODUCTION

The main objective of this experimental investigation is to investigate the effect of sink location on the percentage drawdown. Most recently, Razzaque[1994] had worked in a similar field and studied the effect of intake shape on the drawdown. From his work it is very clear that drawdown is effected by the shape of the sink. He also found that the diameter of the sink itself does not effect the drawdown. In the present experimental work the sink diameter is kept nearly constant throughout the investigation. The location of the sink is varied starting from the bottom of the tank surface up to a certain level. A brief summary of different experimental conditions is provided in Table 4.1. In total twenty four experimental runs is made at eight different sink location throughout this experimental investigation. In the following subsections the effect of intake Froude number and the location of sink on the drawdown is described elaborately.

4.2 Verification of the data with some of the previous work

In this work the location of the sink is varied by placing the sink at several height. Thus one can say that, when the sink is at the bottom of the tank, it is similar to plain intake. Razzaque [1994] worked with plain intake and obtained a relation between the percentage drawdown Λ and logarithmic normalized densimetric Froude number [$(\log(F_r / F_{rc}))$]. Where F_{rc} is the critical densimetric Froude number at some selected drawdown such as 5%, 10%, 15%. He formulated the different equation for different drawdown condition. They are;

i. for F_{rc} at $\Lambda = 5\%$

$$Y = 48.0x^2 + 22.4x + 4.56 \qquad (4.1)$$

ii. for F_{rc} at Λ= 10%

$$Y = 67.9\,x^2 + 44.7x + 9.98 \qquad (4.2)$$

iii. for F_{rc} at Λ = 15%

$$Y = 80.9x^2 + 60.2x + 15.1 \qquad (4.3)$$

where **x** is the value of logarithm of normalized Froude number, i.e. **x** = log (Fr/Frc) and its value lies between -.4 to .4 i.e. -.4 < **x** < .4 .

Data obtained for plain intake from this work is plotted in Fig: 4.1a to Fig: 4.1c and is compared with Razzaque's equation. From the corresponding figures it is very clear that the data of this work agrees with those equations of Razzaque [1994].

Jirka & Katavola [1979] worked on similar field. They performed their experiments in rectangular tank and have placed the sink 0.30m above the above the bottom of the sink. In all of their sixteen experiments, a small degree of withdrawal (Λ < 3%) consistently occurred even at values of Fr well below the incipient condition. This phenomenon have also occurred in this work. It is clear from Fig: 4.1d that at very low values of Fr the value of Λ is not zero rather it is within a value of 3%. Interfacial viscous effects and ambient diffuse interface seem to be responsible for this. They also found that Λ increases significantly as a function of Fr, and a gradual leveling of the curve to the value Λ = 50% as Fr approaches infinity, i.e. when the height of interface becomes zero. For conditions of the interface positions below the intake level, the withdrawal curve has symmetric branch around Λ = 50%. This situation has also occurred in this work and one can easily verify it from Fig:4.1d. The difference between the position of sink of Jirka and this experimental work is that here the sink is placed at the bottom of the tank but Jirka has put it on side wall.

4.3 Dependence of percentage drawdown , Λ, on intake Froude number, F_d

The intake Froude number plays a vital role in the percentage drawdown. Harleman [1959], Goldring [1981], Razzaque [1994] studied the effect of intake Froude number on the drawdown. All of them reported that F_d is a vital parameter for the prediction of the drawdown. In Table 4.2 data of eleven runs are provided and these data are plotted in the Fig:4.3a to Fig: 4.3d. From these figures it is very clear that for higher values of F_d , the value of Λ decreases. This phenomenon agrees with that of Razzaque [1994]. It can be explained by considering that the increase in intake Froude number increases the critical height and at larger critical heights the vertex angle of the drawdown cone becomes sharper which reduces the proportion of the flow area covered by the flow from the diffused part of the lower layer. The figures those are provided, representing the drawdown history at different sink location. From these figures it may be inferred that the variation of Λ, with Fd, reduces at higher heights of the sink.

The density gradient also effects Λ, a steeper density gradient i.e. higher values of g' causes the value of Fd to be low and thus provides higher values of Λ. This type of phenomenon is also described by Goldring [1984] and Islam [1988]. This may be explained in a way that larger temperature differences causes more heat diffusion along the interface which increases the average temperature of the diffused upper portion of the lower layer. This diffusion is responsible for the increased percentage drawdown.

4.4 Effect of sink location on Λ

The location of sink play a vital role in determining Λ. Through this work the sink was elevated gradually within the lower layer of the fluid and data's are plotted in Fig: 4.4a to Fig:4.4b. In Fig: 4.4a Λ is plotted with instantaneous densimetric Foude number F_r for different sink location. The figures show that Λ varies for the same Fr for different sink location. The value of Λ decreases at higher sink location for the same Fr. Again, a symmetrical curve as described by Zirka & Katavola [1979] is not observed till the sink reaches a certain elevation.

4.4.1 Dependence of the critical densimetric Froude number Fr with sink elevation

From Fig: 4.4a to Fig:4.4b a conclusion may be made that the pattern of the flow changes with the location of sink. When the sink is very near to the bottom surface it behaves much like plain intake. But as the height of the sink gradually increases the flow behavior changes and after a certain height the nature of the flow becomes as those described by Zirka & Katavola. In Table-4.3 the value EX/H and the corresponding critical densimetric Froude number at 5%, 10%, 15% drawdown is provided. These data are plotted in the Fig: 4.4.1a to Fig: 4.4.1c, and it is found that after a certain value of EX/H the value of F_{rc} appears to be constant. For all the three values of Λ as mentioned above the critical value of $(EX/H)_{cr}$ **is 1/5 or 0.2 .**

In Fig: 4.4.1d, the experimental runs having EX/H greater than .2 are plotted. The curve shows that after a particular EX/H ratio drawdown history curve of all runs fall in the same region.. Densimetric Froude number becomes a dominating tool for determining the value of Δ and the effect of F_d and F_l becomes less important. Best fit curves are drawn considering all the data obtained from the drawdown history, for EX/H > 0.2. The maximum deviation of the curve is $\pm 6.5\%$. The best fit equations are summarized below;

$$\Lambda = 4.60[\log (F_r)]^3 + 11.5[\log (F_r)]^2 + 7.71[\log (F_r)] + 2.31 \qquad (4.4)$$

$$\text{for } -0.75 \leq \log (F_r) < 0.75$$

$$\Lambda = 1.44[\log (F_r)]^3 - 14.8[\log (F_r)]^2 + 53.2[\log (F_r)] - 16.5 \qquad (4.5)$$

$$\text{for } 0.75 \leq \log (F_r) < 4.00$$

4.5 CONCLUSIONS

This investigation shows that the location of sink play an important role in selecting the strata of fluid at sink level. Following facts are established from this investigation

1. The percentage drawdown is decreased for a particular density gradient and particular diameter when the intake Froude number is increased.
2. Sink location plays an important role in determining the drawdown history. For EX/H≥0.2 the value of F_d and F_l has less significant effect on dradown history of fluid, rather in such state the effect of densimetric Froude number becomes notable.
3. For EX/H ≥0.2 densimetric Froude number becomes predominant in determining the value of Λ. In this region the value of F_d and F_l becomes least predominant.
4. A generalized relationship between densimetric Froude number and percentage drawdown for a sharp round sink located at EX/H > 0.2 is established.

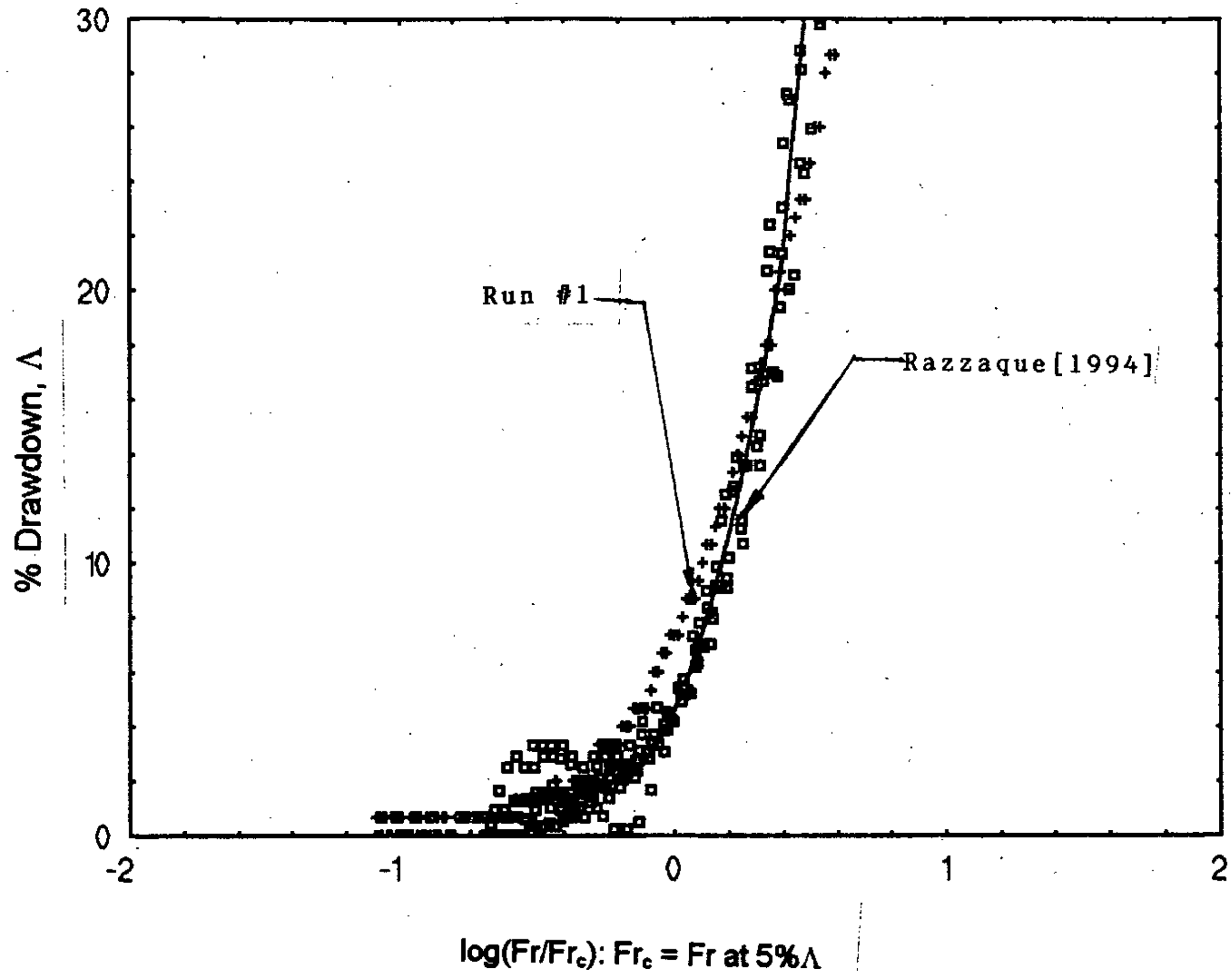

Fig: 4.1a Verification of the data set of Run # 1 with Razzaque[1994]

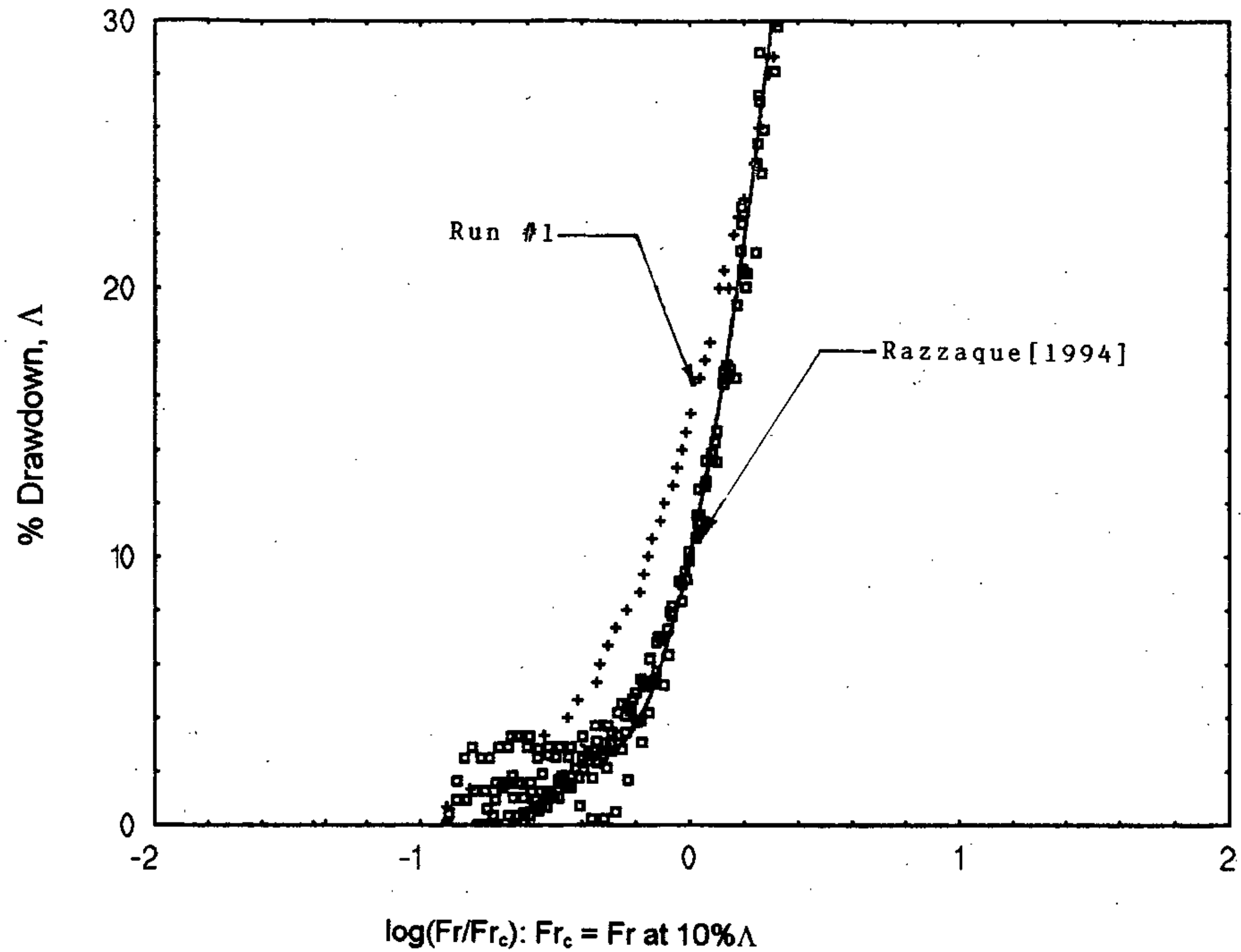

Fig: 4.1b Verification of the data set of Run # 1 with Razzaque[1994]

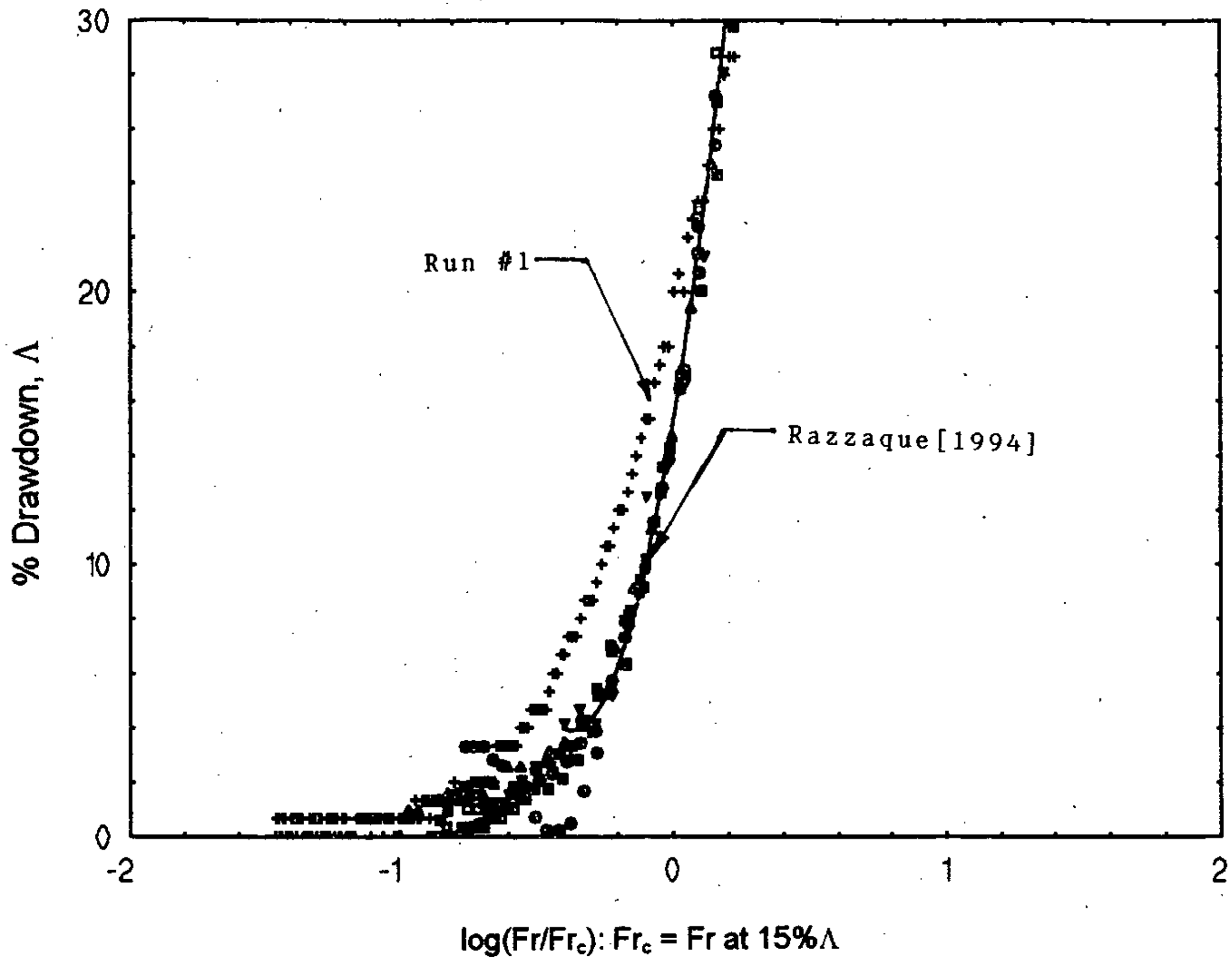

Fig: 4.1c Verification of the data set of Run # 1 with Razzaque[1994]

89/78

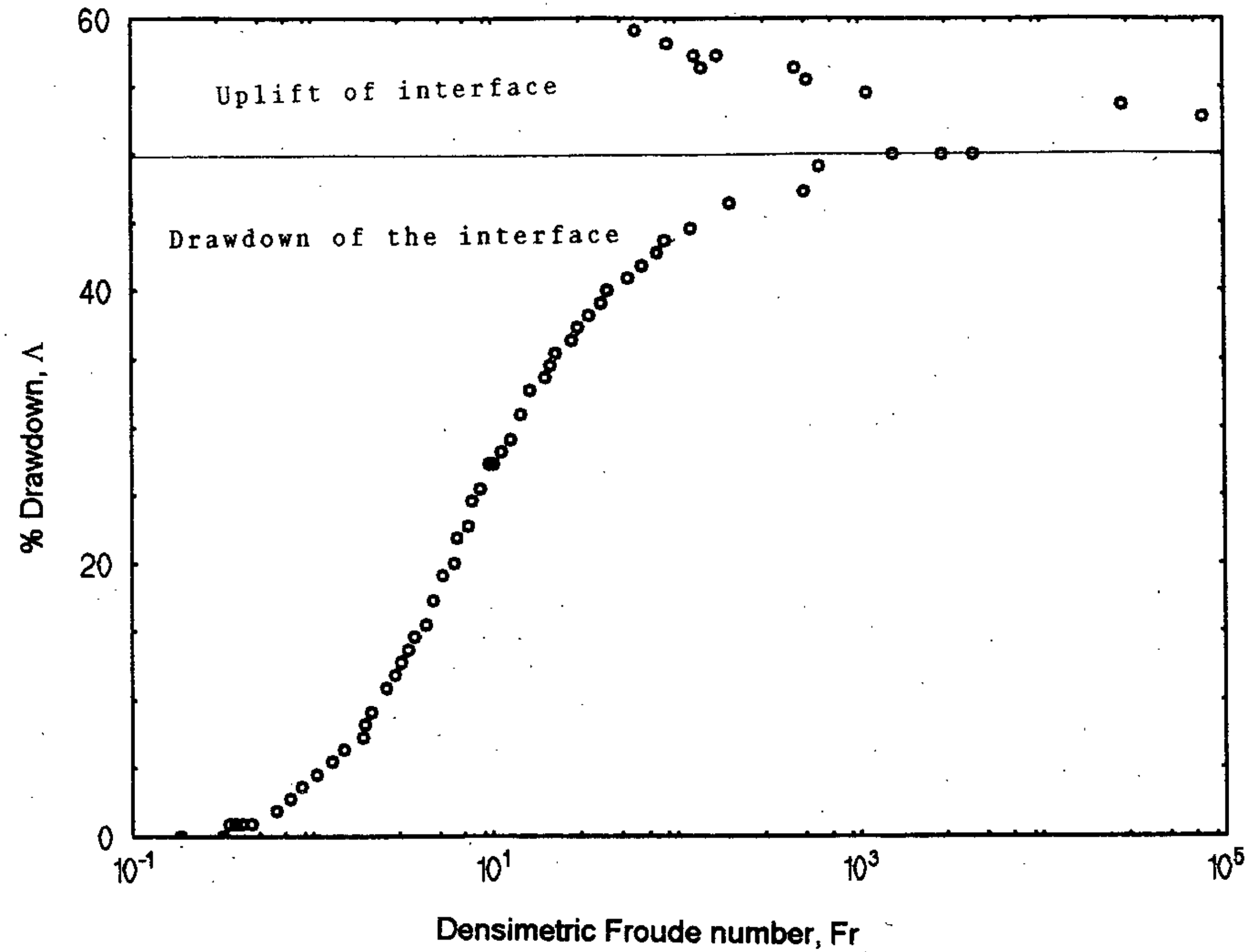

Fig: 4.1d Drawdown history of run #10

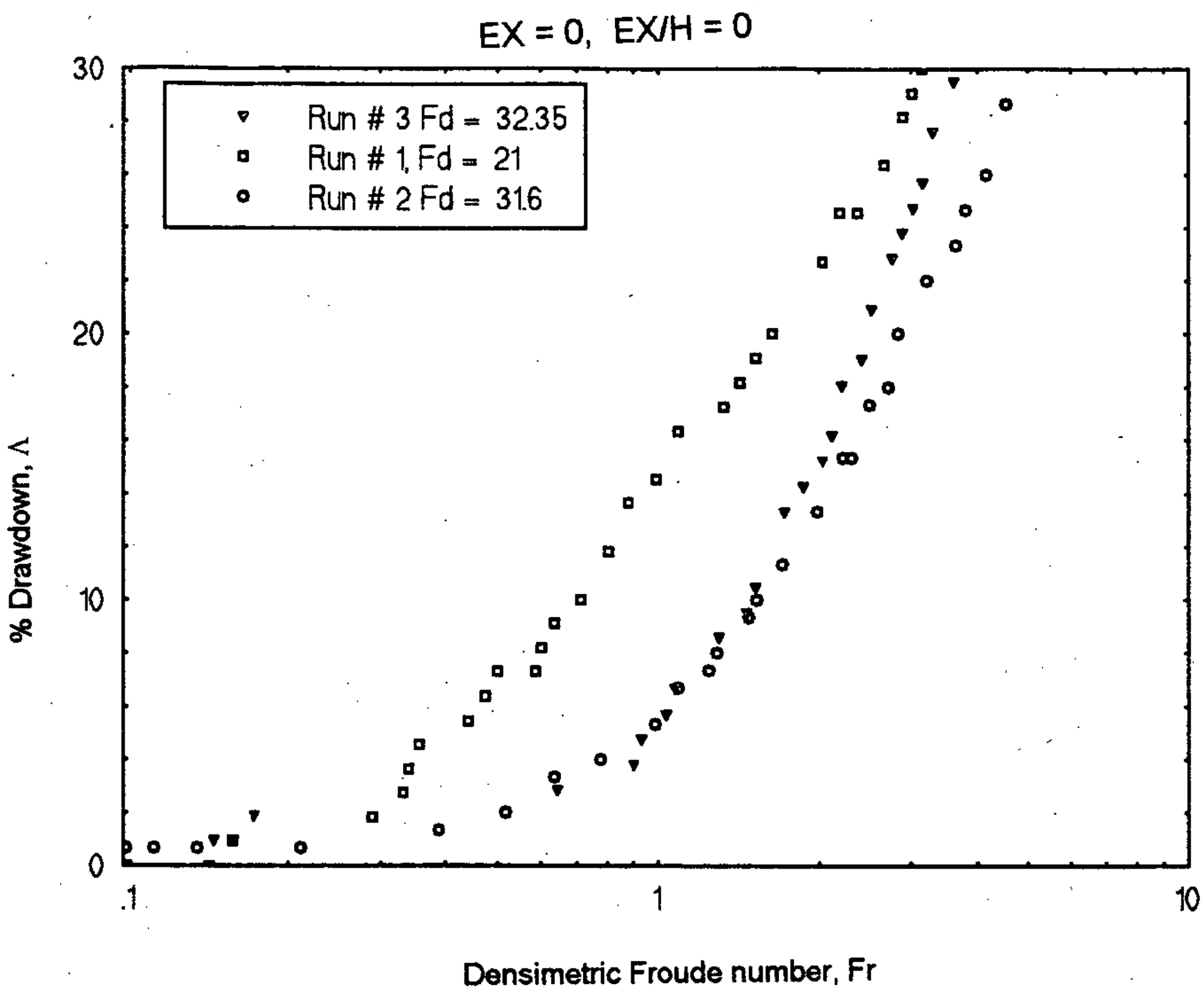

Fig: 4.3a Dependence of Λ on Intake Froude number, Fd

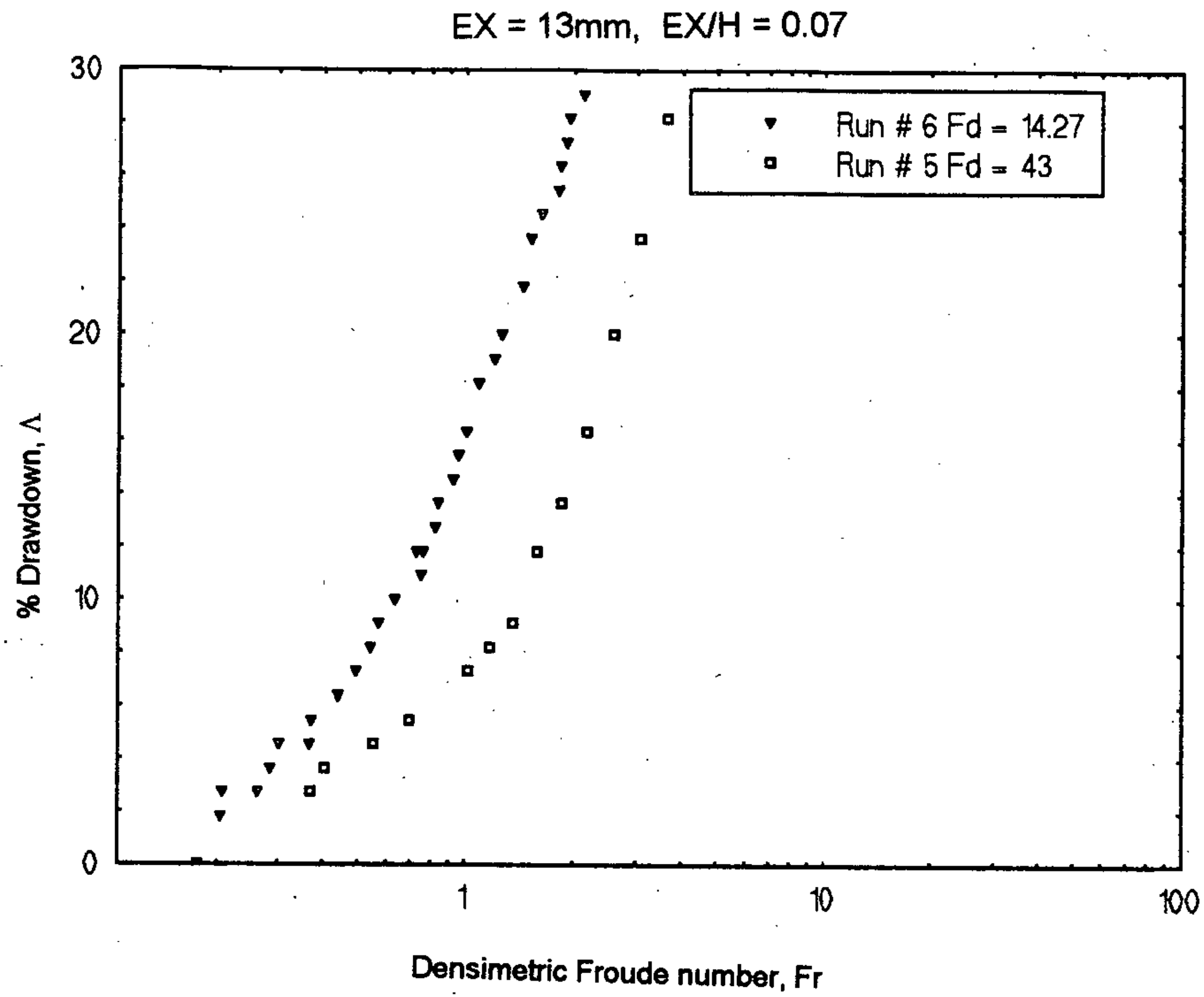

Fig: 4.3b Dependence of Λ on Intake Froude number, Fd

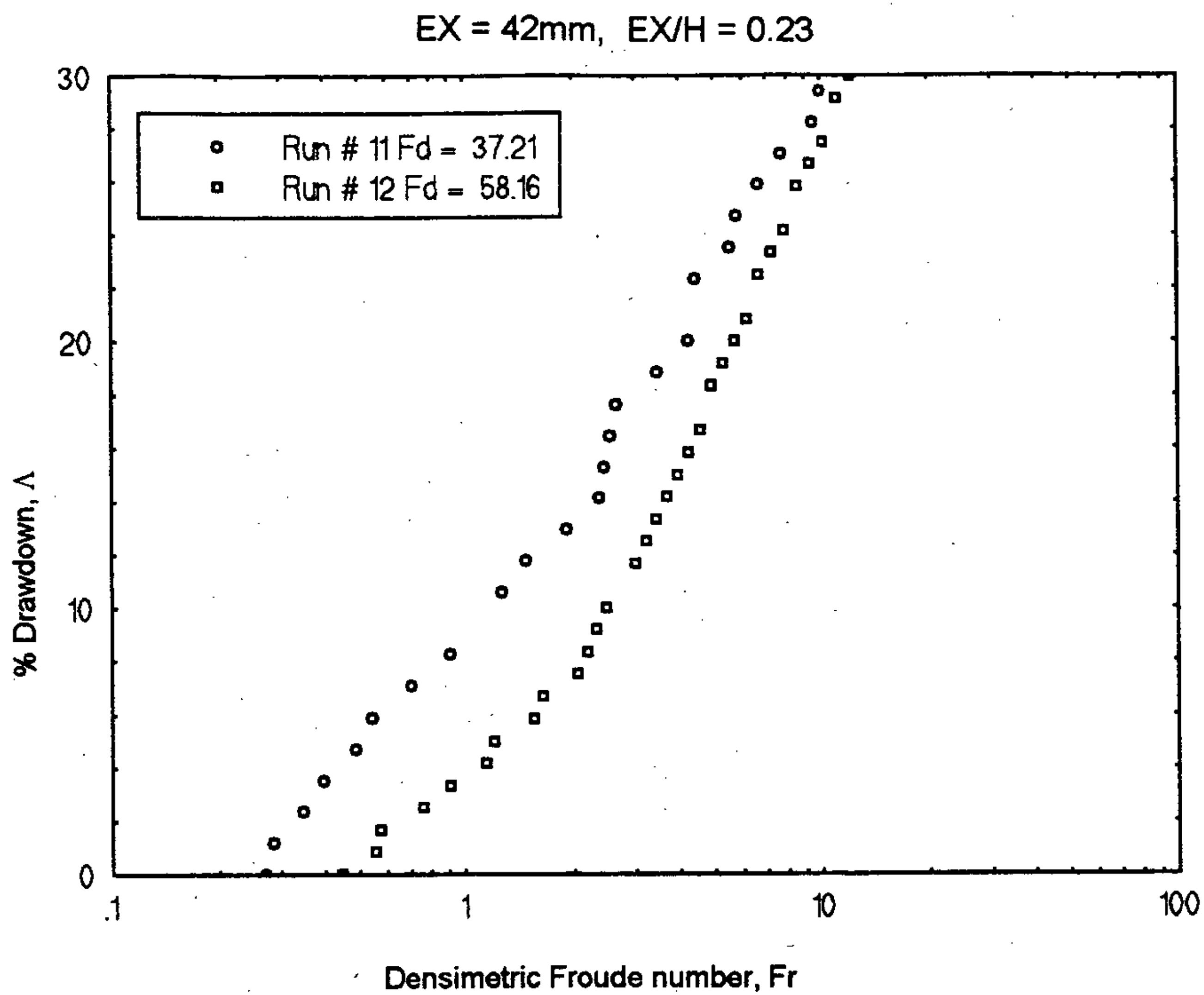

Fig: 4.3c Dependence of Λ on Intake Froude number, Fd

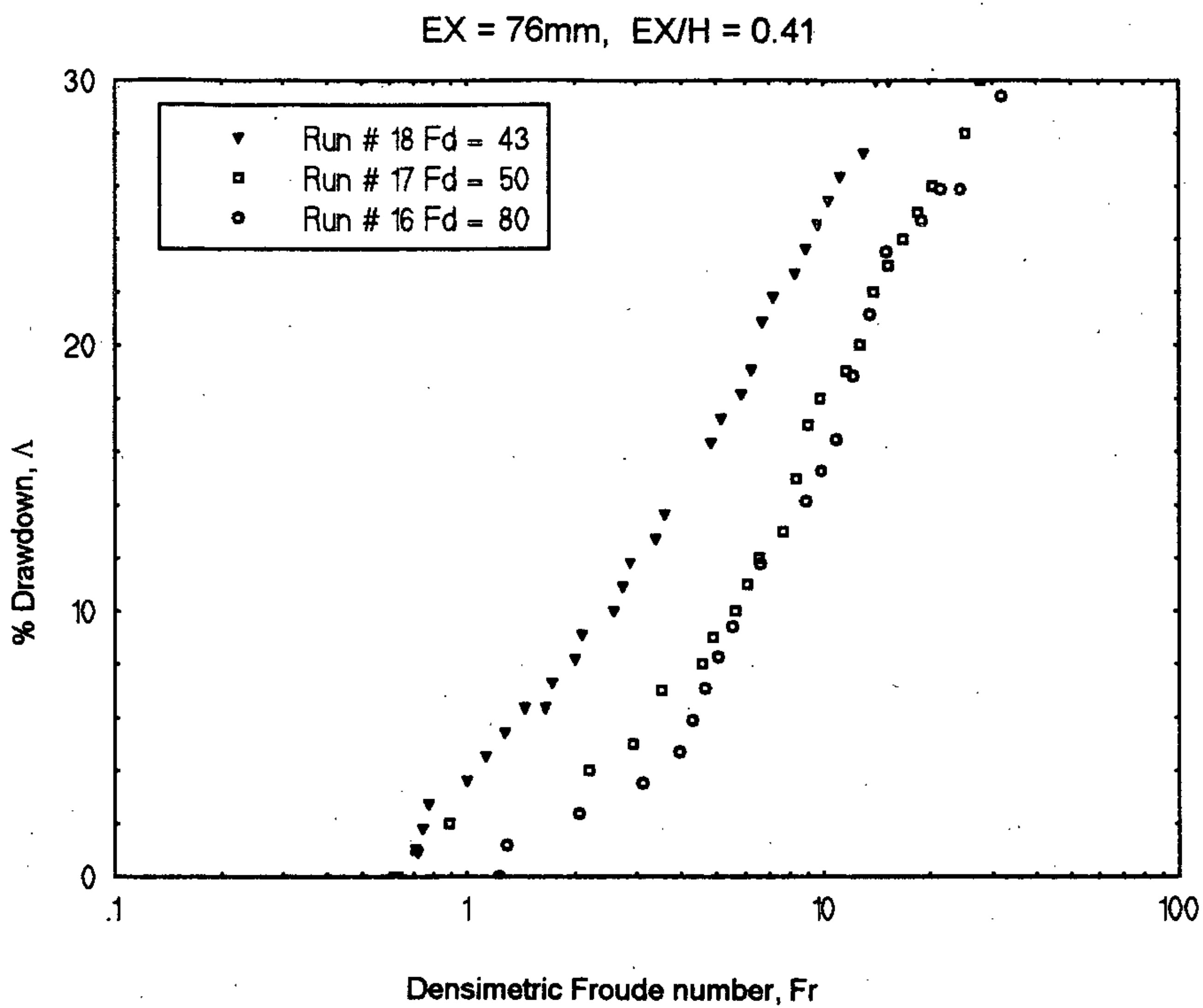

Fig: 4.3d Dependence of Λ on Intake Froude number, Fd

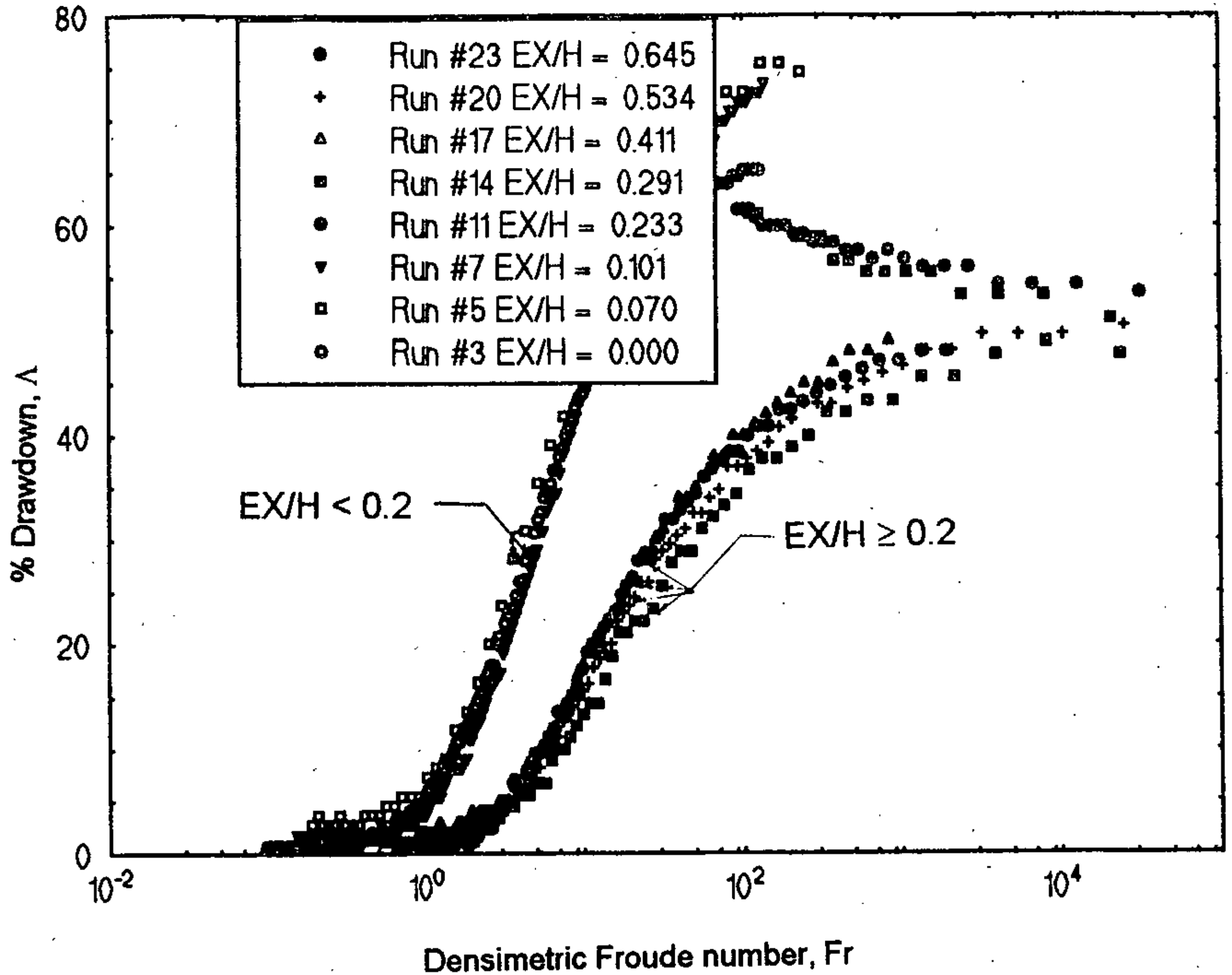

Fig: 4.4a Drawdown history at several location of sink

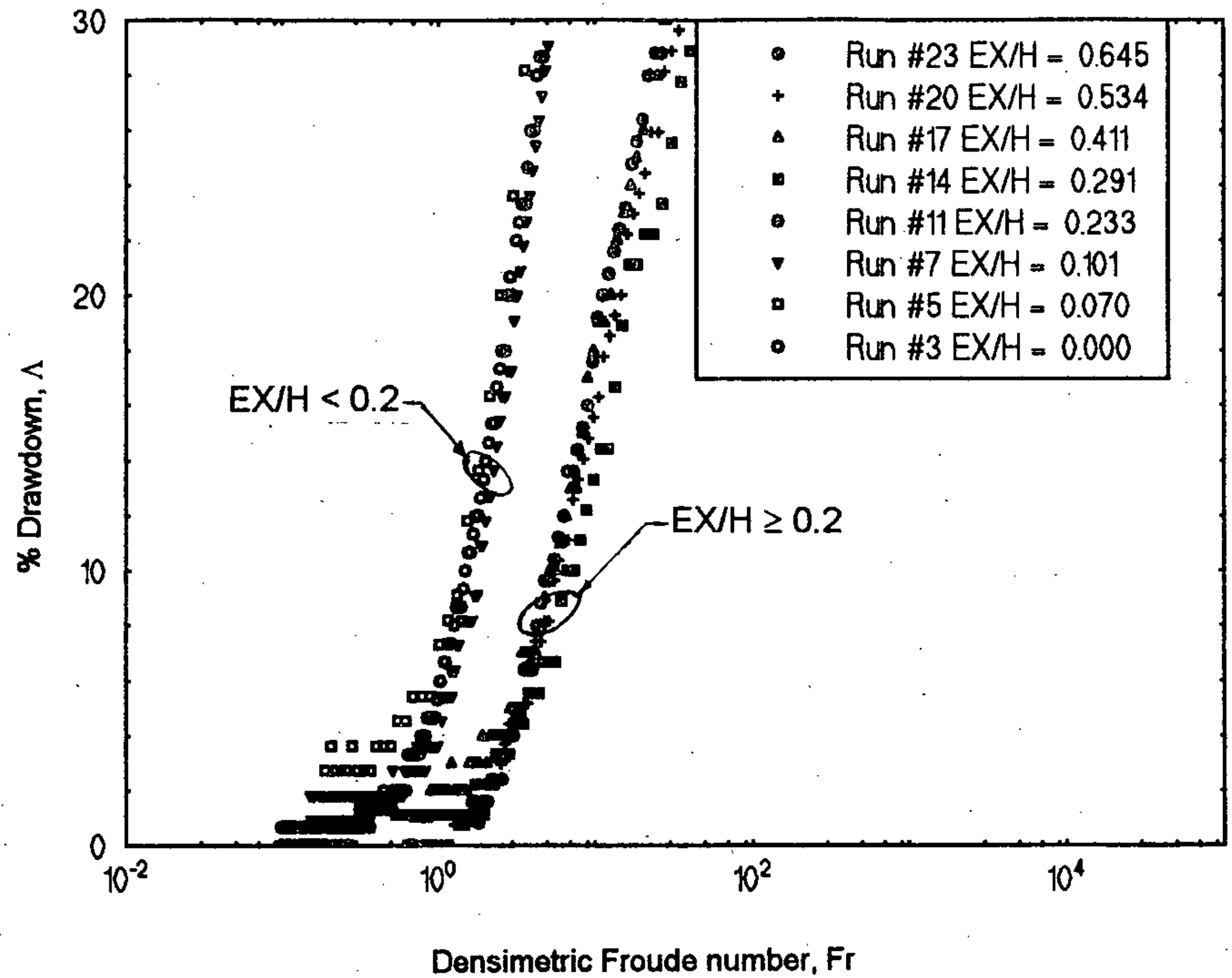

Fig: 4.4b Drawdown history at several location of sink

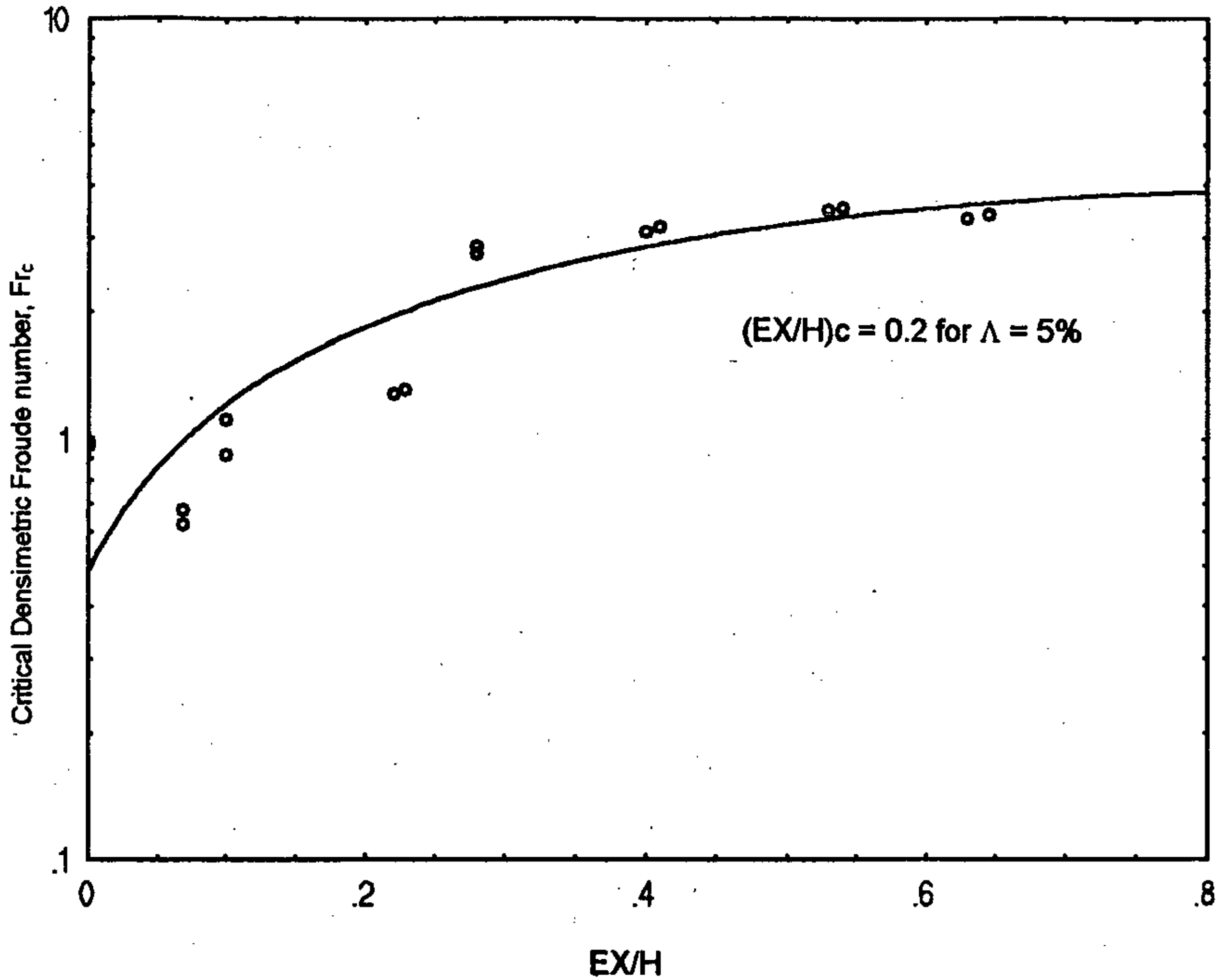

Fig: 4.4.1a Determination of critical value of (EX/H)

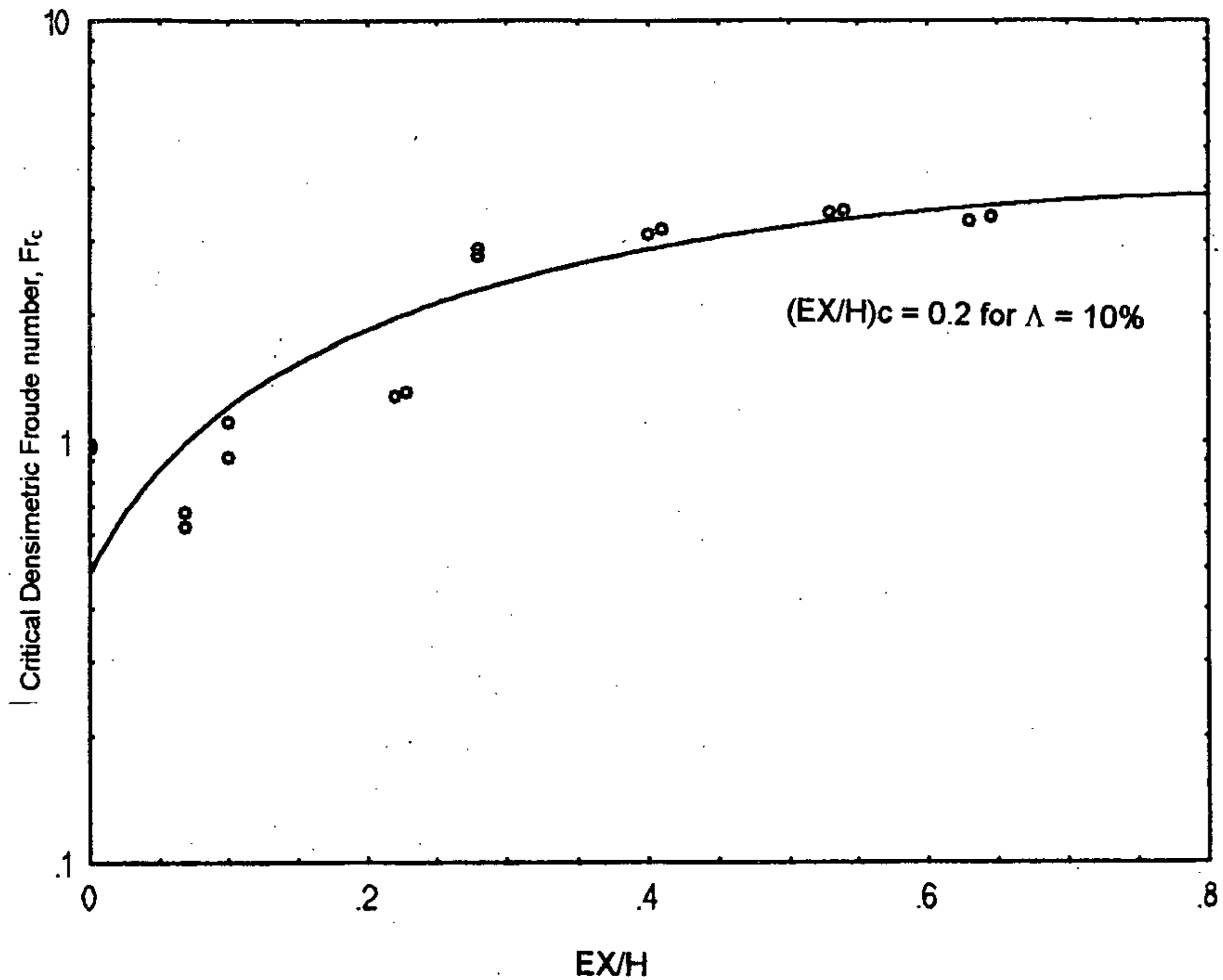

Fig: 4.4.1b Determination of critical value of (EX/H)

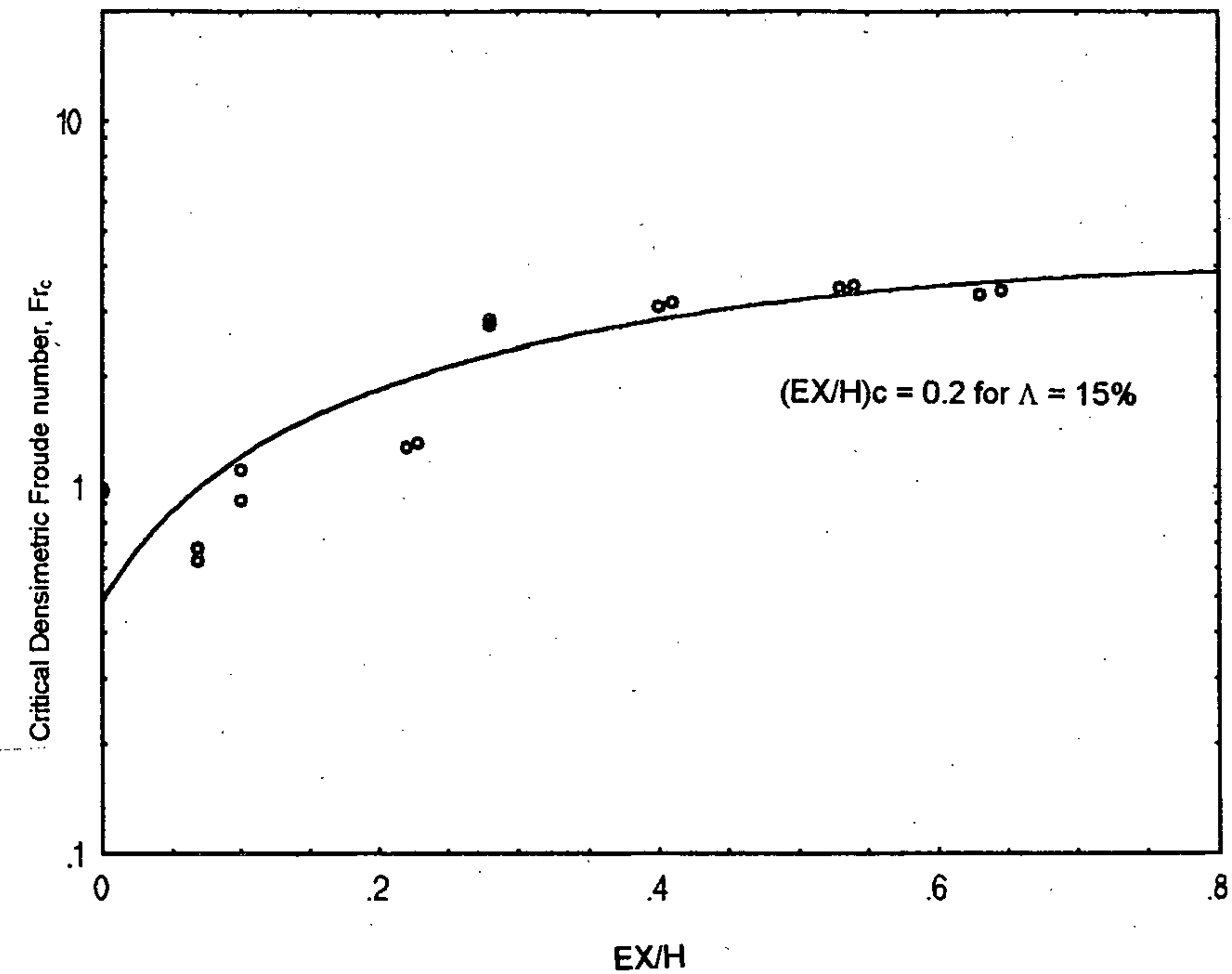

Fig: 4.4.1c Determination of critical value of (EX/H)

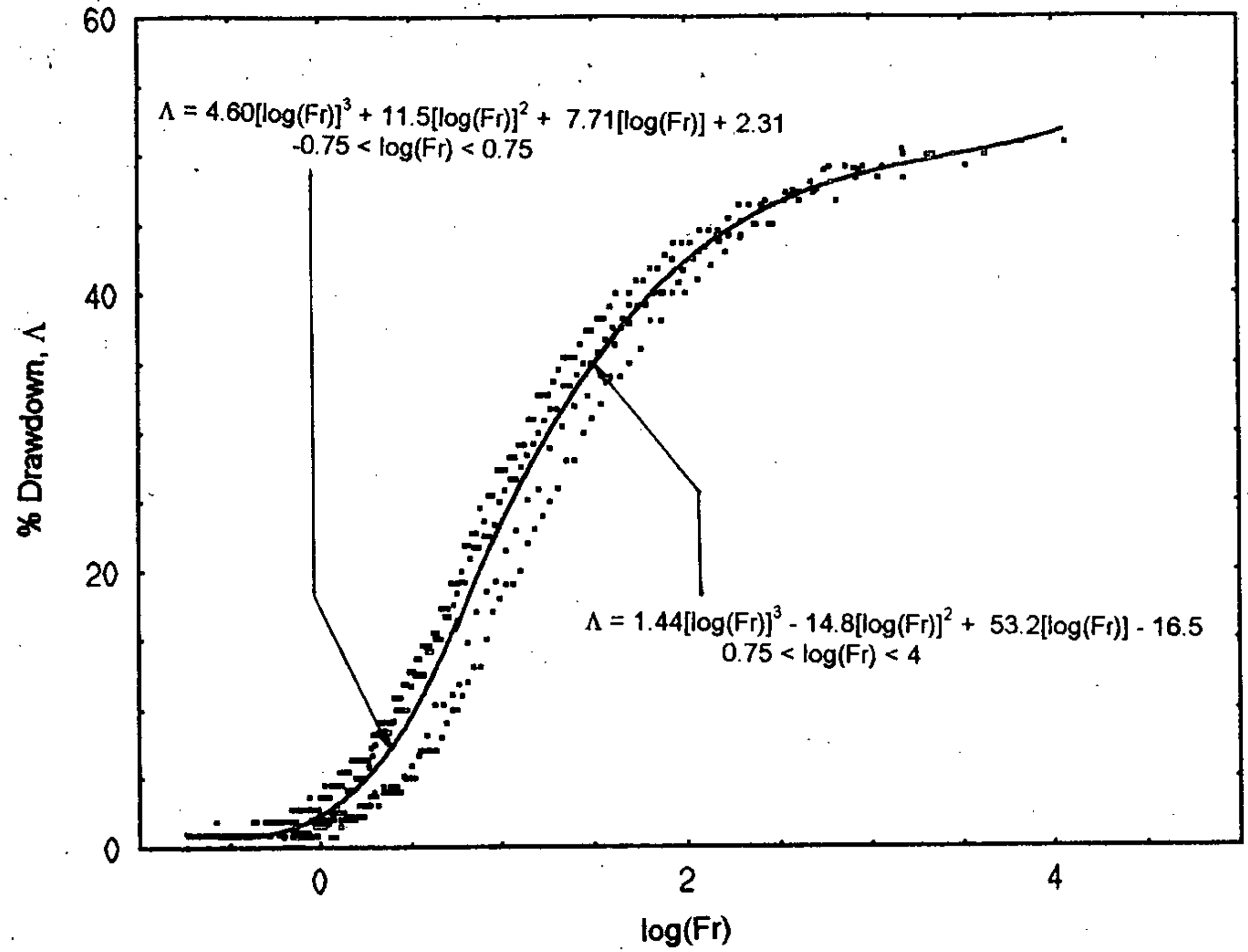

Fig: 4.4.1.d Drawdown history at several location of sink (EX/H>0.2)

TABLE 4.1

CODE	RUN	EX mm	D mm	Q L/MIN	l mm	H mm	T_1 °C	T_2 °C	g	F_d	F_l
L30	1	0	21.5	17.38	37	186	35	20	40	21	5.6
L28	2	0	21.5	22.41	60	185	34	23	30.34	31.6	2.43
L29	3	0	21.5	23.35	33	192	36.5	26	31.51	32.35	11.34
L31	4	13	19	19.63	38	189	41	22	57.2	27.5	5.02
L34	5	13	19	22	38	184	33	22	29.35	43	7.6
L35	6	13	19	7.30	44	191	33	22	29.35	14.27	1.75
L42	7	19	19	18.94	39.1	187	35	23	33.62	34.57	5.7
L43	8	19	19	18.82	36.2	189	35	23	28.62	37	7.4
L44	9	19	19	20.2	41.0	188	35	24	31.31	38	5.58
L46	10	42	19	15.1	40.2	183.7	37	26	33.24	27.73	4.26
L47	11	42	19	17.10	52	180	35.5	27	23.54	37.21	3.0
L52	12	42	19	34.11	41.5	182.1	38.5	26	38.56	58.16	8.24
L48	13	54	19	50	41.8	187.6	39	25.5	41.63	82	11.43
L49	14	54	19	33	44.5	185.3	36	27	27.21	66	8
L51	15	54	19	22.5	43.1	184.5	38.5	27	36	39.76	5.13
L53	16	76	19	38.24	49.2	188.4	35	26.5	25.15	80.75	7.48
L54	17	76	19	26.28	45.5	184.5	37.5	27.5	31	49.9	5.6
L55	18	76	19	24.17	53	180.7	38	27	34	43.78	3.36
L39	19	100	19	22.94	43	185	35	22	35.8	40.5	5.26
L40	20	100	19	20.44	38	187	36.5	23	38.69	34.8	6.15
L41	21	100	19	19.5	36	190	36	24	34.67	35.23	7.13
L36	22	120	19	16.63	40	188.4	34.5	24	29.66	32.33	5.02
L37	23	120	19	21.08	44	186	35	22.5	34.73	37.88	4.64
L38	24	120	19	8.33	51	180.5	33	24	24.84	17.75	1.50

TABLE 4.2

RUN	Diameter mm	EX mm	Q L/MIN	L mm	H mm	EX/H	F_d
1	21.5	0	17.38	37	186	0.000	21
2	21.5	0	22.41	60	185	0.000	31.6
3	21.5	0	23.35	33	192	0.000	32.35
4	19	13	19.63	38	189	0.068	27.5
5	19	13	22	38	184	0.070	43
6	19	13	7.30	44	191	0.068	14.27
11	19	42	17.10	52	180	0.233	37.21
12	19	42	34.11	41.5	182.1	0.231	58.16
16	19	76	38.24	49.2	188.4	0.403	80.75
17	19	76	26.28	45.5	184.5	0.411	49.9
18	19	76	24.17	53	180.7	0.420	43.78

TABLE 4.3

RUN	EX mm	Q L/MIN	H mm	EX/H	F_{rc}		
					Δ=5%	Δ=10%	Δ=15%
1	0	17.38	186	0	.986	1.52	2.2
3	0	23.35	192	0	.962	1.48	1.97
4	13	19.63	189	.068	.626	.875	1.08
6	13	7.30	191	.068	.678	.756	.940
7	19	18.94	187	.100	1.11	1.88	2.45
8	19	18.82	189	.100	.917	1.41	2.45
10	42	15.1	183.7	.228	1.31	2.45	4.05
12	42	34.11	182.1	.228	1.28	2.51	3.95
13	54	50	187.6	.280	2.76	4.46	6.69
14	54	33	185.3	.291	2.86	4.02	6.80
16	76	38.24	188.4	.400	3.11	5.39	8.50
17	76	26.28	184.5	.410	3.19	5.52	8.50
19	100	22.94	185	.540	3.54	6.38	10.5
20	100	20.44	187	.530	3.5	5.79	9.35
22	120	16.63	188.4	.630	3.34	5.52	8.91
23	120	21.08	186	.645	3.42	5.27	8.10

CHAPTER - V

CLOSURE OF THE THESIS

5.1 INTRODUCTION

The objective of this experimental work is to study the selective withdrawal from stratified fluid system. Results of this work is presented in previous chapter. In the following subsections a brief description of the overall work and a guideline or suggestion for future extension of this work is provided.

5.2 Review of the present work

Twenty four 'experimental run' were carried out at eight different locations of the sink. From the experimental data it is evident that location of sink plays an important role in the drawdown history. If the sink is located very near to the bottom of the tank, it works the same as plain intake; but when the sink is elevated to a height such that EX/H>0.2, the behavior of the withdrawal becomes very significant. For such a height, the effect of F_l and F_d becomes insignificant in the drawdown history, densemitric Froude number Fr becomes the governing parameter in controlling the drawdown history. A brief summery of the findings of this work is followed,

1. The percentage drawdown is decreased for a particular density gradient and particular diameter when the intake Froude number is increased.
2. Sink location plays an important role in determining the drawdown history. For EX/H≥0.2 the value of F_d and F_l has less significant effect on drawdown history of fluid, rather in such state the effect of densimetric Froude number becomes notable.
3. For EX/H ≥0.2 densimetric Froude number becomes predominant in determining the value of Λ. In this region the value of F_d and F_l becomes least predominant.
4. A generalized relationship between densimetric Froude number and percentage drawdown for a sharp round sink located at EX/H > 0.2 is established.

5.3 Guideline and recommendation for future work

Following recommendations are made for future work.

1. The present work may be extended by varying the thickness of the stratified layer, diameter of the sink, height of the bottom layer to investigate the effect of the critical location of the sink and the drawdown history.
2. A generalized relation between percentage drawdown and the value of the intake Froude number may be established.
3. The present flow phenomenon is very simple relative to the real life. Thus the parameters involved in the real flow such as topographical effect, wind shear and heat loss at the free surface, steady and unsteady cross flow, multiple intake system, etc. may be included in the experiments.
4. A method for computational prediction of the present work may be developed.

REFERENCES

Baines W. D., Martin W. W. & Smith D. M. (1983), "Development of Stratification in a Rectangular Tank by Horizontal Inflow", J. Fluids Engineering, ASME, Vol. 105, pp. 59-64.

Baker H. D., Ryder E. A. & Baker N. H. (1953), "Temperature Measurement in Engineering", Vol. I, John Wiley & Sons, Inc., New York, Chapman & Hall Limited, London.

Baker H. D., Ryder E. A. & Baker N. H. (1961), "Temperature Measurement in Engineering", Vol. II, John Wiley & Sons, Inc., New York, London.

Bohan J. P. & Grace Jr. J. L. (1973), "Selective withdrawal from Man-Made Lakes U.S. Army Engineering, Waterways Experiment Station", Tech. Report No. H-73-4.

Brooks N. H. & Koh R. C. Y (1969), "Selective Withdrawal from Density Stratified Reservoirs", J. Hydr. Divn. ASCE, Vol. 95, HY4, pp. 1369-1400.

Debler W. R. (1959), "Stratified flow into a line sink", J. Eng. Mech. Divn., ASCE, pp. 51-65.

Goldring B. T. (1981), "The effect of a hood on drawdown criteria in zero cross flow", Report No. RD/L/2032/N81, Central Electricity Research Laboratory, Leatherhead, England.

Harleman D. R. F., Morgan R. L. & Purple R. A. (1959), "Selective withdrawal from a vertically stratified fluid paper 10-C", Proc. of the 8th congress of IAHR, Montreal, Canada.

Harleman D. R. F. (1959), "Stratified flow Handbook of Fluid Dynamics", Editor: Streeter V.L., McGraw Hill.

Hino M. & Onishi S. (1969), "Investigation of Axisymmetric Stratified Flow towards a Point sink Coastal Engineering in Japan", Vol. 12, pp. 179-187.

Hocking G. C. (1991), "Withdrawal from two layer fluid through line sink", J. Hydr. Engineering, ASCE, Vol. 117, No. 6, pp. 800-805.

Hocking G. C. (1991), "Critical Withdrawal from two layer fluid through line sink", Vol. 25, pp. 1-11.

Holman J. P. (1984), "Experimental Methods for Engineers, 4th ed., McGraw Hill Int. Book Co.

Imberger J. & fischer H. B. (1970), "Selective withdrawal from a stratified reservoir Environmental protection agency, water quality office, Water Pollution Res. Series 15040 EJZ 12/70.

Imberger J. (1972), "Two-dimensional sink flow of a stratified fluid contained in a duct", J. Fluid Mech., Vol. 53, pp. 329-349.

Imberger M. & Munson B. (1986), "The flow of two-layer fluid system into a line sink", Report No. 86-WA/FE-7, Winter Annual Meeting, ASME, December 7-12, Anaheim, California.

Islam A. K. M. S. (1988), "Prediction of selective withdrawal phenomena in stratified cross flowing streams", Ph.D. Thesis, Imperial College, University of London, England.

Ivey G. N. & Blake S. (1985),"Axisymmetric withdrawal and inflow in a density stratified container", J. Fluid Mech., Vol. 161, pp. 115-137.

Jirka G.H. Watanabe M. (1980)
Thernmal structure of cooling ponds
J. Hydr. Divn, ASCE, Vol 106. HY5, pp 701-715.

Kao T. W. (1965)
A free streamline solution for stratified flow into a line sink J. Fluid Mech., Vol 21, pp 535-543.

Kao T. W. (1966)
Selective withdrawal criteria of stratified fluids J. Hydr. Divn., ASCE, Vol 102, HY6, pp 717-729.

Koh R.C.Y. (1966a)
Viscous stratified flow towards a sink
J. Fluids Mech., Vol 24, pp 555-575.

Koh R.CY. (1966b)
Unsteady stratified flow into a line sink J. Hydr. Res., Vol 4, No. 2 pp 21-34.

Lawrence G.A. & Imberger J. (1979)
Selective withdrawal through a point sink in a continuously Stratified fluid with pycnocline. Report No. ED-79-002,
Centre for water Research, Univ. of Western Australia.

Lawarence G.A. (1980)
Selective withdrawal through a point sink 2nd Int. symp. on stratified Flows. IAHR,
Trondheim, Norway, pp 411-425.

Lubin B. T. & Springr G. S. (1967)
The formation of a dip on the surface of a liquid draining from a tank J. Fluid Mech., Vol 29, part 2, pp385-390.

Magony J. J & pritchard W. G. (1977)
Withdrawal from a reservoir of stratified fluid Report No. 79, Fluid Mech. Res. Inst. University of Essex, Colchester, Essex.

Makarov I.I. & Zisman S.L. (1972)
On the peculiarities of water supply to thermal and nuclear power plants from stratified streams and reservoirs proc. IAHR Symp. on Stratified Flows, Novosibirsk, pp369-381.

McGuirk J.J. & Islam A.K.M.S. (1986)
Selective withdrawal from a stratified flow into a line sink pric. of Int. Symp. on Buoyant Flows, Athens, Greece.

McGuirk J.J. & Islam A.K.M.S. (1987)
Numerical modelling of the influence of a hood on axisymmetric withdrawal from a density stratified environment Int.l Conf. on Stratified Flows, Caltech, California, U.S.A.

Moffat R.J. (1988)
Describing the uncertainties in experimental results J. Experimental thermal and Fluid Science, Vol 1, pp 3-17.

Onishi S. Imamura K., Terata H. & Shibuya H. (1982)
Study on selective withdrawal by axisymmetric intake with finite opening Coastal Engineering in Japan, Vol 25, pp 251-260.

pao H.p. & Kao T.W. (1974)
Dynamics of establishment of selective withdrawal of a stratified Fluid from a line sink; part 1: Theory
J. Fluid Mech., Vol 65, pp 657-688.

Rahman M. (1978)
Temperature structure in large bodies of water J. Hydr. Res., Vol 17, pp 207-215.

Spiegel R.H. & Farrant B. (1984)
Selective withdrawal through a point sink and pycnocline formation in linearly stratified flow
J. Hydr. Res., Vol 22, No 1, pp 35-51

Streeeter V.L. & Wylie E. B. (1979)
Fluid Mechanics, 7th ed.
McGraw Hill Book Co.

Turner J. S. (1973)

Buoyancy Effects in Fluids
Cambridge University Press, Cambridge.

Vanden-Broeck J. & Keller J. B. (1987)
Free surface flow due to a sink
J. Fluid Mech., Vol. 175, pp. 109-117.

Wen X. & Ingham D. B. (1992)
Flow induced by a submerged source or sink in a three layer fluid
J. Computers Fluids, vol. 21, No. 1, pp. 133-144.

Wood I. R. (1978)
Selective withdrawal from two-layer fluid
J. Hydr. Divn., ASCE, HY12, pp. 1647-1659.

Yih C. S. (1980)
Stratified Flows
McMillam, New York.

Zhou Q. & Graebel W.P. (1990)
Axisymmetric draining of a cylindrical tank with a free surface
J. Fluid Mech., Vol. 221, pp. 511-532.

Razzaque[1994], M.Sc. Thesis,
Axisymmetric Withdrawal From a Two-Layered Fluid System, Mechanical Engineering Department, Bangladesh University of Engineering & Technology, Dhaka.

APPENDIX - A

UNCERTAINTY ANALYSIS

A.1 INTRODUCTION

Errors will creep into all experiments regardless of the care which is exerted. If the experimenter knew what the error was, he or she should correct it and it would no longer be an error. But in most situations, we cannot talk very confidently about what the error in a measurement is, we can only talk about what it `might be'- about the limits that we feel bound the possible error. The term `uncertainty' is used to refer to `a possible value that an error may have'. Kline and McClintock [1953] attributed this definition and it still seems an appropriate and valuable concept.

This chapter is devoted to determine the interval around each measured parameter within which its true value is believed to lie and it will lead to the ultimate goal, that is to estimate how great an effect the uncertainties in the individual measurements have on the calculated results. An uncertainty estimate is only as good as the equation(s) it is based on. If those equations are incomplete and do not acknowledge all the significant factors that affect the result, then the analysis will either underestimate or overestimate the uncertainty in the results.

A.2 THE BASIC MATHEMATICS

In the present experiments, each test point was run only once, and hence they were single sample experiments. A precise method of single sample uncertainty analysis has been described in the engineering literature by the works of Kline and McClintock [1953] and Moffat [1988].

If a variable x, has a known uncertainty W_1, then the form of representing this variable and its uncertainty is,

$x_1 = x_1$ (measured) $\pm W_1$ (20:1) [A.1]

This statement should be interpreted to mean the following:

* The best estimate of x_1 is x_1 (measured)
* There is an uncertainty in x_1 that may be as large as $\pm W_1$
* The odds are 20 to 1 against the uncertainty of x_1 being larger than $\pm W_1$.

It is important to note that such specification can only be made by the experimenter based on the total laboratory experience.

Now suppose, a set of measurements is made and the uncertainty in each measurement may be expressed with the same odds. These measurements are then used to calculate some desired result R using the independent variables $x_1, x_2, x_3, \ldots\ldots\ldots x_n$, where,

$$R = R(x_1, x_2, x_3, \ldots\ldots\ldots\ldots\ldots\ldots x_n) \qquad [A.2]$$

Let, $W_1, W_2, W_3, \ldots\ldots\ldots\ldots\ldots\ldots W_n$ be the uncertainties in the independent variables given with the same odds. Then the uncertainty W_R in the result having these odds is given in Kline and McClintock [1953] as,

$$W_R = \left[\left(\frac{\partial R}{\partial x_1} W_1\right)^2 + \left(\frac{\partial R}{\partial x_2} W_2\right)^2 + \ldots\ldots\ldots + \left(\frac{\partial R}{\partial x_n} W_n\right)^2\right]^{1/2} \qquad [A.3]$$

where, the partial derivative of R with respect to x_i is the sensitivity coefficient for the result R with respect to the measurement x_i. In most situations, the overall uncertainty in a given result is dominated by only a few of its terms. Terms in the uncertainty equation that are smaller than the largest term by a factor of 3 or more can usually be ignored (Moffat, 1988). This is a natural consequence of the Root-Sum-Square (RSS) combination: Small terms have very small effects.

Sometimes the estimate is wanted as a fraction of reading, rather than in engineering units. While this can always be calculated using equation A.3, it is also possible to do the calculation of relative uncertainty directly. In particular, whenever the equation describing the result is a pure product form such as equation (A.4), than the relative uncertainty can be found directly.

That is, if

$$R = x_1^a x_2^b x_3^c \ldots\ldots\ldots\ldots x_m^n \qquad [A.4]$$

then,

$$\frac{W_R}{R} = \left\{ \left(a \frac{W_1}{x_1}\right)^2 + \left(b \frac{W_2}{x_2}\right)^2 + \ldots\ldots\ldots\ldots + \left(m \frac{W_M}{x_M}\right)^2 \right\}^{1/2} \qquad [A.5]$$

A.3 UNCERTAINTY ANALYSIS OF THE PRESENT EXPERIMENTAL DATA

Uncertainty in Flow rate

The intake flow rate (withdrawal) is measured by an orificemeter. The pressure difference between the upstream and downstream locations of orificemeter is determined with a piezometer. The flow rate is calculated as, Q = AL/t, Where, Q = flow rate, A=area of the tank, L=Height of fall water in time 't'. Now, according to equation (A.5)

Here, A = 1.44 m^2

L = 300 ± 1mm ;(maximum range)

L = 280 ± 1mm ;(minimum range)

t = 1080 ± .01sec;(maximum range)

t = 420 ±.01sec;(minimum range)

Thus;

$$\frac{W}{Q} = \left(\frac{W_L}{L}\right) + \left(\frac{W_t}{t}\right)$$

So, maximum, $\frac{W_Q}{Q} = \left(\frac{1}{280} + \frac{0.01}{480}\right) = 0.35\%$

whereas minimum, $\frac{W_Q}{Q} = \left(\frac{1}{300} + \frac{.01}{300}\right) = 0.33\%$

Uncertainty in density, ρ

The density of water is calculated using the following correlation,

$\rho = a + bt + ct^2 + dt^3 = 266.5 + 6.466\,(T + 273) - 0.01788\,(T + 273)^2 + 0.0000148\,(T + 273)^3$

$$\frac{\partial \rho}{\partial t} = b + 2ct + 3dt^2$$

At T = 50°C, $\rho = 988.3598$ kg/m^3 and

$$\frac{\partial \rho}{\partial t} = 6.466 - 2 \times 0.01788\,(50 + 273) + 3 \times 0.0000148\,(50 + 273)^2 = -0.4523$$

At T = 25°C, $\rho = 997.21$ kg/m^3 and

$$\frac{\partial \rho}{\partial t} = 6.466 - 2 \times 0.01788\,(25 + 273) + 3 \times 0.0000148\,(25 + 273)^2 = -0.2476$$

Now, for T = 50 ± 1°C

$$W_\rho = \frac{\partial \rho}{\partial t} . W_t = 0.4523$$

and $\rho = 988.3598 \pm 0.4523$ kg/m^3 will be used in later calculations.

Uncertainty in effective gravitational acceleration, g'

$$g' = \frac{\Delta\rho}{\rho} g = \Delta\rho . \rho^{-1} g \quad \text{and} \quad \frac{W_{g'}}{g'} = \left[\left(-1 \frac{W_\rho}{\rho}\right)^2\right]^{\frac{1}{2}}$$

$\rho = 988.3598 \pm 0.4523$ kg/m^3

$$\frac{W_{g'}}{g'} = \left[\left(\frac{0.4523}{988.3598}\right)^2\right]^{\frac{1}{2}} = 0.05\%$$

Uncertainty in Froude Number Calculation

The intake Froude number is defined as, $F_d = \dfrac{Q}{\sqrt{g' d^5}} = Q(g')^{-\frac{1}{2}} d^{-\frac{5}{2}}$

d = 21.5 ± 0.1 mm; maximum range

= 19.0 ± 0.1 mm; minimum range

$$SO,\ \frac{W_F}{F} = \left\{ \left(\frac{W_Q}{Q}\right)^2 + \frac{1}{4}\left(\frac{W_{g'}}{g'}\right)^2 + \frac{25}{4}\left(\frac{W_d}{d}\right)^2 \right\}^{\frac{1}{2}}$$

$$minimum\ \frac{W_{F_d}}{F_d} = \left\{ (0.0033)^2 + \frac{1}{4}(0.0005)^2 + \frac{25}{4}\left(\frac{0.1}{21.5}\right)^2 \right\}^{\frac{1}{2}} = 1.20\%$$

$$maximum,\ \frac{W_{F_d}}{F_d} = \left\{ (0.0035)^2 + \frac{1}{4}(0.0005)^2 + \frac{25}{4}\left(\frac{0.1}{19}\right)^2 \right\}^{\frac{1}{2}} = 1.36\%$$

The uncertainty in the calculation of other Froude numbers will be of this order.

Uncertainty in percentage drawdown determination

Determination of percentage drawdown, Λ involves a ratio of temperature differences. The uncertainty in percentage drawdown, Λ determination may be calculated as follows:

$$\Lambda = \frac{T_m - T_2}{T_1 - T_2} = \frac{x}{y} = xy^{-1}\ (say)$$

maximum possible $T_m - T_2$ = 12°C ±0.1°C

minimum possible $T_m - T_2$ = 8°C ±0.1°C

maximum possible $T_1 - T_2$ = 15°C ±0.1°C

minimum possible $T_1 - T_2$ = 10°C ±0.1°C

$$\frac{W_\Lambda}{\Lambda} = \left[\left(\frac{W_x}{x}\right)^2 + \left(-1\frac{W_y}{y}\right)^2 \right]^{\frac{1}{2}}$$

Using this equation uncertainty in percentage drawdown determination is found to be within 1.06% to 1.60%.

APPENDIX - B

THERMOCOUPLE THERMOMETRY

B.1 INTRODUCTION

The thermocouple technique is the most widely used method of measuring temperatures. The usual thermocouple thermometer circuit consisting of three metals is shown below.

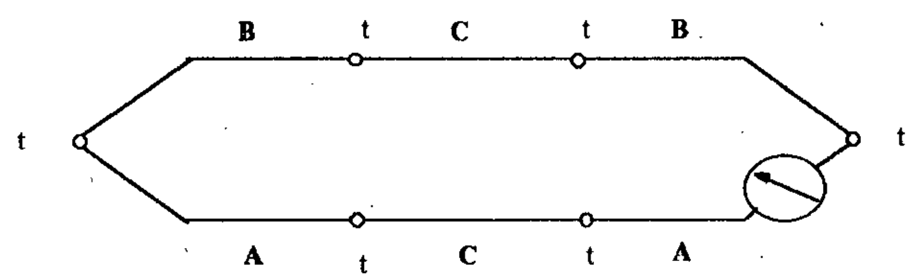

Where A and B are the thermocouple constituents and C is the lead wire. Let, E_{AB} be the average thermoelectric power over the temperature ranges t_1 to t_i and t_j to t_2 then, thermoelectric emf,

$$E_{ACABCB} = e_{AB}(t_1 - t_2) - e_{AB}(t_i - t_j)$$

If both the ends of the leads are kept at same temperature; i.e. if $t_i = t_j$ then the introduction of lead wires into the thermocouple circuit will not practically cause any change. That is the circuit will act as if the thermocouple itself is extended from hot junction to cold junction without any intermediate lead wire.

B.2 EFFECT OF INTRODUCTION OF INTERMEDIATE METALS

Thermoelectric circuits always include indicating instruments, switches etc. The portion of the circuit through any such device nearly always consists of several metals. The law of intermediate metals states: ***if in any circuit of solid conductors the temperature is uniform from any point P through all the conducting matter to a point Q, the thermoelectric emf in the circuit is the same as if P and Q were put in contact.*** Thus if the temperature throughout any such switch or indicating device is uniform, no error will result. Likewise, the smaller the variations in the thermoelectric properties among the various metals used, the smaller the resulting error will be for a given degree of nonuniformity in temperature within the group of switches and indicating devices. The metals for this portion of the circuit are customarily limited to copper, brass, lead-tin solder, silver and manganin, as the thermoelectric properties of these metals do not differ greatly, i.e. they have low thermoelectric powers with respect to one another (Baker et. al., 1953).

B.3 THERMAL INSULATION

It is usually sufficient for the switches and instruments to be kept in a room provided with ordinary thermostating (i.e. ± 4°F or 2.5°C) and at a distance of 6 feet or more from any hot and cold surface such as window, radiator, poorly insulated steam pipe and not exposed to any drafts or direct sunshine. In very precise work (i.e. to be within ± 0.01 to ± 0.001°F) additional precaution may be required, such as packing the instruments in cotton or emerging them in constant temperature oil baths. If instruments must be placed in thermally exposed position, protection by some adequate form of thermal insulation is necessary even in low precision work (Baker et. al., 1953).

B.4 THERMOCOUPLE WIRES

Four pairs of thermoelectric wire materials are widely used. These are:

- Copper against Constantan (60% Copper with 40% Nickel)
- Iron against Constantan
- Chromel P (90% Nickel with 10% Chromium) against Alumel (95% Nickel with Al, Si and Mn comprising the remainder)
- Platinum against Platinum-Rhodium (90% Platinum with 10% Rhodium or 87% Platinum with 13% Rhodium)

Standards and tables for thermoelectric e.m.f.s have been established for these four combinations of materials. Matched pairs of wires are furnished commercially to conform within manufacturing tolerances to these tables. Manufacturer of thermocouple wire also furnish tables applying specifically to their own products.

B.5 T-TYPE THERMOCOUPLE

Copper against Constantan is widely used for low temperature. The ease with which copper can be fabricated in a pure homogeneous condition tends toward reliability in this couple. The thermoelectric power is high, i.e. 23.8 $\mu V/^{o}F$ (42.8 $\mu V/^{o}C$) in the range of 0°C to 100°C. In case of Chromel-alumel pair it is 22.8 $\mu V/^{o}F$ (41 $\mu V/^{o}C$) whereas in case of Iron-constantan it is 30 $\mu V/^{o}F$ (54 $\mu V/^{o}C$). But Iron-constantan couple can not be used in water for long time as iron has a tendency to be oxidized to form rust.

B.6 CALIBRATION OF THERMOCOUPLE WIRES

Thermocouple wire is available commercially in matched pairs, with specified tolerances. These tolerances are published in standard tables. Each strand of wires, as produced, is calibrated. Selected strands of two materials are then paired such that the temperature e.m.f. relationship for each such pair does not deviate by more than the stated amount. Common tolerances are ± 0.25 percent to ± 0.75 percent.

Laboratory calibration has only to do with wire that is found to be homogeneous in thermoelectric properties along its length. As such it is not necessary to calibrate every couple, individually, which may be made up out of a given pair of matched strands of wire. This couple can be taken from each end of a pair of strands, or, if the length is great, at suitable intervals. If the discrepancies amount to more than one-tenth the allowable error, the entire spool should be discarded.

In this work M50 data logger and T-type thermocouple is used to measure the temperature. The thermocouple is calibrated with mercury thermometer. The relation between the mercury thermometer(actual) temperature and the data logger reading (observed temperature) is shown in Fig: A1, and it is certain that with the working range of the temperature (25°C to 45°C) the relationship may assumed to be linear.

Frequently, the interest lie more in the measurement of temperature differences or in the determination of temperature pattern, than in learning the absolute values of these temperatures. In this case, all thermocouple for the job should be made from the same pair of strands.

B.7 JUNCTIONS AND SPLICES

The term `junction' applies to each of the electrically conducting joints made between the thermocouple wires to form the thermocouple. The term `splices' is used when the conducting joint is made between two wires of the same, or thermoelectrically equivalent metals.

In fused junctions there may be a layer of intersolution separating the two metals. Thus in the neighborhood of the junction, there is a portion of the circuit that consists of material other than either of the original thermocouple metals. This can be regarded as a short length of wire composed of a third metal or as an inhomogeneous section. If this portion of the circuit is at the same, uniform temperature, the effect will be the same as though the two metals were joined directly at the point of entry into the uniform temperature region. This point will then be the effective junction. If the temperature within this inhomogeneous portion of the circuit is not uniform, the effective location of the junction will be uncertain. To minimize such uncertainty, it is necessary that the inhomogeneous portion at the junction be made as small as possible. this is best achieved in beaded or butt-welded junction.

Where a splice is made between two wires of the same metal or of metals intended to be thermoelectrically equivalent as in the lead wires, in a region where the temperature varies along their lengths, the splice should be made by fusing the two ends together in a butt-weld or fused splice. Clamping the two wires directly together is also satisfactory if good contact is made (Baker et. al., 1953).

B.8 RAPIDLY CHANGING TEMPERATURE

When the source body is of uniformly changing temperature and moving relatively to the measuring device, the temperature of the materials successively presented in the flow process to the sensitive element is a function of time. An error in the indication of the time for the occurrence of a given temperature magnitude is to be interpreted as an error in location for the point on the moving body. Lag time can be determined by inserting the sensitive element in a constant temperature bath and recording the time-temperature response (Fig. A2 to Fig: A4).

B.9 EFFECT OF VELOCITY

When flow velocity is high and irregular, corresponding temperature variations result. Discrepancies due to this phenomena are, however, less often serious in liquid temperature measurement than in gas-temperature measurement. Geldbach and Müller [quoted from Baker et. al., 1953] observed local temperature changes in streams of water at points where the flow was disturbed by obstacles. For stream velocities upto around 7 m/sec, temperature rise were of the order of 0.02 to 0.04°C and appeared to be proportional to the square of the undisturbed stream velocity.

B10 Temperature profile of stratified fluid system

A typical temperature profile of the present stratified fluid system is shown in Fig: 3.4. Three thermocouples, those are 6"(inch) apart (in horizontal direction), are used to check the variation in temperature profile in the horizontal direction. The variation in temperature along the depth of the tank for different thermocouple is shown in Table A4 and these data are plotted in Fig: A5 & Fig: A6. From these figures it can be inferred that there is no variation in temperature profile in the horizontal direction, or more precisely the mean height of interface and the thickness of the interface remains constant at different location of the tank

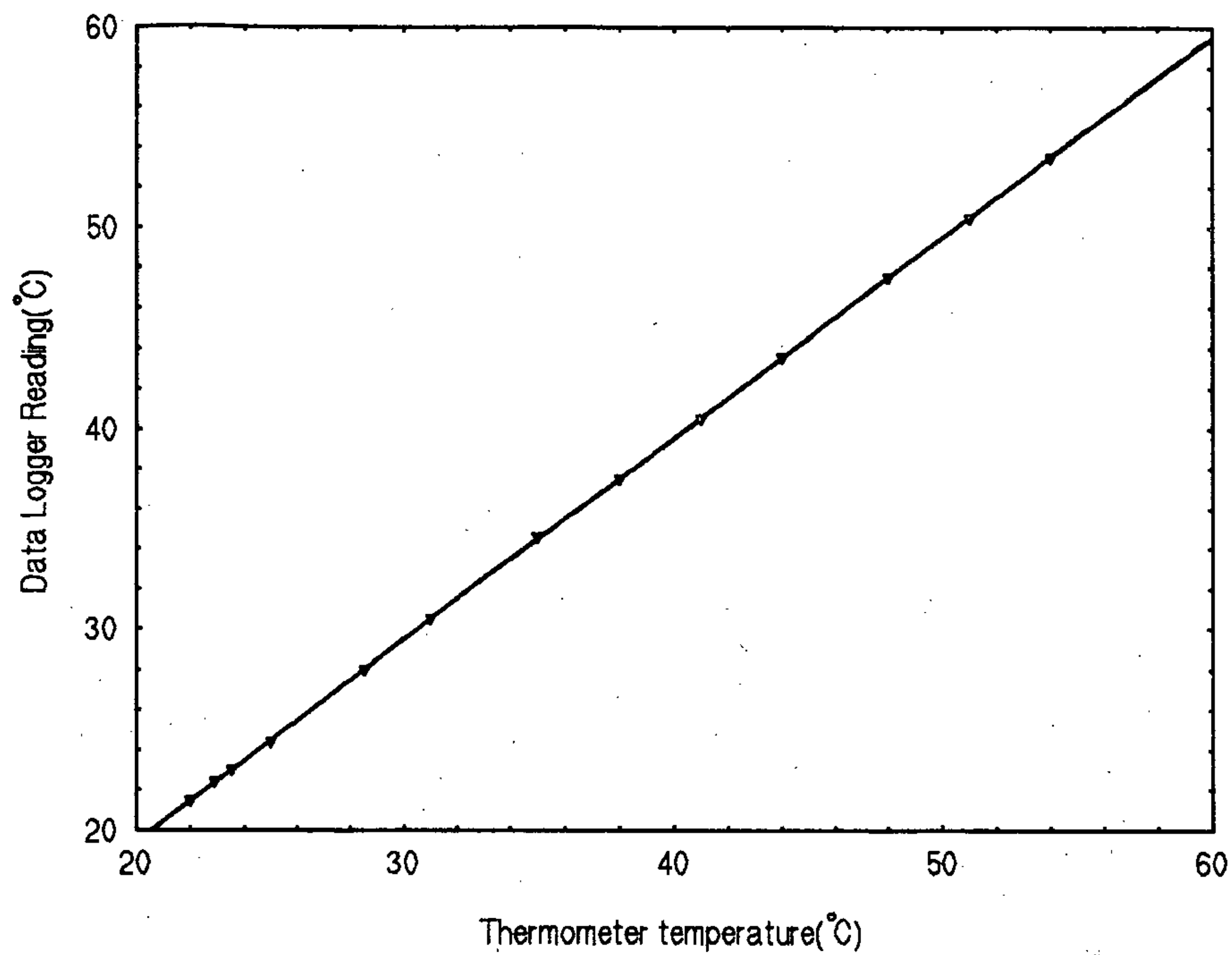

Fig: A1 Calibration of Data Logger

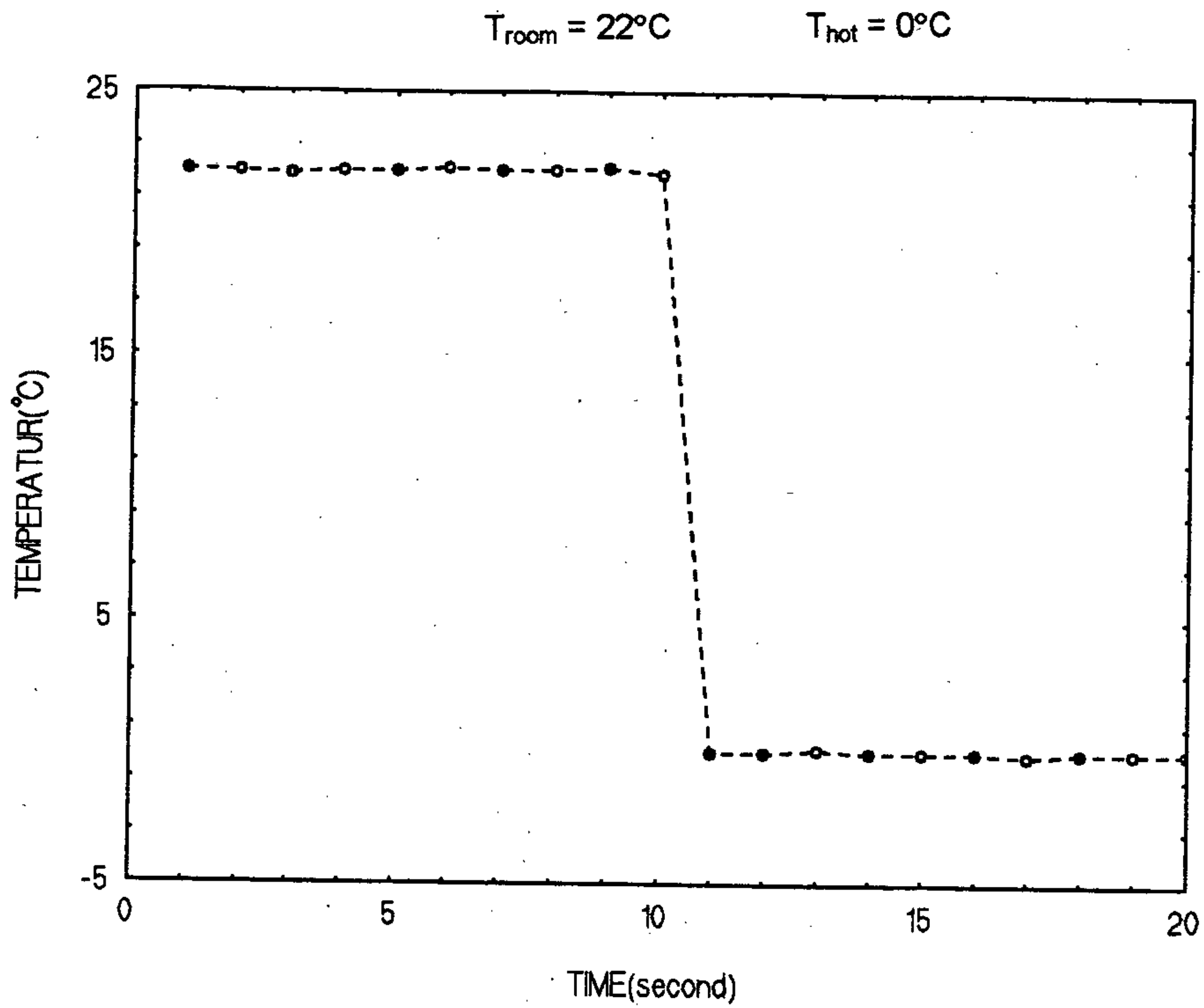

Fig: A2 Response time of T-type thermocouple

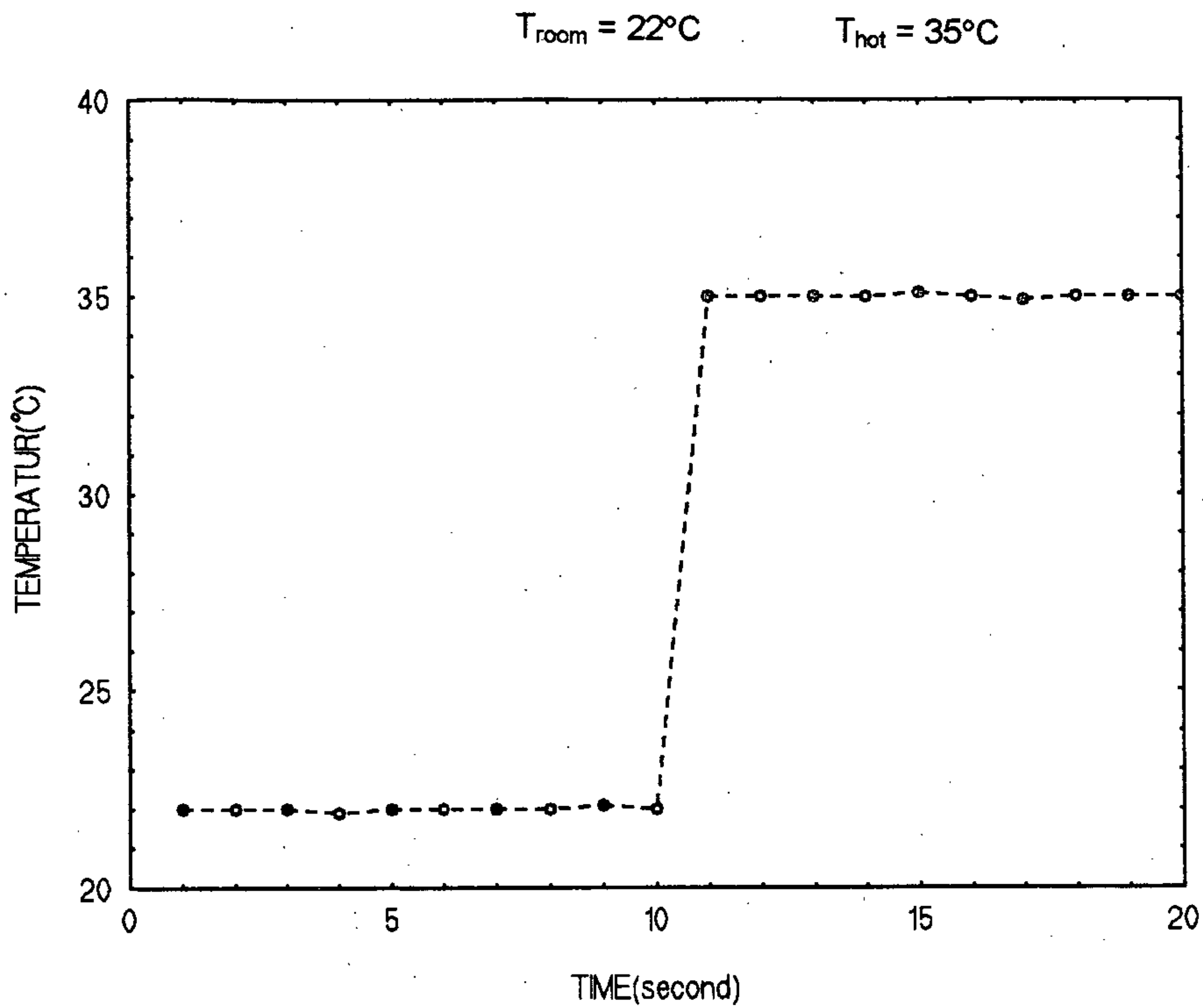

Fig: A3 Response time of T-type thermocouple

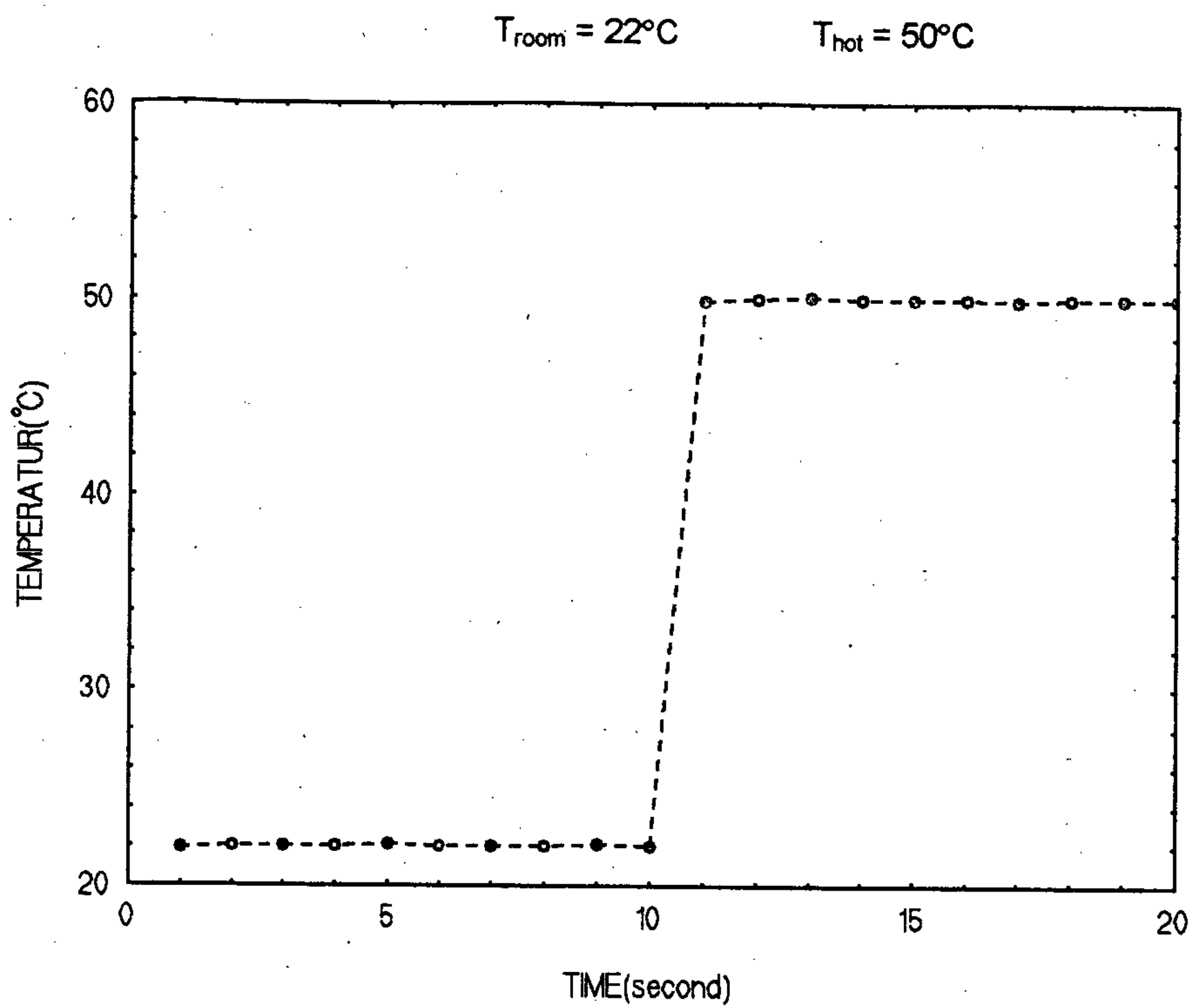

Fig: A4 Response time of T-type thermocouple

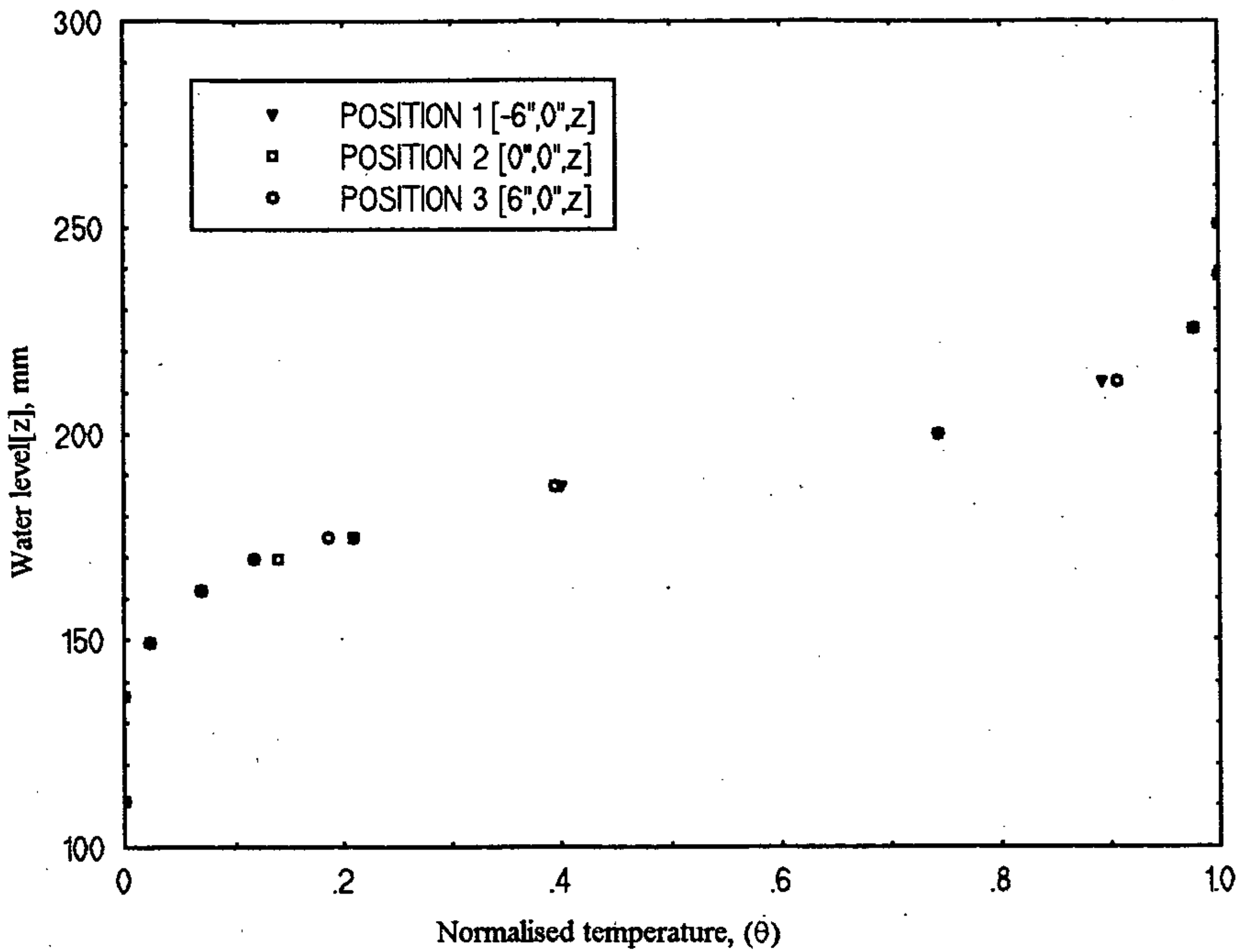

Fig: A5 Verification of one dimensional temperature variation

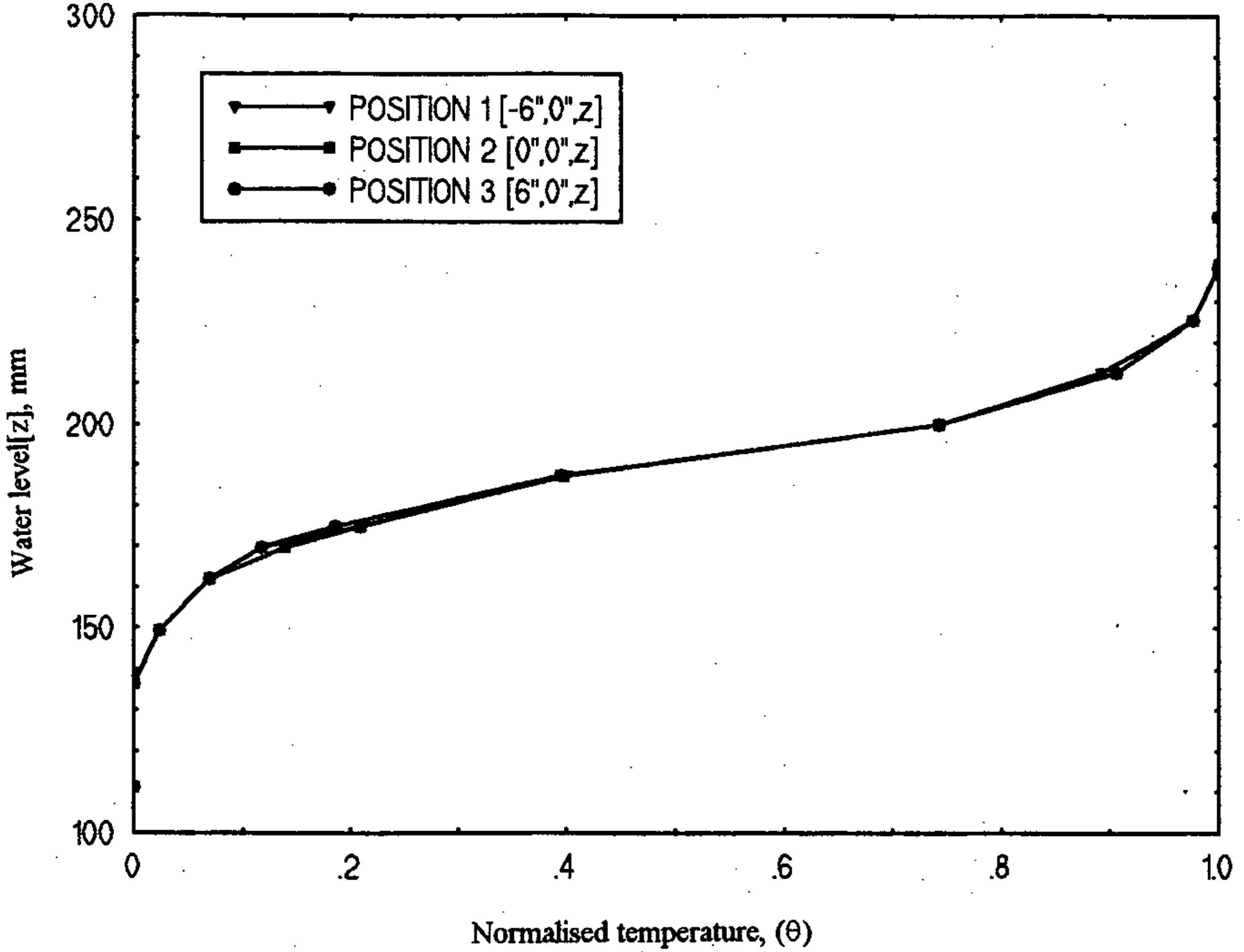

Fig: A6 Verification of one dimensional temperature variation

TABLE A1

HEIGHT OF WATER COLUMN[z]	NORMALIZED TEMPERATURE (θ)		
mm	POSITION 1 [-6",0",z]	POSITION 2 [0",0",z]	POSITION 3 [6",0",z]
111.10	0	0	0
136.50	0	0	0
149.20	0.0232558	0.0232558	0.0232558
161.90	0.0697674	0.0697674	0.0697674
169.52	0.1162790	0.1395350	0.1162790
174.60	0.1860470	0.2093020	0.2093020
187.30	0.3953490	0.3953490	0.4118600
200.00	0.7441860	0.7441860	0.7839023
212.70	0.9069770	0.9069770	0.9100300
225.40	0.9767440	0.9767440	0.9667440
238.10	1	1	1
250.80	1	1	1